Exploring the Proteome: Insights into Eukaryotic Protein Synthesis Using Puromycin Analogs

Thesis by
Shelley Ruth Starck

In Partial Fulfillment of the Requirements
for the Degree of
Doctor of Philosophy

California Institute of Technology
Pasadena, California

2004

(Defended May 20, 2004)

Acknowledgements

I gratefully acknowledge my mentor and advisor Richard W. Roberts, who stands at the forefront for providing scientific support and guidance during my Ph.D. studies. His knowledge of our field and genuine enthusiasm for research is unmatched. This work would not have evolved into such an interdisciplinary body of research without the guidance, insight, and commitment of my colleague and fiancé, Harry Miguel Green. In addition, I sincerely appreciate the time Terry Takahashi, a fellow graduate student, spent giving me advice and guidance, as well as making the best barbeque on earth. William Ja, another fellow graduate student, is responsible for recruiting me to the Roberts group, welcoming me so warmly into the group, and including me in many dinners out. I thank my other colleagues in the Roberts group who helped to make my time in graduate school a wonderful experience, including Ryan Austin, Christopher Balmaseda, Steve Millward, Shuwei Li, Anders Olson, Cindy Qi, Christine Ueda, and Tianbing Xia. Jennifer Treweek and Binghai Li, undergraduates, were a joy to work with during my last year. Thank you Jenn and Binghai for all the late night FLASH columns and HPLC runs! The Roberts group secretary, Margot Hoyt, deserves special recognition for making sure 'things got done.' I must also acknowledge the José Alberola-Ila and the Alberola group, specifically Michelline Laurent, Gabriela Hernandez, and Eric Tse who has since passed away. Finally, I sincerely appreciate the support from my committee members, Peter Dervan, Dennis Dougherty, and Harry Gray, who wrote numerous letters of support on my behalf.

The first person I met at Caltech was Dian Buchness, our division secretary. Her warmth and support during my time at Caltech will always be remembered. Nelson Leonard, my 'scientific grandfather,' was a great source of guidance and wisdom during preparation of a JACS manuscript. Dr. Leonard is true gentleman and an inspiration to all.

Important recognition must be paid to Candace Rypisi, the Caltech Women's Center Director, who provided many programs free of charge to the Caltech community,

especially the women's self-defense class which probably saved my life.

Mrs. Grace Verburg, a P.E.O. chapter member, nominated and helped me win a P.E.O. Scholar Award. Her encouragement and support is gratefully appreciated. The RNA society meeting in Vienna, Austria would not have been possible without this award.

My friends here at Caltech deserve many thanks for being there through it all, including Sarah Monahan, Shira Rogers-Jacobson, Catherine Oertel, Elizabeth Mayo, Pei Yun Lee, Wendy Steiner, Marcia Cooper, Caroline Englebienne and special thanks to Philippe Chatelain, who spent *hours* helping me put this thesis into LaTex. Miguel, my love, thank you for making my time here the happiest ever, from 'sqleep-sqleep in da be' to 'looking at da tinq in da bag.' Dr. Harry Green and Dr. Manuela Martins-Green, my future in-laws, were tremendously supportive and encouraging over the past several years. I can not imagine having more loving future in-laws.

Lastly, I would like to pay tribute to my parents, Richard and Sharon Starck, my siblings Rick, Jason, and Kylie, and the best grandparents known to man, Caesar and Ruth Cappo. Although you were many miles away during my work on this thesis, your love and support were always there. See Dad, the time you spent helping me dissect the worm and the starfish paid off! Columbus you will be missed and never forgotten. Blonde Moment and Totally Blonde live in your memory. Toffee 2000, thank you for your soul-full gaze of support during the months of proposal and thesis writing.

Abstract

Puromycin is a protein synthesis inhibitor that acts as a structural analog of an aminoacyl-tRNA. The ribosome mistakenly inserts puromycin in place of aminoacyl-tRNA resulting in truncated proteins containing the drug at their C-terminus. Herein, the puromycin reaction is re-examined in a cell-free eukaryotic translation extract and in live cells. The framework for puromycin reactivity in terms of potency, product distribution, and mechanism is studied *in vitro*. These insights are used to develop a series of fluorescent puromycin-based reagents to detect protein expression in living cells that does not require transfection, radiolabeling, or the prior choice of a candidate gene. Further, puromycin is used to examine the stereo- and regiochemical nature of protein synthesis both *in vitro* and *in vivo*. These data indicate that the ribosome tolerates a broader range of substrates than previously recognized, including D-amino acids. Overall, these studies yield a series of insights about protein synthesis and the ribosome, including mechanistic observations, the development of reagents to explore the proteome, and a theory about the evolution of amino acid homochirality.

Contents

List of Figures

List of Tables

Chapter 1

Background and Perspective

Protein synthesis is one of the fundamental events in every living cell. The central dogma of biology (Figure 1.1) shows that our genetic material, encoding ~30,000 genes (1, 2), can be transformed into protein through RNA. A specialized type of RNA called mRNA is deciphered with the aid of several translation factors on ribosomes, the molecular decoding machinery of the cell. Ribosomes are RNA and protein complexes that make up more than 25% of the total mass of *Escherichia coli* cells and carry a M_r of 3 million daltons. In an *E. coli* cell, 3 x 10^4 ribosomes select the correct amino acid from over 41 aminoacyl-tRNAs containing a unique anticodon sequence and assemble amino acids into protein at a rate of $10 - 20$ sec^{-1} (3). Yet the macromolecular concentration of an *E. coli* cell is 340 mg/mL, which in terms of

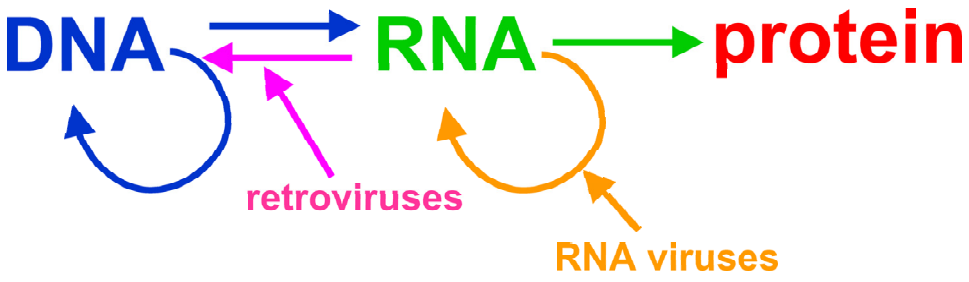

Figure 1.1: Central dogma of biology.

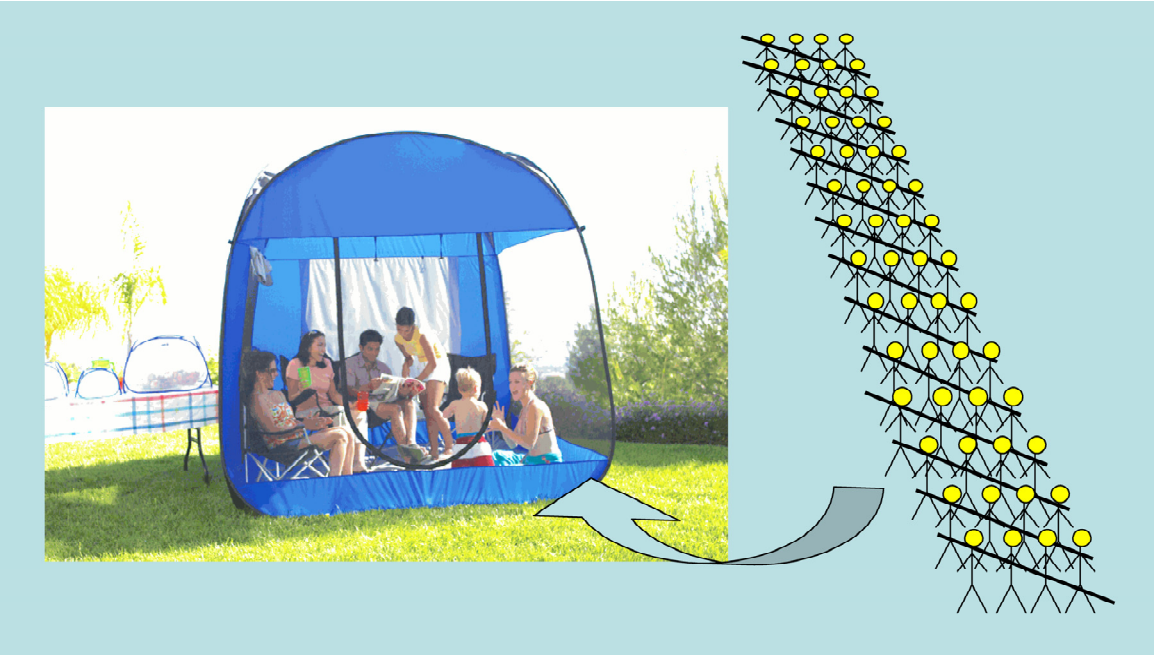

Figure 1.2: The macromolecular concentration of the *E.coli* cell is equivalent to packing 70 humans into this small tent.

volume is equivalent to packing more than 70 humans into a space of a small tent with volume 500 ft^3 (Figure 1.2) (4)! So how can protein synthesis proceed at a rate necessary to sustain life with an error of only 1 in 10 thousand amino acids? This question is one of many that remain unanswered in the area of protein synthesis.

My Ph.D. tenure has overlapped with several spectacular achievements in the area of protein translation. On August 11, 2000, Tom Steitz and co-workers published an atomic resolution crystal structure of the large ribosomal subunit (5). This work unambiguously assigned the location of peptide bond formation to be completely within a region of RNA. This confirmed a theory backed by biochemical evidence (6) that the ribosome is a ribozyme (4). Soon thereafter, a 5.5 $\AA$ map of the entire ribosome assembled with mRNA and aa-tRNAs was published by Harry Noller and colleagues. This account yielded a snapshot of protein synthesis that continues to stand at the structural forefront of biology. In addition to structural insights, kinetic

and equilibrium measurements of ribosomes at discrete steps during translation were published (7). These structural and biochemical data presented in just the last few years have advanced our understanding of translation beyond what could even be imagined just 10 years ago. What lies ahead in this field is the development of tools and reagents to elucidate the proteome at the molecular level within the cell.

In the pages that follow, I describe the design and characterization of compounds to directly study protein synthesis both *in vitro* and in live cells. Much of what we know about translation has been derived from the study of prokaryotic organisms, such as *E. coli*. The lack of comparable insight about translation in higher organisms was the impetus behind the work presented in this thesis.

Chapter 2 reviews the historical use of reagents to probe protein synthesis and examines their drawbacks for understanding protein translation in the context of cells. A re-evaluation of puromycin action using a reticulocyte lysate cell-free translation system is presented, which takes into account the potency, product distribution, and mechanism of various puromycin-oligonucleotide conjugates. Insights derived from these studies lay the framework for the design of reagents to study translation in live cells. Chapter 3 describes the implementation of these reagents to study protein synthesis *in vivo*. Fluorescent puromycin derivatives (of the form X-dC-puromycin) enable direct monitoring of protein expression and provide the potential for both spatial and temporal resolution in living cells and tissues. Chapter 4 revisits the issues surrounding the stereo- and regiochemistry of protein translation and presents a set of data that show the specificity of the ribosome (compared to typical enzymes) to be more relaxed than previously recognized. These new observations support the notion that the ribosome could synthesize peptides and proteins using D- and $\beta-$amino acids. Chapter 5 continues to examine the specificity of the ribosome and highlights the sensitivity of translation to substitution of the reactive amine. Chapter 6 is an *in vivo* analysis of ribosome specificity using the number of live cells as a measurement of ribosome specificity. Further, the effect of sidechain identity on ribosome stereos-

electivity is analyzed in live cells. These results extend the theory that the protein synthesis machinery should be capable of generating polymers that differ substantially from natural peptides and proteins. Finally, in Chapter 7, data is presented that provides prebiotic evidence for the evolution of amino acid homochirality. In summation, these data offer new insights into the chemical nature of eukaryotic protein synthesis and advance our understanding of the proteome.

References

[1] The International Human Genome Sequencing Consortium. Initial sequencing and analysis of the human genome. *Nature*, 409:860–921, 2001.

[2] J.C. Venter, M.D. Adams, E.W. Myers, P.W. Li, R.J. Mural, G.G. Sutton, H.O. Smith, M. Yandell, C.A. Evans, and R.A. et al. Holt. The sequence of the human genome. *Science*, 291:1304–1351, 2001.

[3] K.H. Nierhaus. *Gene Expression: Decoding and Accuracy. In: Nature Encyclopedia of Life Sciences.* Nature Publishing Group, London, 1999.

[4] N. Ban, P. Nissen, J. Hansen, P.B. Moore, and T.A. Steitz. The complete atomic structure of the large ribosomal subunit at 2.4 angstrom resolution. *Science*, 289:905–920, 2000.

[5] P. Nissen, J. Hansen, N. Ban, PB. Moore, and Steitz TA. The structural basis of ribosome activity in peptide bond synthesis. *Science*, 289:920–930, 2000.

[6] HF. Noller, V. Hoffarth, and Zimniak L. Unusual resistance of peptidyl transferase to protein extraction procedures. *Science*, 256:1416–1419, 1992.

[7] M.V. Rodnina and W. Wintermeyer. Fidelity of aminoacyl-tRNA selection on the ribosome: Kinetic and structural mechanisms. *Ann. Rev. Biochem.*, 70:415–435, 2001.

Chapter 2

Puromycin Oligonucleotides Reveal Steric Restrictions For Ribosome Entry and Multiple Modes of Translation Inhibition

This chapter has previously appeared as: S.R. Starck and R.W. Roberts. Puromycin oligonucleotides reveal steric restrictions for ribosome entry and multiple modes of translation inhibition. *RNA* 8:890-903, 2002.

Abstract

Peptidyl transferase inhibitors have generally been studied using simple systems and remain largely unexamined in *in vitro* translation extracts. Here, we investigate the potency, product distribution, and mechanism of various puromycin-oligonucleotide conjugates (1 to 44 nucleotides with 3'-puromycin) in a reticulocyte lysate cell-free translation system. Surprisingly, the potency *decreases* as the chain length of the oligonucleotide is increased in this series, and only very short puromycin conjugates function efficiently ($IC_{50} < 50$ μM). This observation stands in contrast with work on isolated large ribosomal subunits which indicates that many of the puromycin-oligonucleotide conjugates we studied should have higher affinity for the peptidyl

transferase center than puromycin itself. Two $tRNA^{Ala}$-derived minihelices containing puromycin provide an exception to the size trend, and are the only constructs longer than four nucleotides with any appreciable potency ($IC_{50} = 40 - 56\ \mu M$). However, the puromycin minihelices inhibit translation by sequestering one or more soluble translation factors, and do not appear to participate in detectable peptide bond formation with the nascent chain. In contrast, puromycin and other short derivatives act in a factor-independent fashion at the peptidyl transferase center and readily become conjugated to the nascent protein chain. However, even for the short derivatives, much of the translation inhibition occurs *without* peptide bond formation between puromycin and the nascent chain, a revision of the classical model for puromycin function. This peptide bond-independent mode is likely a combination of multiple effects including inhibition of initiation and failure to properly recycle translation complexes that have reacted with puromycin.

2.1 Introduction

Puromycin has played an important role in our understanding of the ribosome and protein synthesis. It has been known for more than 40 years that the molecule is a universal protein synthesis inhibitor that acts as a structural analog of an aminoacyl-tRNA (aa-tRNA) (Figure 2.1) (1). Nathans went on to demonstrate that the ribosome mistakenly inserts puromycin in place of aminoacyl-tRNA resulting in truncated proteins containing the drug at their C-terminus (2). A later examination of this mechanism concluded that puromycin inhibits translation solely through C-terminal labeling of peptides and not through additional pathways (3). This classic model for puromycin supports only a single mode of action, covalent attachment to the nascent chain.

In vitro studies with the drug have largely utilized the 'fragment reaction,' in which peptidyl transferase activity of isolated 50S subunits is measured by the formation of

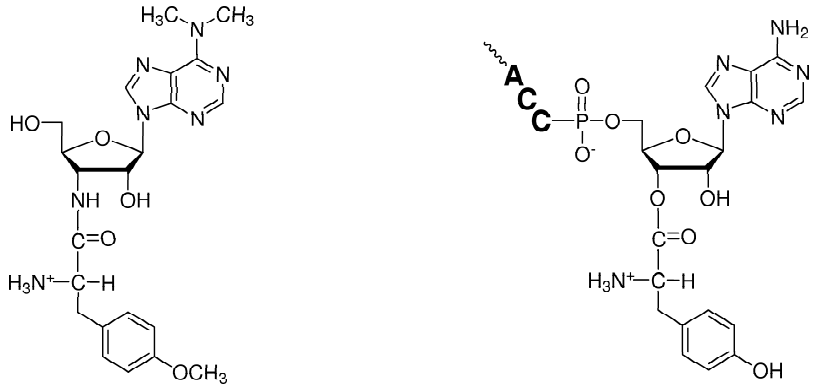

Figure 2.1: Puromycin versus aminoacyl-tRNA.

N-formyl-[^{35}S]Met-puromycin (f-Met-puromycin) from a fragment of *N*-formyl-Met-tRNA$_f^{Met}$ and puromycin (4). Much of what we know about the catalytic activity of the ribosome has been derived from this simple assay (5, 6). However, the reaction is conducted under conditions that are relatively non-physiological (30% ethanol, 400 mM K^+, and $0 - 4$ °C incubation temperature) and the effect of other critical components such as the template, small ribosomal subunit, and soluble translation factors cannot be measured, as they are absent. Thus, the potency of puromycin may not be accurately reflected by its activity under fragment reaction conditions.

To account for these shortcomings, some modifications have been made to more fully recapitulate the protein synthesis machinery. Addition of the small subunit and poly(U)-mRNA followed by P-site charging with *N*-acetyl-Phe-tRNA^{Phe} (Ac-Phe-tRNA^{Phe}) pushes the equilibrium towards subunit association, which allows peptidyl transferase to be carried out in the absence of alcohol (7). However, these adaptations still require salt-washed ribosomes, relatively high concentrations of NH_4Cl and $MgCl_2$ to promote subunit assembly in the absence of initiation factors (7), and fail to yield long polypeptide-puromycin complexes (>12-15 amino acids in the *E. coli* cell-free poly(A) system) (3). Thus even these modifications result in systems

that are biochemically removed from the complete translation apparatus. To date, the majority of studies with translation inhibitors have been conducted using either the classical fragment reaction or a version of the f-Met-tRNA·A-U-G·70S or Ac-Phe-tRNA·poly(U)·70S system (8, 9, 10, 11).

Interest in puromycin and puromycin conjugates has recently increased due to new methods for synthesizing molecular libraries (12, 13), photo-crosslinking reagents for the ribosome (8), peptidyl transferase inhibitors (11, 14), and *in vitro* synthesis of proteins containing specific labels or tags (15). Optimization of each of these processes requires that we understand how puromycin conjugates enter the ribosome in *cis* (when they are tethered to the mRNA in the decoding site) or in *trans* when these molecules enter the ribosome from solution. Considerable effort has recently gone into understanding the *cis* reaction to facilitate the synthesis of the mRNA-peptide fusions for mRNA-display selection experiments (16). Interestingly, the *trans* reaction between puromycin conjugates and the ribosome remains relatively uncharacterized in complete translation systems, and basic features, such as elongation factor dependence, remain unexplored. We were therefore curious to examine the ability of trans substrates to enter the ribosome and inhibit protein synthesis in a complete translation system. A deeper understanding of the trans reaction would be helpful in 1) synthesizing more efficient translation inhibitors, 2) creating better ribosome crosslinking reagents, and 3) using the ribosome to generate a protein tagged at its C-terminus.

Here, we have examined the effect of puromycin and puromycin-oligonucleotide conjugates on translation by constructing a series of oligonucleotides bearing puromycin at their 3'-end. We then assayed their ability to inhibit translation of rabbit globin mRNA in rabbit reticulocyte translation extracts. Our results differ markedly from previous work with isolated large subunits or whole ribosomes charged with artificial templates. The data provide new insights into the action of puromycin and identify constraints on the design of puromycin-based translation inhibitors that can

function in a physiologically relevant context.

2.2 Results and Discussion

2.2.1 Puromycin versus 30P

We began our experiments by comparing translation inhibition by two substrates, puromycin and 30**P** (p(dA)$_{27}$dCdC-**P**), a 30mer DNA oligonucleotide containing puromycin at the 3'-end. Previously, we had used 30**P** to tether puromycin to mRNAs for the synthesis of mRNA-peptide fusions (13). When attached to the mRNA template, 30**P** can act as an efficient peptide acceptor (13, 16). The design of 30**P** was based on previous work with isolated large subunits, which indicated that molecules containing a penultimate cytidine nucleotide adjacent to the aminoacyl nucleotide should be better acceptors than puromycin alone (reviewed in (?)). For example, 2'(3')-*O*-glycyladenosine (A-Gly) has little acceptor activity, whereas 1) addition of ribocytidine (C-A-Gly) gives a compound with similar activity to puromycin (17) and 2) CA-Phe has a lower K_m than A-Phe (18). Under fragment conditions, 4-thio-dT-C-puromycin has a lower K_m (10 μM) (8) than puromycin itself (K_m = 740 μM) (11). Taken together, these data support the notion that an oligonucleotide with dC-puromycin at its 3'-end should have higher acceptor activity than puromycin alone. However, preliminary experiments indicated that 30**P** showed little ability to inhibit translation or act as an acceptor when co-incubated with fusion templates (R.W.R., unpublished observation).

2.2.2 Potency of Puromycin and Puromycin Oligonucleotides

We developed an *in vitro* translation assay to quantify the potency of puromycin and other putative inhibitors such as 30**P**. In the assay, a translation reaction is performed for one hour using rabbit globin mRNA at ~60 nM (total template concentration; the

template is a mixture of α- and β-globin mRNAs) in rabbit reticulocyte lysate. Each reaction differs only in the amount of inhibitor that is added at the beginning of the reaction. We then assay the reactions by tricine-SDS PAGE (19), TCA precipitation, or other methods to determine the amount of globin translation product. This analysis results in a sigmoidal curve and we term the midpoint (the concentration of drug required to give a 50% decrease in globin synthesis relative to a no-inhibitor control) the IC_{50}.

IC_{50} determinations for puromycin and for 30**P** are shown in Figure 2.2. Several features can be seen in the gel analysis. First, globin synthesis decreases as the amount of puromycin is increased from 25 nM to 75 μM, resulting in an IC_{50} of 1.8 μM (Figure 2.2A,C). Our value agrees reasonably well with previous work showing an IC_{50} value of 2.8 μM in rabbit reticulocyte lysate (20). Our IC_{50} is $\sim$10- to 50-fold lower than the published K_d or K_m values for puromycin measured with mammalian ribosomes (21, 22). For example, Lorsch and Herschlag measured a K_m of $60-100$ μM for puromycin with rabbit reticulocyte ribosomes (22). Our lower apparent value is consistent with entry of puromycin at multiple sites in the protein chain, for example any one of the 144 or 148 codons (including stop) in rabbit α- or β-globin (23). The published K_m values thus provide support that we are measuring a composite of multiple mechanistic steps in our IC_{50} experiments.

A second feature observed for both inhibitors is the apparent lack of low molecular weight, truncated protein as the drug concentration is increased, even at the highest puromycin concentrations in this assay. As the puromycin concentration is increased, a gradual decrease in the amount of the globin band is seen with most of the remaining protein appearing as full-length globin. The fact that puromycin does not chase the protein into lower molecular weight species implies two possible mechanisms for its action: 1) that puromycin entry and peptide bond formation occur only at the termination step and not during elongation or 2) that puromycin entry results in fragments too small to be resolved by PAGE techniques (e.g., Met-puromycin). Analysis

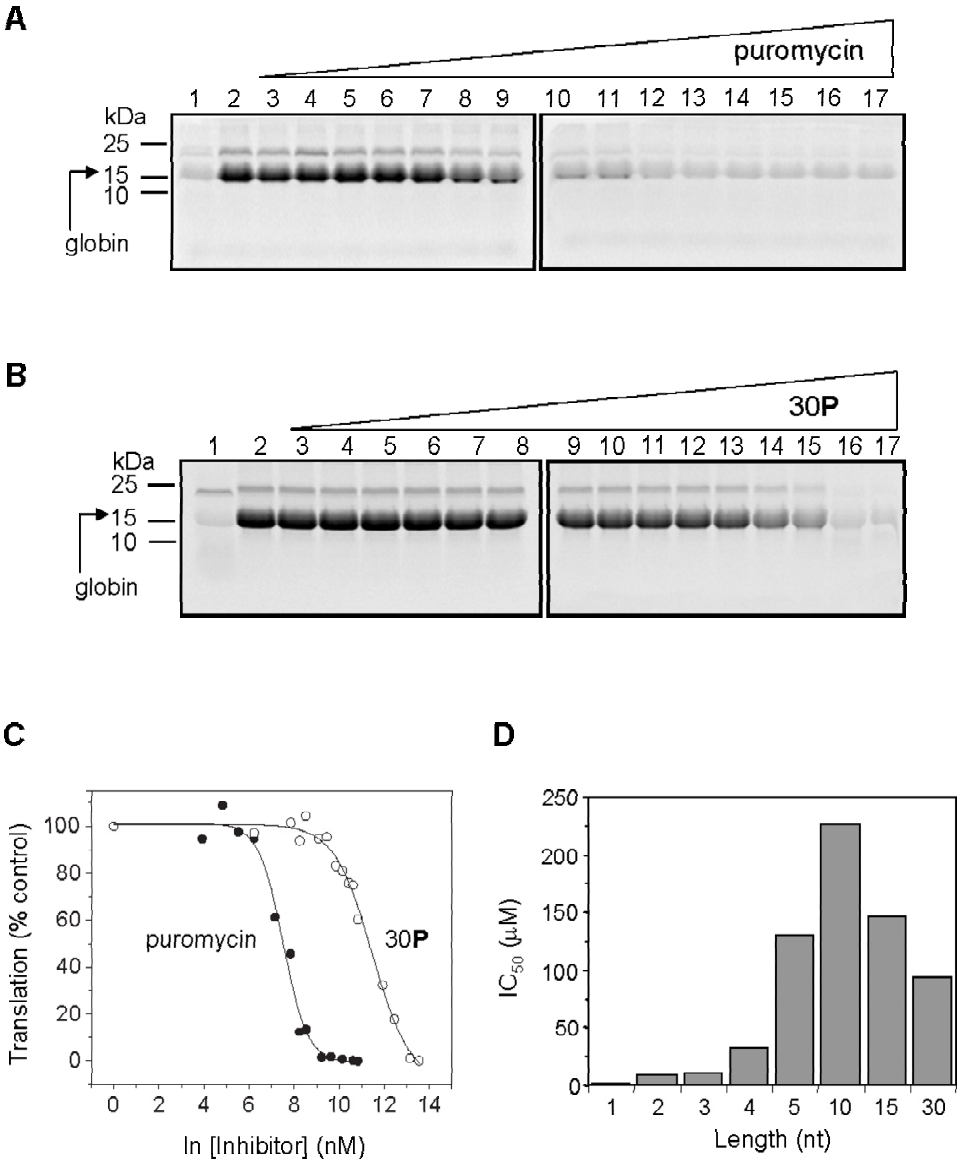

Figure 2.2: IC_{50} determinations for puromycin and 30**P**. (A) Translation of globin with puromycin: lane 1, no template; lane 2, globin alone; lanes 3 – 17, concentrations from 0.025 to 75 μM. (B) Translation of globin with 30**P**: lane 1, no template; lane 2, globin alone; lanes 3 – 16, 0.5 to 750 μM. (C) Percent of globin translation relative to a no-drug control for puromycin (•) and 30**P** (○). (D) Effect of chain length on IC_{50} values for puromycin and simple puromycin-oligonucleotide conjugates.

Inhibitor	IC_{50} (μM)
Linear Conjugates	
Puromycin (**P**)	1.8
r2**P** (prC-**P**)	9
2**P** (pdC-**P**)	10
3**P** (dCdC-**P**)	11
4**P** (dΛdCdC-**P**)	33
5**P** [$(d\Lambda)_2$dCdC-**P**]	130
10**P** [$(d\Lambda)_7$dCdC-**P**]	230
15**P** [$(d\Lambda)_{12}$dCdC-**P**]	150
30**P** [p$(d\Lambda)_{27}$dCdC-**P**]	94
tRNA Mimics	
RNA 12-**P**	56
Ala-minihelix-**P**	40
Oligonucleotides	
5Λ [$(d\Lambda)_2$dCdCdΛ]	>400
10Λ [$(d\Lambda)_7$dCdCdΛ]	1100
30Λ [$(d\Lambda)_{27}$dCdCdΛ]	>200
Ala-minihelix	83
Puromycin Derivatives	
biotin-puromycin	54
biotin-2**P** [biotin-dC-puromycin]	11
fluorescein-puromycin	120
N-trifluoroacetyl-puromycin	>250

Table 2.1: IC_{50} values for puromycin and puromycin oligonucleotide conjugates.

of the longer 30**P** oligonucleotide showed very weak inhibition with an IC_{50} ~100 μM, more than 50-fold weaker than puromycin (Figure 2.2B,C). In these experiments, the oligonucleotide phosphate concentration is significant compared to the divalent cation concentration in the translation extract (3 mM PO_4^- versus 0.5 mM Mg^{+2}). Indeed, the IC_{50} for an identical oligonucleotide lacking puromycin (30A; Table 2.1) was found to be >200 μM. Therefore, it appears that inhibition from 30**P** occurs from a combination of the action of puromycin as well as the high concentration of oligonucleotide in the translation reaction. This result indicates that the *trans* reaction is likely to be insignificant for mRNA-puromycin conjugates, as these are typically used at 100 nM to 1 μM concentrations (16). Comparing puromycin to 30**P** suggested that increasing the size of the puromycin conjugate decreases its potency. Further, addition of the -dAdCdC- sequence adjacent to puromycin did not enhance its efficacy as an inhibitor.

We therefore constructed a series of puromycin conjugates ranging from 1 to 44 nucleotides to examine these issues in more detail. Regarding size, we constructed a series of puromycin-DNA oligonucleotides with chain lengths of 2 (2**P**), 3 (3**P**), 4 (4**P**), 5 (5**P**), 10 (10**P**), and 15 (15**P**) nucleotides, in addition to puromycin and 30**P** (Table 2.1). Regarding compatibility with the acceptor site, we constructed a riboversion of 2**P** (prC-**P** = r2**P**) and two puromycin-RNA mimics of aa-tRNA. None of these molecules inhibited translation as effectively as puromycin. Generally, the IC_{50} values increase as the chain length is increased (Table 2.1 and Figure 2.2D). For example, addition of one nucleotide decreases the IC_{50} of puromycin by 5-fold (compare puromycin versus 2**P** or r2**P**; Table 2.1). The sugar moiety at the penultimate nucleotide makes little difference as the potency of r2**P** and 2**P** are nearly identical, in line with previous work on the Ac-Phe-tRNA·poly(U)·70S translation system (18). The IC_{50} values increase steadily from chains of one to five nucleotides. Above five nucleotides, puromycin conjugates give similar weak inhibition, with IC_{50} values ranging from 90 to 230 μM. The worst inhibitor is (dA)7dCdC-**P** (10**P**), which has an

IC_{50} value of 230 μM, similar to some oligonucleotides that lack puromycin entirely.

The data present a puzzle as to why the larger oligonucleotides are unable to act as effective inhibitors. The functional portion of all the molecules in the series is identical, the 3'-puromycin moiety. However, the potency of each ranges over more than 100-fold. Generally, the data support a model where size is a critical feature, suggesting that larger molecules are poor inhibitors due to difficulty entering the ribosome. Large molecules such as 30**P** are thus unable to enter the ribosome readily in a passive fashion. This hypothesis poses a problem since aa-tRNAs ranging from 75 to 90 nucleotides efficiently act as substrates in protein synthesis. However, aa-tRNAs enter the ribosome as a ternary complex with elongation factor (EF-Tu in bacteria and eEF1A in eukaryotes) and GTP.

We therefore tested whether puromycin conjugates that resembled aa-tRNAs would have greater efficacy as inhibitors. Previously, two alanylated $tRNA^{Ala}$-derived RNAs (denoted RNA 12 and Ala-minihelix) have been shown to bind bacterial EF-Tu with nanomolar affinity ($K_d = 4.5 - 29$ nM) (24). In addition, the Ala-minihelix has been shown to be as effective as Ala-$tRNA^{Ala}$ as an acceptor substrate in the bacterial fragment reaction (25). We constructed two puromycin-minihelix analogs of these sequences, RNA 12-**P** and Ala-minihelix-**P** (Figure 2.5), and examined their activity in our translation assay. Both RNA 12-**P** and Ala-minihelix-**P** are modest inhibitors of translation with IC_{50} values of 56 and 40 μM, respectively (Table 2.1). These values are more than 20-fold weaker than puromycin, but they are better than the longer oligonucleotide conjugates 10**P** and 30**P** by 2- to 4-fold, respectively. Interestingly, an Ala-minihelix lacking puromycin entirely (Ala-minihelix with 3'-adenosine), (Table 2.1) gave an IC_{50} of 83 μM, much better than any of the other simple oligonucleotides tested.

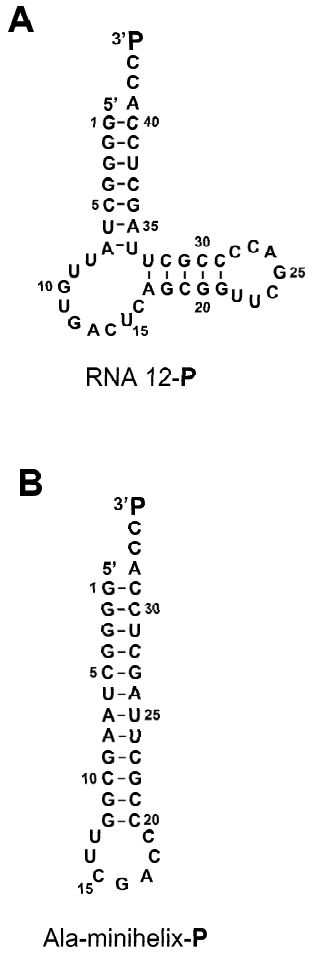

Figure 2.3: Secondary structure of tRNΛ mimics containing puromycin. Both (Λ) RNΛ 12-**P** and (B) Λla-minihelix-**P** were derived from *E. coli* $\text{tRN}\Lambda^{\Lambda\text{la}}$ (24).

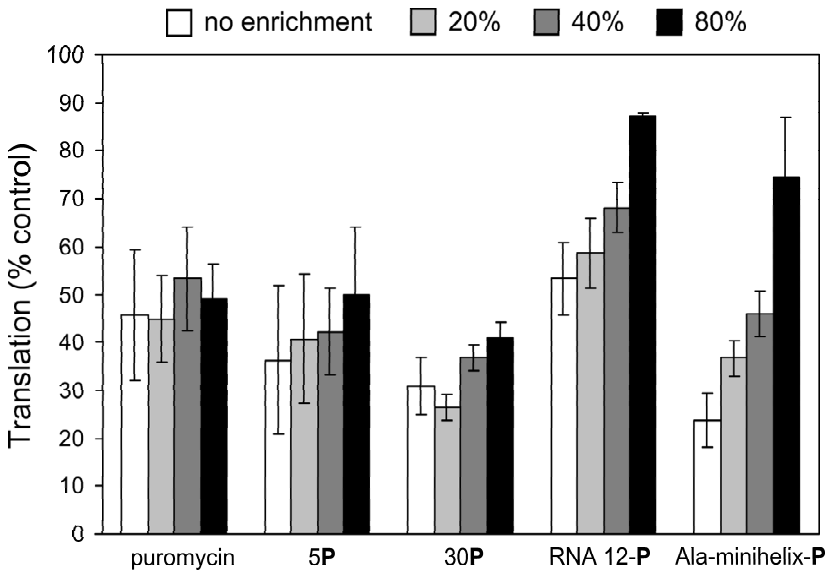

Figure 2.4: Effect of ribosome-depleted lysate on puromycin oligonucleotide-inhibited translation reactions. Addition of ribosome-depleted lysate does not change the amount of globin product significantly for reactions inhibited by puromycin, 5**P**, or 30**P**, but restores translation for both RNA 12-**P** and Ala-minihelix-**P**. The percent enrichment is given by the ratio of ribosome-depleted lysate to native lysate used in the reaction. The drug concentrations for each reaction are puromycin (3.8 μM), 5**P** (76 μM), 30**P** (56 μM), RNA 12-**P** (46 μM), and Ala-minihelix-**P** (46 μM). The values (mean $\pm$ S.E.) are the percent of translation compared to an untreated control.

2.2.3 Elongation Factor Dependence

The relatively strong inhibition by the puromycin-free Ala-minihelix implied that these compounds might inhibit translation by sequestering soluble translation factors. We generated a ribosome-depleted lysate (see Experimental Procedures) to test the role of soluble translation factors on the function of RNA 12-**P**, Ala-minihelix-**P**, and other puromycin conjugates. We added this ribosome-depleted fraction back to our normal translation reactions and assayed the translation of globin. If inhibitors act by sequestering soluble translation factors, then translation should be at least partially restored if more factors are added to the lysate. Inhibitors that work in a factor-independent fashion should be unaffected and inhibitors that require translation factors should become more potent.

Increasing amounts of ribosome-free lysate (relative to the amount of native lysate) had little or no effect on puromycin, 5**P**, or the 30**P** conjugates within experimental error (Figure 2.4). However, the added extract helped to recover translation in the presence of RNA 12-**P** and Ala-minihelix-**P** (Figure 2.4). At the highest level of enrichment (80%), translation was restored 34% and 50% in the presence of RNA 12-**P** and Ala-minihelix-**P**, respectively. This is a notable response since the extent of translation was fairly constant for puromycin, 5**P**, and 30**P** despite the increasing amounts of ribosome-depleted lysate. These results are consistent with a model where RNA 12-**P** and Ala-minihelix-**P** act by sequestering translation factors. These data also present the first clear evidence that puromycin and simple puromycin conjugates function in a translation factor-independent fashion in an intact translation system. The most likely candidate for interaction with the aminoacyl-tRNA^{Ala} mimics, RNA 12-**P** and Ala-minihelix-**P**, is elongation factor 1A (eEF1A). Both Ala-tRNA^{Ala}-derivatives, RNA 12 and Ala-minihelix, bind eEF1A with low nanomolar affinity ($K_d = 29$ and 84 nM, respectively). The three differences between these compounds and our analogs are 1) the amide linkage attaching the amino acid to the ribose, 2) the *O*-methyl tyrosine sidechain, and 3) the N6-dimethyl moiety. The sidechain likely has little effect

on elongation factor binding as many unnatural hydrophobic amino acids may be inserted into proteins in both bacteria (26) and in eukaryotes (27). The amide linkage and N6-dimethyl adenosine in our tRNA mimics may result in somewhat reduced affinity for the elongation factor (28).

We presently favor a model where RNA 12-**P** and Ala-minihelix-**P** act by sequestering eEF1A for two reasons: 1) inhibition occurs as the concentration of RNA-12-**P** or Ala-minihelix-**P** becomes comparable to the endogenous eEF1A concentration ($\sim$20 μM) and 2) this concentration is approximately 1000-fold higher than the reported K_ds for the Ala-RNA 12 and Ala-minihelix with eEF1A (29, 24). In this scenario, addition of minihelix titrates away the available pool of elongation factor until translation is entirely shutdown.

2.2.4 Product Distribution

The IC_{50} analysis using short tricine-SDS-PAGE gels revealed a lack of low molecular weight protein products for puromycin or any of the puromycin derivatives (Figure 2.2). These observations were somewhat unexpected, as it seemed puromycin should be able to enter the ribosome and become attached to the nascent chain at any time during elongation (2, 3). We were therefore curious 1) if puromycin entry occurred to a significant extent and 2) if our various conjugates differed in their ability to enter the ribosome.

We first analyzed the extent and distribution of products by constructing biotinylated versions of several puromycin conjugates. The four biotinylated puromycin conjugates tested include 1) biotin-puromycin, 2) biotin-dC-**P** (biotin-2**P**), 3) biotin-RNA 12-**P** (biotin-dT at position 11; see Figure 2.5) and 4) biotin-Ala-minihelix-**P** (biotin-dT at position 13; see Figure 2.5). We reasoned that any [^{35}S]Met-labeled peptide that became attached to these analogs, from one amino acid (initiator [^{35}S]Met) to full-length globin, could be easily detected by purification on streptavidin or monomeric avidin (see Experimental Procedures) followed by scintillation counting

or SDS-PAGE analysis.

Two of the derivatives, biotin-2**P** (Figure 2.5A,B) and biotin-RNA 12-**P** (data not shown), retain essentially the same IC_{50} as their parent compounds. However, these two biotin conjugates appear to act in decidedly different ways. Purification on streptavidin showed that [^{35}S]Met is not incorporated into biotin-RNA 12-**P**, indicating that this compound does not participate in peptide bond formation despite the fact that it can act as an inhibitor (data not shown). Our assay does not address whether the RNA 12-**P**·eEF1A·GTP ternary complex makes its way to the ribosome and is subsequently rejected during ribosomal substrate proofreading.

Biotin-2**P** is attached to significant amounts of nascent peptide (Figure 2.5C). This attachment occurs in a concentration dependent fashion, with a maximum at 35 μM of the conjugate. Even under optimal conditions, the amount of protein that is attached to puromycin is less than 40% of the total amount of protein made in the absence of drug (TCA precipitated globin) (Figure 2.5C). High-resolution tricine-SDS-PAGE analysis further supports these observations as lower molecular weight products are observed with puromycin and 5**P**, but not with RNA 12-**P** despite nearly complete inhibition of globin synthesis (data not shown).

The attachment of biotin-2**P** to the nascent peptide provided an excellent means to determine where puromycin entered the ribosome during elongation. After translation in the presence of biotin-2**P**, we purified the [^{35}S]Met-adducts using monomeric avidin-agarose (Pierce) (K_d, biotin = 10^{-8} M), released the products, and analyzed the fragments by tricine-SDS-PAGE. This gel identifies three discrete product bands (Figure 2.6). The highest molecular weight band is close to the full-length material (α-globin = 15.5 kDa and β-globin = 16 kDa), whereas the lower molecular weight bands appear to correspond to globin fragments of approximately 6 and 13 kDa (Figure 2.6). Biotin-2**P** concentrations up to 35 μM provide a concomitant increase in the amount of globin-biotin-2**P** complex (Figure 2.6A). Increasing concentrations also shift the product distributions of the three protein bands. Between 0.7 and 35 μM,

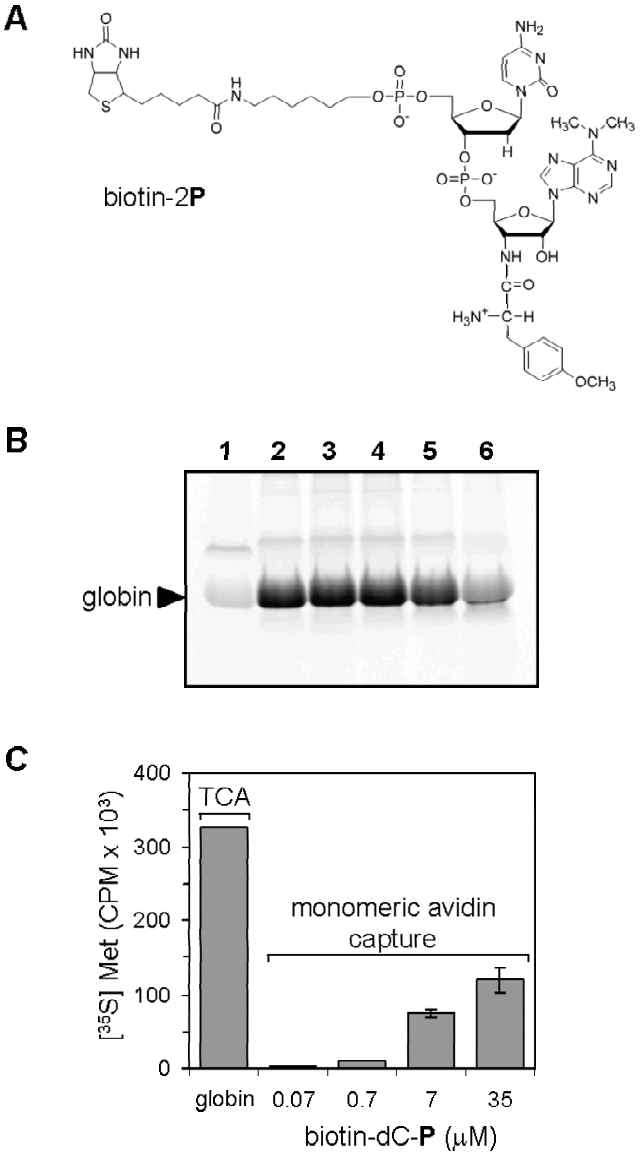

Figure 2.5: Translation inhibition and product formation for biotin-2**P**. (A) Structure of biotin-2**P**. (B) Translation inhibition with increasing amounts of biotin-2**P** assayed by tricine-SDS-PAGE: Lane 1, no globin and no biotin-2**P**; lane 2, globin alone; lane 3, 0.07 μM; lane 4, 0.7 μM; lane 5, 7.0 μM; and lane 6, 35 μM. (C) Isolation of [^{35}S]Met-labeled fragments linked to biotin-2**P** from reactions in (B) assayed by monoavidin capture.

the amount of the 6 and 13 kDa bands increases relative to the full-length product (Figure 2.6B). At 0.7 μM biotin-2**P**, the full-length product constitutes ~50% of the total counts, whereas at 35 μM, the 6, 13, and full-length bands have nearly equal intensity. The shift to lower molecular weight biotin-2**P**-globin fragments is fully consistent with increased ribosome entry at high drug concentrations.

It is important to note that quantification of protein-puromycin complexes in our assay is dependent on the presence of the [^{35}S]Met-label within the complex. However, initiator [^{35}S]Met is readily removed by a methionine aminopeptidase (MetAP) (30). Therefore, short peptide-puromycin complexes without the internal methionine (internal methionine is residue 32 in α-globin and 55 in β-globin) may not be detected in our radioassays. An exception to this is [^{35}S]Met-puromycin, which is not recognized by degradation machinery in reticulocyte lysate. Other than MetAP, no other degradation activity is expected to occur with our products (30).

Interestingly, neither biotin-puromycin (IC_{50} = 54 μM; Table 2.1) nor biotin-Ala-minihelix-**P** (data not shown) function efficiently as translation inhibitors, indicating that attachment of biotin interferes with their function. Addition of biotin to Ala-minihelix-**P** may block elongation factor binding and relieve eEF1A-mediated inhibition. The poor function for biotin-puromycin is more puzzling. Addition of the 5'-biotin-phosphate moiety to puromycin may interfere with A-site binding. In line with this observation, fluorescein-puromycin (5'-fluorescein-phosphate moiety) also functions very poorly as a translation inhibitor, with an IC_{50} of 120 μM (Table 2.1). Whatever the origin, the poor potency of 5'-biotin-puromycin and 5'-fluorescein-puromycin provide a clear design constraint, namely that fluorescent and affinity tag labels should be appended to 5'-end of a dC-**P** or rC-**P** dinucleotide to maximize their incorporation into nascent chains.

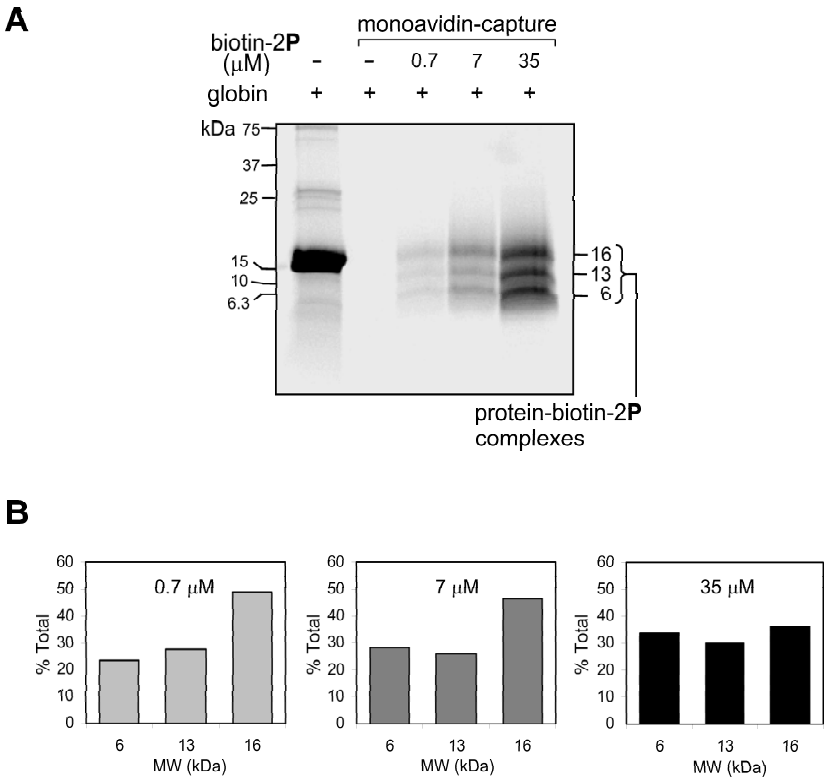

Figure 2.6: Analysis and quantitation of globin fragments attached to biotin-2**P** after translation. (A) High-resolution tricine-SDS-PAGE analysis of fragments bound to biotin-2**P**. Fragments were captured after translation with monomeric avidin, released and analyzed (see Experimental Procedures). Three distinct globin products are seen with approximate molecular weights of 6, 13, and 16 kDa. Increasing concentrations of drug results in an increasing amount of biotin-2**P**-bound product. (B) Ratio of [^{35}S]Met counts in 6, 13 and 16 kDa bands. As the biotin-2**P** concentration is increased, the product distribution shifts toward the lower molecular weight fragments. Fragments ~32 (α-globin) and ~55 amino acids (β-globin) may not be seen since the [^{35}S]Met-label is not present (see Conclusions).

2.2.5 Puromycin Entry At Ribosome Pause Sites

The monomeric avidin capture experiments demonstrate that three [^{35}S]Met-puromycin-containing protein fragments are generated using biotin-2**P**. These data indicate that puromycin entry occurs preferentially at relatively few positions. Mechanistically, these preferences could occur if 1) ribosomes were paused at these sites or 2) these positions were hyper-reactive to puromycin. Our results cannot distinguish these two models, but there is presently no data to indicate that certain codons are hyper-reactive to puromycin.

In contrast, there is support for pausing at discrete locations within the message (31). Wolin and Walter found that eukaryotic ribosomes (wheat or rabbit) pause at two internal positions (on glycine residues 77 and 159) and at the start and terminus of the preprolactin mRNA (31). In our sequences, β-globin contains glycines at positions 47 and 120, and α-globin contains glycine at position 52 and 60. These glycines could be the source of pausing in our templates. It is not clear why pausing would occur at these positions as opposed to other glycines in the open reading frames, in line with Wolin's and Walter's observations. We note that in β-globin mRNA Gly47 and Gly120 occur in the same sequence context, directly after a phenylalanine residue. Our biotin-capture assay may therefore provide a technically straightforward way to assay discrete ribosome pause sites.

2.2.6 Preincubation and Carboxypeptidase Analysis

Puromycin added at the start of the reaction (at concentrations several-fold higher than the ribosome concentration) may inhibit the formation of an initiation complex by binding in the A- or P-sites and perturb the assembly of an initiation complex. Formation of Met-puromycin or short peptide-puromycin fragments (not bearing the internal [^{35}S]Met) would also be an explanation for the complete loss of translation at high puromycin concentrations. Both of these predictions could not be resolved simply

by SDS-PAGE analysis as carried out in Figure 2.2. Instead, preincubation of lysate reactions with template prior to addition of puromycin could indicate whether A- or P-site binding or some other binding mode predominates. Further, the examination of puromycin potency with template preincubation could clarify whether the production of Met-puromycin or short protein-puromycin complexes is the principal action of puromycin.

We therefore preincubated our translation reactions for 30 seconds, 1 minute, or 5 minutes prior to addition of biotin-2**P**, and determined the IC_{50} and product distributions. Reaction products were purified on streptavidin-agarose and quantitated by scintillation counting (see Experimental Procedures). Reactions with biotin-2**P** concentrations <35 μM for all preincubation times indicate that the amount of both free and bound globin remains nearly unchanged (compare no preincubation with 1 min preincubation, Figure 2.7A,B). We observe nearly equivalent IC_{50} values for biotin-2**P** whether biotin-2**P** is added at the beginning of translation (IC_{50} = 11 μM) or after translation has had time to commence on all templates (IC_{50} = 16 μM). This suggests that inhibition results from biotin-2**P** occupation of regions not sensitive to initiation complex formation and/or a mechanism that inhibits ribosome recycling. The observation that maximum complex formation occurs at ~35 μM concentration is qualitatively similar to the concentration optimum of 20 μM for crosslinking, obtained with 4-thioT-rC-puromycin on bacterial ribosomes (8).

At very high drug concentrations (e.g., 140 μM), one and five minute preincubations result in a 4- to 5-fold increase in the amount of globin attached to biotin-2**P**, respectively (Figure 2.7B, 5 min preincubation not shown). The increase in biotin-2**P**-globin products likely represents the fraction of templates that initiate translation in the first 1 to 5 minutes. The large excess of biotin-2**P** present then results in attachment of the drug to the majority of the nascent chains. Further rounds of translation are possibly arrested by biotin-2**P** blocking initiation, inhibition of ribosome recycling, or inactivation of 60S subunits from obstruction of the exit tunnel

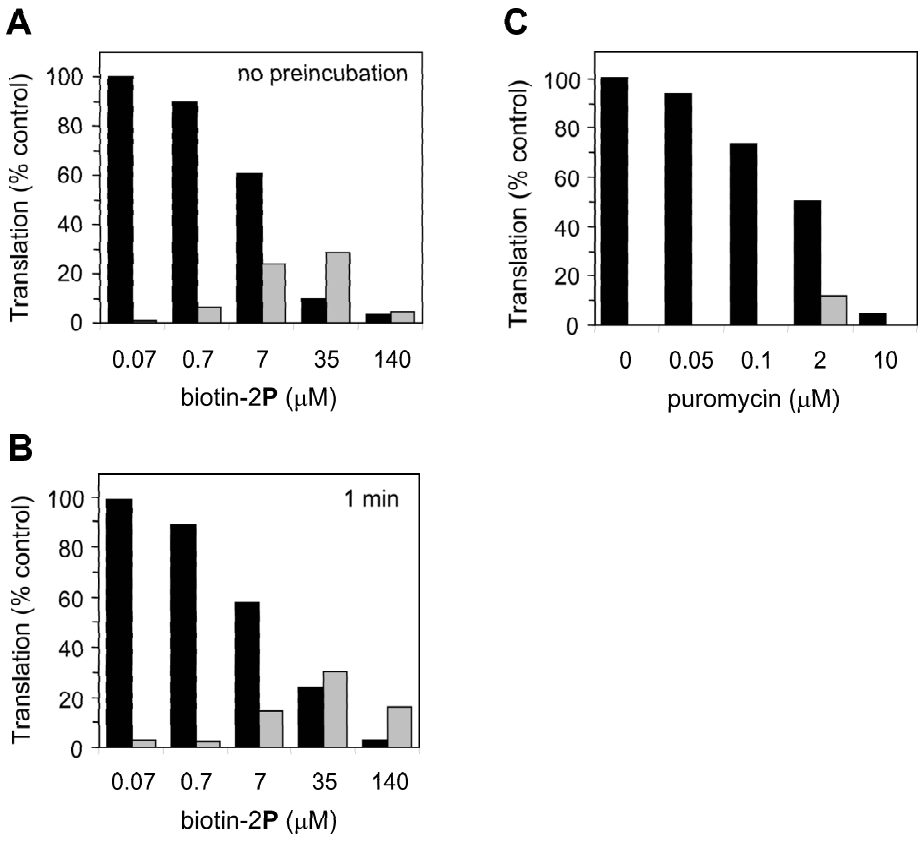

Figure 2.7: Analysis of puromycin-conjugated globin 1) by streptavidin-capture of biotin-2**P** and 2) carboxypeptidase Y treatment. Translation reactions were preincubated at 30 °C for (A) 0 min and (B) 1 min prior to addition of biotin-2**P**. The inhibition profiles for all cases, given by the globin translation (black bar), are the same within experimental error. The amount of globin fragment attached to biotin-2**P** (grey bar) increases only for the high concentration sample (140 μM). (C) Globin fragments containing a C-terminal puromycin are carboxypeptidase Y-resistant. Graph of the total globin made (black bar) and carboxypeptidase Y-resistant globin (grey bar) as a function of puromycin concentrations. The synthesis of puromycin-reacted globin products show an optimum at $\sim$2 μM of puromycin.

with peptide-puromycin- oligonucleotide conjugates.

Our data do not support the notion that the majority of inhibition results from production of Met-puromycin, since preincubation has little effect on the amount of [^{35}S]Met material isolated. Additionally, no Met-puromycin is detected in lysate reactions using the cation-exchange TLC assay developed previously to study the formation of Met-puromycin (22) (data not shown). Finally, we observe no significant shift in the IC_{50} value with preincubation, as would be expected if the majority of puromycin entry occurred in the first few codons. Overall, these analyses are consistent with the conclusion that short peptide-puromycin conjugates are not produced in significant quantity in our reactions.

Another method to identify puromycin-labeled protein is carboxypeptidase analysis, which was originally used to demonstrate puromycin attachment to nascent protein chains (2). After carboxypeptidase Y (CPY) digestion of puromycin-treated translation reactions, very little CPY-resistant protein was detected (Figure 2.7C). Indeed, CPY-resistant protein is detected above the no-drug control only when the drug concentration approaches the IC_{50} value of the compound (2 μM for puromycin). This data confirms that puromycin is able to enter the ribosome and become attached to the nascent protein. However, the amount of CPY-resistant product (12% of the no-drug control) is minimal (Figure 2.7C) and resembles the fraction of globin that becomes attached to biotin-2**P** (Figure 2.7A,B). These experiments further support the multiple-mode hypothesis for puromycin action 1) bonding to the C-terminus of a nascent protein and 2) through a mechanism that does not result in covalent attachment to protein.

2.2.7 Role of the Free Amine

Puromycin is produced by *Streptomyces alboniger* despite its sensitivity to the drug (32). *S. alboniger* inhibits the lethality of the drug by *N*-acetylation of the reactive amino group, thereby eliminating its acceptor activity in protein synthesis (33). We

constructed an *N*-acetylated version of puromycin (*N*-trifluoroacetyl-puromycin) and measured the IC_{50} value to see if this modification eliminated activity of the drug. For example, if the acetylated version could bind the P-site, it might inhibit translation at high concentrations. Our results demonstrate that the *N*-acetylated puromycin molecule is virtually inactive in blocking protein synthesis in reticulocyte lysate (IC_{50} >250 μM) (Table 2.1). The free amine group on puromycin is thus essential for both the peptide-bond dependent and peptide bond-independent action of puromycin.

2.2.8 Revised Model for Puromycin Action: Multiple Modes of Inhibition

Broadly, we observe two modes of puromycin action: 1) a covalent attachment mode and 2) a non-covalent mode. The covalent mode represents the classical activity of puromycin, peptide bonding to the C-terminus of the nascent chain (2, 3). This model implies that the number of moles of globin made in the absence of drug should equal the total moles of free globin plus puromycin-bound globin when the drug is present. Our observations differ from this prediction (Figures 2.5 – 2.8). The non-covalent mode is evident from the summation of free [^{35}S]Met-globin and [^{35}S]Met-globin bound to biotin-2**P**, which does not nearly equal the amount of protein synthesis in a no-drug control at drug concentrations >35 μM (Figure 2.8). The non-covalent mode can be broken down into a combination of multiple effects including 1) inhibition of ribosome recycling, 2) inhibition of an initiation or translation-competent complex, and 3) sequestration of soluble factors (tRNA mimics only) (Figure 2.9). Inhibition of ribosome recycling could result from a combination of events including 1) failure of puromycin-reacted ribosomes to be recognized by the normal recycling apparatus or 2) inactivation of the large subunit from congestion in the exit tunnel/P-site with a peptide-puromycin-oligonucleotide conjugate, preventing further rounds of translation.

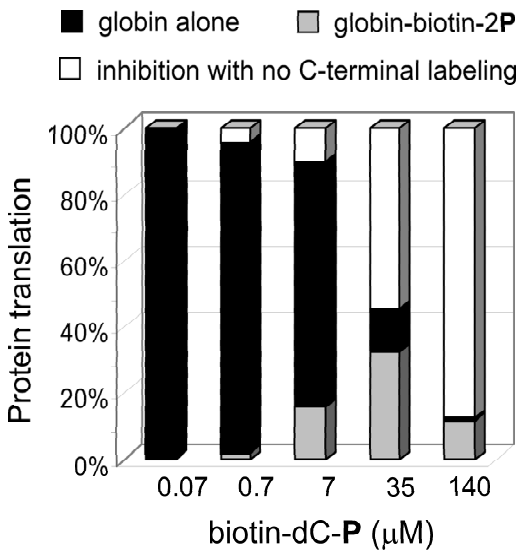

Figure 2.8: Quantitation of free globin, biotin-2**P** conjugated globin, and amount of protein synthesis inhibition. Plot of the amount of globin (black bar), biotin-2**P** conjugated globin (grey bar), and the amount of translation inhibition (white bar) as a function of biotin-2**P** concentration. The free globin protein product falls steadily above 7 μM biotin-2**P**, whereas the amount of puromycin-reacted product shows an optimum around 35 μM of the drug. The sum of the two globin fractions does not equal 100% above 7 μM of biotin-2**P**.

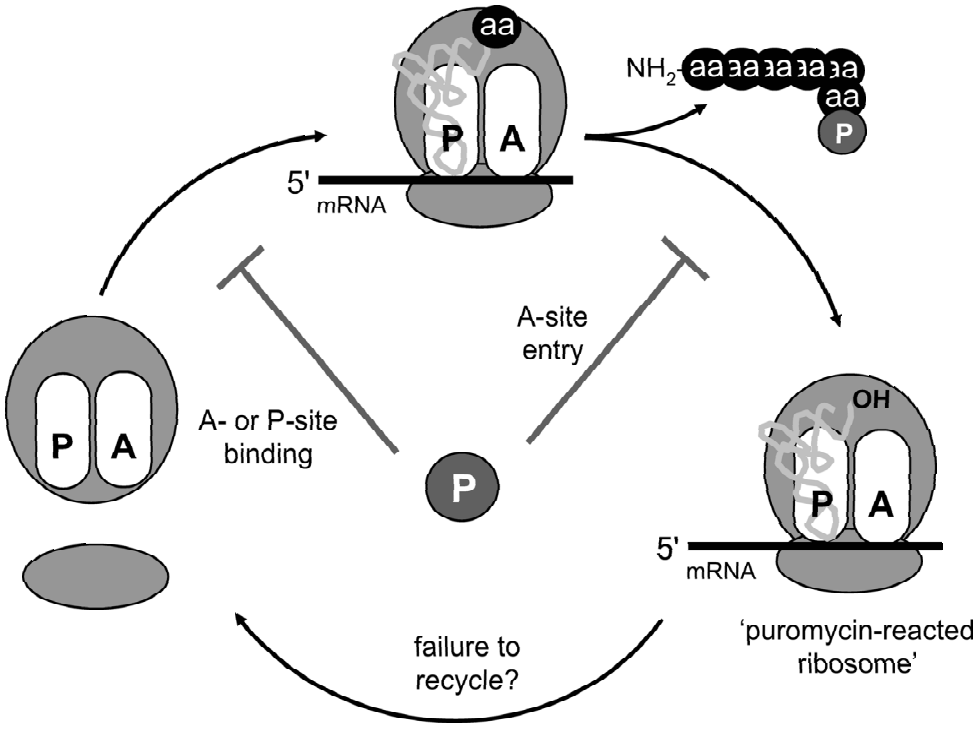

Figure 2.9: Revised model for the action of puromycin-oligonucleotides. Puromycin-oligonucleotides may function in a peptide bond-dependent mode, attaching to the nascent peptide to give puromycin-bound protein products. These same puromycin-oligonucleotides may also act in a peptide bond-independent fashion that represents a composite of different mechanisms including 1) inhibition of translation initiation by binding in the A- or P-sites, 2) inhibition of ribosome recycling, and 3) sequestering soluble translation factors (tRNA mimics only).

2.2.9 Size, Rather than Affinity, Determines Potency of Puromycin Conjugates

We observe that the efficacy of our puromycin conjugates depends primarily on their size, rather than their affinity for the ribosome. Overall, larger derivatives show weaker potency as inhibitors, with some functioning only a few-fold better than oligonucleotides lacking puromycin. This finding is in stark contrast to studies on isolated bacterial 50S subunits. For example, the overall affinity of 2'-(3')-*O*-aminoacyl derivatives of CA is considerably greater than that of the analogous adenosine derivatives. Previous work demonstrates that 4-thio-dT-rC-**P** has a K_m value of 10 μM with bacterial ribosomes (8) as compared with a K_m of 740 μM for puromycin itself (11) under the fragment assay conditions. However, our data show that the 2**P** conjugates (prC-**P** and pdC-**P**) are five times less potent than puromycin (Table 2.1). Certainly this result is not intuitive since the dC (analogous to the penultimate C in tRNA) is expected to Watson-Crick base pair in the A-loop (8, 14) and is therefore expected to be a better acceptor than puromycin alone. The presence of yet another base should contribute to the free energy of stabilization through base stacking in the A-loop (14). Our results demonstrate that addition of another dC to make dCdC-**P** (3**P**) decreases rather than improves the potency of the inhibitor (Table 2.1). Thus, the efficacy of our puromycin conjugates does not show correlation with expected A-site affinity.

The present literature would also predict that adding nucleotides to the 5'-end of our conjugates would have no effect on acceptor activity. This prediction also differs from our observations. For example, CCA-Phe and CACCA-Phe bind equivalently to bacterial ribosomes (34, 35). In contrast, we observe that adding nucleotides beyond dCdC-**P** diminishes the IC_{50} for the conjugates significantly (Table 2.1). For example, addition of dA to give dAdCdC-**P** (4**P**) results in a 3-fold loss of activity relative to 3**P** and a compound that is 18-fold worse than puromycin (Table 2.1).

Our results lead us to conclude that entry into the A-site, rather than affinity

for the ribosome, is the primary determinant of activity in the series of molecules we have investigated. Puromycin-conjugate function apparently is determined by how efficiently they are able to enter or leak into the ribosome. The path puromycin conjugates must traverse to act as substrates appears to allow only relatively small molecules to enter in a factor-independent fashion.

2.3 Conclusions

Our experiments demonstrate that puromycin and its derivatives may inhibit translation in multiple ways. First, small puromycin derivatives can enter the peptidyl transferase center and become attached to the nascent protein chain in a factor-independent fashion. Derivatives that resemble tRNA can inhibit translation by sequestering soluble factors, likely eEF1A. Puromycin attachment occurs predominantly at discrete locations within the template and near the end of the open reading frame. Second, our data indicate that puromycin can function in a peptide bond-independent mode. This inhibition is likely due to a combination of puromycin binding that blocks initiation, failure of ribosomes to recycle properly, or some other non-productive mode.

Our results have both practical and broader implications. First, these data should aid in the design and testing of efficient peptidyl transferase inhibitors as well as the synthesis of protein-puromycin conjugates *in vitro*. Entry of biotin-2**P** at discrete locations along the message may provide a fast, simple means to assay translational pausing within a particular template. Biotin-2**P** may also find use in cellular labeling experiments, to tag portions of cells that are actively synthesizing proteins for fluorescence *in situ* detection (B. Hay, personal communication). Finally, our data demonstrate striking differences in peptidyl transferase inhibitor potency when minimal translation systems are compared to those that are physiologically more complete.

2.4 Experimental Procedures

2.4.1 Reagents

Puromycin hydrochloride and d-biotin were obtained from Sigma Chemical Co. (St. Louis, MO). Rabbit reticulocyte Red Nova lysate was purchased from Novagen (Madison, WI). Rabbit globin mRNA was obtained from Life Technologies Gibco BRL (Rockville, MD) and Novagen (Madison, WI). L-[^{35}S]methionine ([^{35}S]Met) (1175 Ci/mmol) was obtained from NEN Life Science Products (Boston, MA). Carboxypeptidase Y and Immunopure immobilized monomeric avidin and streptavidin-agarose were from Pierce (Rockford, IL). GF/A glass microfiber filters were from Whatman. Polygram IONEX-25 SA-Na cation exchange TLC plates were purchased from Alltech (Deerfield, IL). Microcon YM-3 (3,000 MW cutoff) centrifugal filter columns were obtained from Millipore (Bedford, MA).

2.4.2 Oligonucleotides

RNA and DNA oligonucleotides and puromycin-oligonucleotide conjugates were synthesized using standard phosphoramidite chemistry at the California Institute of Technology oligonucleotide synthesis facility. Puromycin-CPG was obtained from Glen Research (Sterling, VA). Oligonucleotides were synthesized with the 5'-trityl intact, desalted via OPC cartridge chromatography (Glen Research) (DNA oligonucleotides only), cleaved, and evaporated to dryness. 5'-Biotin phosphoramidite and biotin-dT (Glen Research) were used to make the biotin-puromycin conjugates. The dried samples were resuspended and desalted by sephadex chromatography. The puromycin-oligonucleotides pC-**P** (r2**P**), pdC-**P** (2**P**), biotin-dC-**P** (biotin-2**P**), dCdC-**P** (3**P**), dAdCdC-**P** (4**P**), and $(dA)_2$dCdC-**P** (5**P**) were desalted on Sephadex G-10 (Sigma), all others were desalted on Sephadex G-25 (Sigma). Urea PAGE analysis confirmed that each oligonucleotide was a single species. Short oligonucleotides display anomalously slow electrophoretic mobility due to the positively charged puromycin.

The RNA r2**P** was deprotected with 1 M tetrabutylammonium fluoride (TBAF) in tetrahydrofuran (THF) (Aldrich) according to the method described in (36) and purified to homogeneity using HPLC with a Dionex DNAPac PA-100 semi-preparative column (9 x 250 mm) with buffer A (10 mM NH_4OAc (pH 5.5) + 10% acetonitrile) and buffer B (200 mM NH_4OAc (pH 5.5) + 10% acetonitrile); a linear gradient of 90% buffer B in 20 min was used with a flow rate of 1.5 mL/min. The RNAs Ala-minihelix-**P** and RNA 12-**P** (including biotinylated-derivatives) were deprotected with *N*-methylpyrrolidinone (Aldrich), anhydrous triethylamine (Aldrich), and anhydrous triethylamine-hydrogen fluoride (Aldrich) as described in (37) and purified by 20% denaturing PAGE. Puromycin and puromycin-oligonucleotides concentrations were determined with the following extinction coefficients ($M^{-1}cm^{-1}$) at 260 nm: puromycin (ϵ = 11,790), r2**P** (ϵ = 18,920), d2**P** (ϵ = 19,100), 3**P** (ϵ = 26,210), 4**P** (ϵ = 41,200), 5**P** (ϵ = 52,200), 10**P** (ϵ = 112,200), 15**P** (ϵ = 172,200), 30**P** (ϵ = 352,200), Ala-minihelix-**P** (ϵ = 324,100), and RNA 12-**P** (ϵ = 409,700).

2.4.3 IC_{50} Determination

Translation reactions containing [^{35}S]Met were mixed in batch on ice and added in aliquots to microcentrifuge tubes containing an appropriate amount of puromycin, puromycin-conjugate, or oligonucleotide dried in vacuo. Typically, a 20 μl translation mixture consisted of 0.8 μL of 2.5 M KCl, 0.4 μL of 25 mM MgOAc, 1.6 μL of 12.5X translation mixture without methionine, (25 mM dithiothreitol (DTT), 250 mM HEPES (pH 7.6), 100 mM creatine phosphate, and 312.5 μM of 19 amino acids, except methionine) (Novagen), 3.6 μL of nuclease-free water, 0.6 μL (6.1 μCi) of [^{35}S]Met (1175 Ci/mmol), 8 μL of Red Nova nuclease-treated lysate (Novagen), and 5 μL of 0.05 μg/μL globin mRNA (Gibco). Inhibitor, lysate preparation (including all components except template), and globin mRNA were mixed simultaneously and incubated at 30 °C for 60 min. For some assays (e.g., detection of small protein fragments and biotin-capture experiments, see below) the amount of [^{35}S]Met (1175

Ci/mmol) in a 20 μL reaction was increased to 4.2 μL (43 μCi) and no nuclease-free water was added. Then 2 μL of each reaction was combined with 8 μL of tricine loading buffer (80 mM Tris-Cl (pH 6.8), 200 mM DTT, 24% (v/v) glycerol, 8% sodium dodecyl sulfate (SDS), and 0.02% (w/v) Coomassie blue G-250), heated to 90 °C for 5 min, and applied entirely to a 4% stacking portion of a 16% tricine-SDS-polyacrylamide gel containing 20% (v/v) glycerol (19) (30 mA for 1h, 30 min). Gels were fixed in 10% acetic acid (v/v) and 50% (v/v) methanol, dried, exposed overnight on a PhosphorImager screen, and analyzed using a Storm PhosphorImager (Molecular Dynamics). IC_{50} determination for N-trifluoroacetyl-puromycin was conducted as above except the inhibitor was initially dissolved in dimethyl sulfoxide (DMSO) and the final DMSO concentration in each translation reaction was 5% (v/v). Fluorescein-puromycin (dissolved in 3 mM Na_2CO_3/$NaHCO_3$) was added in aliquots to lysate preparations as described above, except 1 μL of 0.25 μg/μL globin mRNA (Novagen) and additional nuclease-treated water was used in each 20 μL reaction.

2.4.4 Lysate Enrichment Assay

Ribosome-depleted rabbit reticulocyte lysate was prepared by ultracentrifugation of 80 μL/rotor tube of Red Nova lysate at 95,000 RPM for 30 min at 4 °C in a Beckman Airfuge Ultracentrifuge (A-100 rotor with 5 x 20 mm tubes). Lysate preparation (15 μL) and template (5 μL of 0.05 μg/μL globin mRNA) were mixed simultaneously in microcentrifuge tubes containing puromycin and puromycin-oligonucleotides dried *in vacuo*. A typical 20 μL reaction mixture contained the following: 0.8 μL of 2.5 M KCl, 0.4 μL of 25 mM MgOAc, 1.6 μL of 12.5X Translation Mixture without methionine, 0.6 μL of [^{35}S]Met (1175 Ci/mmol), 6.8 μL of Red Nova nuclease-treated lysate plus 0, 1.4, 2.7, or 5.3 μL of ribosome-depleted lysate and 5.3, 4.0, 2.6, or 0 μL of nuclease-free water for 0, 20, 40, and $\sim$ 80% enrichment (relative to the amount of native lysate/reaction), respectively. The samples were analyzed as described above for IC_{50} determination.

2.4.5 TLC Assay for Detection of Met-puromycin

The standard assay as described for IC_{50} determination was carried out except 45 μCi of [^{35}S]Met was used in each translation mix. After incubation, aliquots (1 μL) were spotted onto Polygram IONEX-25 SA-Na cation exchange TLC plates (9 X 11 cm) and developed in 2 M ammonium acetate (pH 5.2) plus 10% acetonitrile as described in (22). The plates were dried, exposed overnight on a PhosphorImager screen, and analyzed on a Storm PhosphoImager. The position of 4**P** was determined through UV-shadow of the sample TLC plate and the position of [^{35}S]Met-tRNA is assumed from an equivalent experiment described in (22).

2.4.6 Monomeric Avidin- and Streptavidin-capture of Biotinylated Puromycin Conjugates

Biotin-RNA 12-**P** (biotin-dT at position 11 in Figure 2.4), biotin-Ala-minihelix-**P** (biotin-dT at position 13 in Figure 2.4), or biotin-2**P** were evaporated to dryness in microcentrifuge tubes followed by simultaneous addition of 15 μL of lysate preparation (components are the same as for IC_{50} determination, but with 43 μCi of [^{35}S]Met/reaction) and 5 μL of 0.05 μg/μL globin mRNA. The reactions were incubated at 30 °C for 60 minutes. For the monoavidin-agarose experiments [50% slurry (v/v)], the high affinity biotin-binding sites were blocked with a solution of 2 mM D-biotin in phosphate buffered saline (PBS) (137 mM NaCl, 2.7 mM KCl, 4.3 mM $Na_2HPO_4 \cdot 7H_2O$, 1.4 mM KH_2PO_4, and 0.1% Triton X-100) followed by removal of D-biotin from low affinity biotin-binding sites using 0.1 M glycine (pH 2.8) (0.1% Triton X-100) according to manufacturer instructions. Typically, 0.6 mL of the monoavidin-agarose 50% slurry (v/v) was pre-blocked as described above, washed 3 times with PBS, and resuspended in 1 mL of PBS. Aliquots of this suspension (125 μL) were combined with 7.5 μL of the reaction lysate mixture and 0.575 mL of PBS for each reaction. The samples were rotated at 4 °C for 1.5 h and then washed with PBS un-

til the CPM of [^{35}S]Met were < 1000 in the wash. The biotin-immobilized molecules were eluted with 2 mM D-biotin in PBS and concentrated to < 20 μL in YM-3 Microcon centrifugal filters. Tricine loading buffer (20 μL) was added to the concentrated samples and applied entirely to a 4/16% tricine-SDS-polyacrylamide gel (30 mA, 5 h). For streptavidin-capture experiments, 0.6 mL of streptavidin-agarose [50% slurry (v/v)] was washed 3 times with PBS and resuspended in 1 mL of PBS. To 100 μL of this suspension, 3 μL of the reaction lysate and 0.4 mL of PBS were added. The samples were rotated at 4 °C for 3 h and washed with PBS until the CPM of [^{35}S]Met were <500 in the wash. The amount of immobilized [^{35}S]Met-protein-puromycin conjugate was determined by scintillation counting of the streptavidin-agarose beads. An incorporation assay was used to determine the amount of globin synthesized (no inhibitor control) in an equivalent volume of lysate. After incubation, 3 μL of the lysate reaction was mixed with 150 μL of 1 N NaOH/2% H_2O_2 and incubated at 37 °C for 10 min to hydrolyze the charged tRNAs. Then 1.35 mL of 25% trichloroacetic acid (TCA)/2% casamino acids was added to the samples, vortexed, and put on ice for 10 min. The samples were filtered on GF/A filters (pre-soaked in 5% TCA), washed 3 times with 4.5 mL of cold 5% TCA, dried under high heat, and scintillation counted to determine the amount of [^{35}S]Met-globin.

2.4.7 Preincubation Assay with Biotin-2P

Lysate preparation (15 μL, prepared as described above with 43 μCi [^{35}S]Met/reaction) and globin mRNA (1 μL of 0.25 μg/μL, Novagen) were preincubated at 30 °C for 0, 1, or 5 min. After addition of biotin-2**P** (3 μL aliquots) and nuclease-free water (1 μL), the reactions were incubated at 30 °C for an additional 60 min. Analysis of the translation reactions via streptavidin-agarose capture was carried out exactly as described above.

2.4.8 Carboxypeptidase Y Assay

Translation reactions were prepared and treated as described for IC_{50} determination (43 μCi [^{35}S]Met/reaction). A portion of each lysate reaction (2.5 μL) was resuspended in 23 μL of 0.1 M sodium acetate (pH 5.0) and carboxypeptidase Y [15 μL of 1 mg/mL in 0.05 M sodium citrate (pH 5.3)] was added followed by incubation at 37 °C for 14 h. After incubation, the samples were concentrated to <5 μL and 10 μL of tricine loading buffer was added. The samples were analyzed using 4/16% tricine-SDS-PAGE as described above.

Acknowledgements

We thank Ms. Jie Xu for synthesis of *N*-trifluoroacetyl-puromycin, and Terry T. Takahashi for comments on this manuscript. This work was supported by NIH Grant R01 GM60416 to R.W.R. and by NIH training grant GM 07616 (S.R.S.).

References

[1] M.B. Yarmolinsky and G. de la Haba. Inhibition by puromycin of amino acid incorporation into protein. *Proc. Natl. Acad. Sci. U.S.A.*, 45:1721–1729, 1959.

[2] D. Nathans. Puromycin inhibition of protein synthesis: incorporation of puromycin into peptide chains. *Proc. Natl. Acad. Sci. U.S.A.*, 51:585–592, 1964.

[3] J.D. Smith, R.R. Traut, G.M. Blackburn, and R.E. Monro. Action of puromycin in polyadenylic acid-directed polylysine synthesis. *J. Mol. Biol.*, 13:617–628, 1965.

[4] RE. Monro and KA. Marcker. Ribosome-catalysed reaction of puromycin with a formylmethionine-containing oligonucleotide. *J. Mol. Biol.*, 25:347–350, 1967.

[5] HF. Noller, V. Hoffarth, and Zimniak L. Unusual resistance of peptidyl transferase to protein extraction procedures. *Science*, 256:1416–1419, 1992.

[6] R.R. Samaha, R. Green, and H.F. Noller. A base pair between tRNA and 23S rRNA in the peptidyl transferase centre of the ribosome. *Nature*, 377:309–314, 1995.

[7] S. Chládek, D. Ringer, and J. Žemlička. L-phenylalanine esters of open-chain analog of adenosine as substrates for ribosomal peptidyl transferase. *Biochemistry*, 12:5135–5138, 1973.

[8] R. Green, C. Switzer, and HF. Noller. Ribosome-catalyzed peptide-bond formation with an A-site substrate covalently linked to the 23S ribosomal RNA. *Science*, 280:286–289, 1998.

[9] M. Michelinaki, P. Namos, C. Coutsogeorgopoulos, and D.L. Kalpaxis. Aminoacyl and peptidyl analogs of chloramphenicol as slow binding inhibitors of ribosomal peptidyltransferase: A new approach for evaluating their potency. *Mol. Pharm.*, 51:139–146, 1996.

[10] O.W. Odom and B. Hardesty. Use of 50S-binding antibiotics to characterize the ribosomal site to which peptidyl-tRNA is bound. *J. Biol. Chem.*, 267:19117–19122, 1992.

[11] M. Welch, J. Chastang, and M. Yarus. An inhibitor of ribosomal peptidyl transferase using transition-state analogy. *Biochemistry*, 34:385–390, 1995.

[12] N. Nemoto, E. Miyamoto-Sato, Y. Husimi, and H. Yanagawa. *In vitro* virus: Bonding of mRNA bearing puromycin at the 3'-terminal end to the C-terminal end of its encoded protein on the ribosome *in vitro*. *FEBS Lett.*, 414:405–408, 1997.

[13] R.W. Roberts and J.W. Szostak. RNA-peptide fusions for the *in vitro* selection of peptides and proteins. *Proc. Natl. Acad. Sci. U.S.A.*, 94:12297–12302, 1997.

[14] P. Nissen, J. Hansen, N. Ban, PB. Moore, and Steitz TA. The structural basis of ribosome activity in peptide bond synthesis. *Science*, 289:920–930, 2000.

[15] E. Miyamoto-Sato, N. Nemoto, K. Kobayashi, and H. Yanagawa. Specific bonding of puromycin to full-length protein at the C-terminus. *Nucleic Acids Res.*, 28:1176–1182, 2000.

[16] R. Liu, J. Barrick, J.W. Szostak, and R.W. Roberts. Optimized synthesis of

RNA-protein fusions for *In Vitro* protein selection. *Methods Enzymol.*, 317:268–293, 2000.

[17] I. Rychlík, S. Chládek, and J. Žemlička. Release of peptide chains from the polylysyl-tRNA ribosome complex. *Biochim. Biophys. Acta*, 138:640–642, 1967.

[18] A. Bhuta, K. Quiggle, T. Ott, D. Ringer, and S. Chládek. Stereochemical control of ribosomal peptidyltransferase reaction. Role of amino acid side-chain orientation of acceptor substrate. *Biochemistry*, 20:8–15, 1981.

[19] H. Schagger and G.V. von Jagow. Tricine-sodium dodecyl sulfate-polyacrylamide gel electrophoresis for the separation of proteins in the range from 1 to 100 kDa. *Anal. Biochem.*, 166:368–379, 1987.

[20] EJ. Hengesh and AJ. Morris. Inhibition of peptide bond formation by cytidyl derivatives of puromycin. *Biochim. Biophys. Acta*, 299:654–661, 1973.

[21] DM. Graifer, OS. Fedorova, and GG. Karpova. Interaction of puromycin with acceptor site of human placenta 80 S ribosomes. *FEBS Lett.*, 277:4–6, 1990.

[22] J.R. Lorsch and D. Herschlag. Kinetic dissection of fundamental processes of eukaryotic translation initiation *in vitro*. *EMBO*, 18:6705–6717, 1999.

[23] A. Fersht. *Enzyme Structure and Mechanism*. W. H. Freeman and Company, New York, 1985.

[24] IA. Nazarenko and OC. Uhlenbeck. Defining a smaller RNA substrate for elongation factor Tu. *Biochemistry*, 34:2545–2552, 1995.

[25] N.Y. Sardesai, R. Green, and P. Schimmel. Efficient 50S ribosome-catalyzed peptide bond synthesis with an aminoacyl minihelix. *Biochemistry*, 38:12080–12088, 1999.

[26] J. Ellman, D. Mendel, S. Anthony-Cahill, CJ. Noren, and PG. Schultz. Biosynthetic method for introducing unnatural amino acids site-specifically into proteins. *Methods Enzymol.*, 202:301–336, 1991.

[27] DA. Dougherty. Unnatural amino acids as probes of protein structure and function. *Curr Opin Chem Biol*, 4:645–652, 2000.

[28] E. Baksht, N. de Groot, M. Sprinzl, and F. Cramer. Properties of tRNA species modified in the 3'-terminal ribose moiety in an eukaryotic ribosomal system. *Biochemistry*, 15:3639–3646, 1976.

[29] TW. Dreher, OC. Uhlenbeck, and KS. Browning. Quantitative assessment of EF-1α·GTP binding to aminoacyl-tRNAs, aminoacyl-viral RNA, and tRNA shows close correspondence to the RNA binding properties of EF-Tu. *J. Biol. Chem.*, 274:666–672, 1999.

[30] A. Varshavsky. The N-end rule: Functions, mysteries, uses. *Proc. Natl. Acad. Sci. U.S.A.*, 93:12142–12149, 1996.

[31] S.L. Wolin and P. Walter. Ribosome pausing and stacking during translation of a eukaryotic mRNA. *EMBO*, 7:3559–3569, 1988.

[32] J.N. Porter, R.I. Hewitt, C.W. Hesseltine, G. Krupka, J.A. Lowery, W.S. Wallace, N. Bohonos, and J.H. Williams. Achromycin: A new antibiotic having trypanocidal properties. *Antibiotics and Chemo.*, 11:409–410, 1952.

[33] J.A. Pérez-González, J. Vara, and A. Jiménez. Acetylation of puromycin by *Streptomyces alboniger* the producing organism. *Biochem. Biophys. Res. Commun.*, 113:772–777, 1983.

[34] P. Bhuta, G. Kumar, and S. Chládek. The peptidyltransferase center of *Escherichia coli* ribosomes: binding sites for the cytidine 3'-phosphate residues of

the aminoacyl-tRNA 3'- terminus and the interrelationships between the acceptor and donor sites. *Biochim. Biophys. Acta*, 696:208–211, 1982.

[35] J.L. Lessard and S. Pestka. Studies on the formation of transfer ribonucleic acid-ribosome complexes. xxiii. chloramphenicol, aminoacyl-oligonucleotides, and *Escherichia coli* ribosomes. *J. Biol. Chem.*, 247:6909–6912, 1972.

[36] N. Usman, K.K. Ogilvie, J.-Y. Jiang, and R.J. Cedergren. The automated chemical synthesis of long oligoribonucleotides using 2'-*O*-silylated ribonucleoside 3'-*O*-phosphoramidites on a controlled-pore glass support: Synthesis of a 43-nucleotide sequence similar to the 3'-half molecule of an *Escherichia coli* formylmethionine tRNA. *J. Am. Chem. Soc.*, 109:7845–7854, 1987.

[37] F. Wincott, A. DiRenzo, C. Shaffer, S. Grimm, D. Tracz, C. Workman, D. Sweedler, C. Gonzalez, S. Scaringe, and N. Usman. Synthesis, deprotection, analysis and purification of RNA and ribozymes. *Nucleic Acids Res.*, 23:2677–2684, 1995.

Chapter 3

A General Approach to Detect Protein Expression *In Vivo* Using Fluorescent Puromycin Conjugates

This chapter has previously appeared as: S.R. Starck, H.M. Green, J. Alberola-Ila, R.W. Roberts. A General Approach to Detect Protein Expression *In Vivo* using fluorescent puromycin conjugates. *Chem. Biol.* In press.

Abstract

Understanding the expression of known and unknown gene products represents one of the key challenges in the post-genomic world. Here, we have developed a new class of reagents to examine protein expression *in vivo* that does not require transfection, radiolabeling, or the prior choice of a candidate gene. To do this, we constructed a series of puromycin conjugates bearing various fluorescent and biotin moieties. These compounds are readily incorporated into expressed protein products in cell lysates *in vitro* and efficiently cross cell membranes to function in protein synthesis *in vivo* as indicated by flow cytometry, selective enrichment studies, and western analysis. Overall, this work demonstrates that fluorescent-puromycin conjugates offer a general

means to examine protein expression *in vivo*.

3.1 Introduction

Complete sequencing of the human genome (1, 2) shows that less than 50% of the putative gene transcripts correspond to known proteins. A complete understanding of the proteome awaits the identification of thousands of unassigned gene products and assignment of their role in signaling cascades (3), membrane trafficking (4), apoptosis (5), and other cellular processes. Currently, there are large-scale techniques to study cellular protein levels indirectly using DNA and mRNA arrays (6). However, these techniques do not directly monitor the level of protein synthesis. Methods to directly monitor protein expression *in vivo* are extremely useful, particularly in the study of higher organisms with many different cell and tissue types.

Currently, protein expression is studied using pulse-labeling with a radioactive tracer or by transformation with fluorescent reporters based on the green fluorescent protein (GFP) and mutants (BFP, CFP, and YFP) (7). Pulse-labeling experiments typically require the cell(s) to be destroyed and are not amenable to microscopy experiments with simultaneous protein synthesis detection. Genetically encoded GFP mutants and fusion proteins have seen broad biological applications including study of Ca^{2+} localization (8) protein tyrosine kinase activity (9), and mRNA trafficking and protein synthesis localization in cultured neurons (10, 11). However, the use of GFP-based constructs is limited to cells that can be efficiently transfected. Additionally, DNA transfection protocols often require several days to produce cells yielding robust GFP-based fluorescent signals and also inundate the protein synthesis machinery with a non-native transcript due to the use of strong upstream promoters. Finally, transfection-based strategies generally require choice of a particular candidate gene product.

We reasoned that puromycin-based reagents might provide a general means to ex-

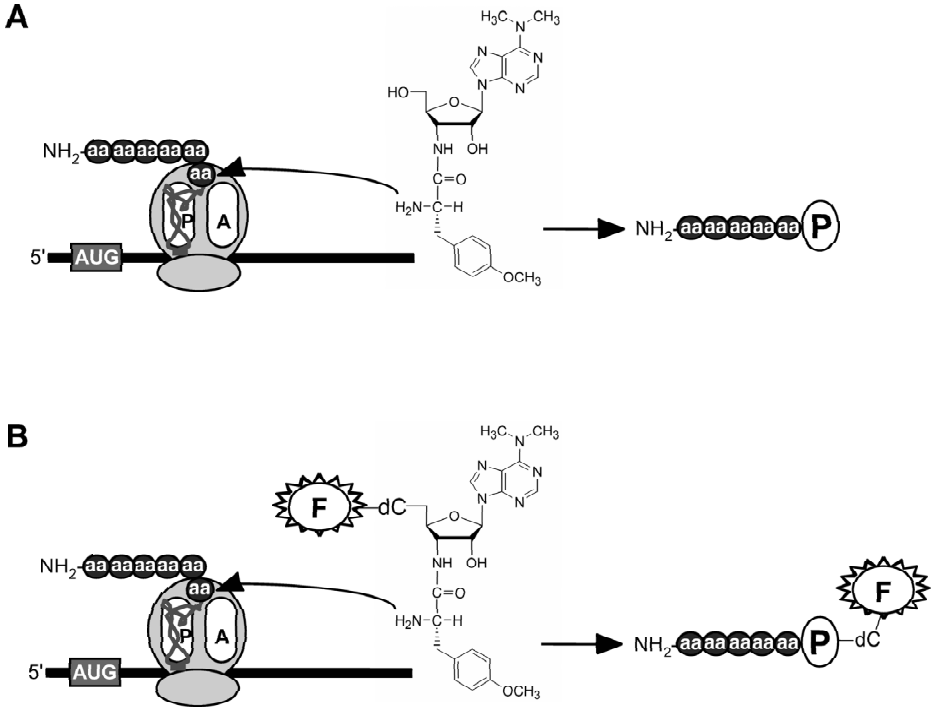

Figure 3.1: (A) Puromycin (**P**) participates in peptide bond formation with the nascent polypeptide chain. (B) Puromycin-dye conjugates, of the form X-dC-puromycin where X = fluorescein (**F**), are also active in translation and become covalently linked to protein.

amine protein expression. Puromycin is a structural analogue of aminoacylated-tRNA (aa-tRNA) and participates in peptide-bond formation with the nascent polypeptide chain (Figure 3.1A) (12, 13). Previously, various puromycin derivatives of the form X-dC-puromycin have been examined and shown to be functional during *in vitro* translation experiments (14, 15, 16, 17). In principle, a fluorescent or biotinylated variant of puromycin should be functional in protein synthesis *in vivo* if it is able to enter cells in a non-destructive fashion (Figure 3.1B). In this way, selective labeling of newly synthesized proteins would enable direct monitoring of protein expression

and provide the potential for both spatial and temporal resolution.

Here, we demonstrate that a variety of puromycin conjugates can be used as detectors of protein synthesis in live cells. This work shows that puromycin conjugates can easily enter cells and covalently label newly synthesized proteins, enabling direct detection of protein expression *in vivo*.

3.2 Results

3.2.1 Design of Puromycin Conjugates

To label newly synthesized proteins, our puromycin conjugates would have to satisfy three general criteria: 1) functionality in peptide bond formation, 2) cell permeability, and 3) ready detection in a cellular or biochemical context. In addressing the first issue, it had been previously shown that puromycin derivatives bearing substitutions directly off the 5'-OH functioned poorly *in vitro* (e.g., biotin-puromycin $IC_{50} = 54\,\mu M$) (17), whereas conjugates with the general form X-dC-puromycin (e.g., biotin-dC-puromycin) were substantially more effective ($IC_{50} = 11\,\mu M$) (17). We therefore chose to design molecules by varying the substituents appended to dC-puromycin (Figure 3.2A).

In order to facilitate cellular entry and detection, we considered a number of factors including 1) type and position of the label, 2) the linker between the label and dC-puromycin, 3) background fluorescence properties, and 4) membrane permeability including net charge and hydrophobicity. We then designed and synthesized various dC-puromycin conjugates to address these issues systematically. The first series of puromycin conjugates (**1**, **3**, **4**, **6**, **8**; Figure 3.2A) either contain fluorescent dyes (compounds **1** and **4**), biotin (compound **6**), or both (compounds **3** and **8**). Two different fluorescent dyes were utilized (Cy_5 and fluorescein) to provide detection at a range of emissions. Biotin labels were introduced to enable detection via western blot analysis or affinity purification. We also prepared a series of compounds (**2**, **5**,

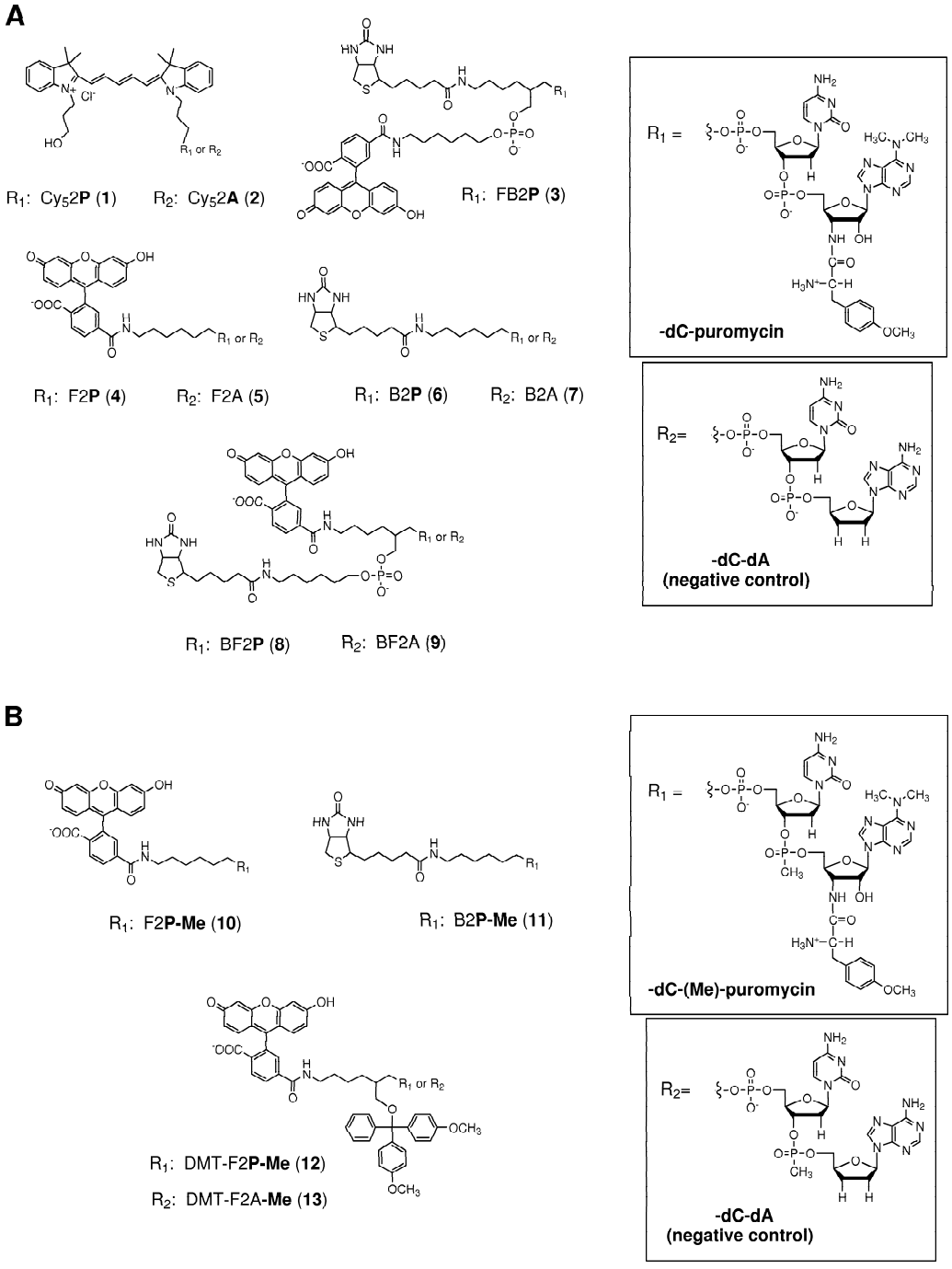

Figure 3.2: (A) Structure of puromycin conjugates and negative control conjugates. (B) Structure of phosphonate-based conjugates.

7, **9**; Figure 3.2A), which lack the 3'-amino acid moiety to serve as negative controls.

A second series of conjugates with a phosphonate linkage between dC and puromycin were prepared to examine whether reduction of charge would enhance cell membrane solubility and facilitate cellular entry (Figure 3.2B). Three compounds (**10**, **11**, **12**; Figure 3.2B) were constructed bearing fluorescein (**10**, F2**P**-Me), biotin (**11**, B2**P**-Me), or the hydrophobic dimethoxytrityl group (DMT) and fluorescein (**12**, DMT-F2**P**-Me). A DMT bearing fluorescein-dC-dA conjugate (DMT-F2A-Me) served as a negative control (**13**; Figure 3.2B). The DMT group was added to gauge whether the addition of a hydrophobic group would further enhance entry into cells.

3.2.2 Analysis of Puromycin-conjugate Activity *In Vitro*

We began our analysis by examining the activity of each of our conjugates *in vitro* for their ability to inhibit protein translation. Previously, we had used this activity assay to measure the IC_{50} for various puromycin conjugates (17) and analogs (18), as well as demonstrate a direct relationship between the IC_{50} and the efficiency of protein labeling (17). Using this approach, we measured IC_{50} values for the compounds in Figure 3.2A and 3.2B (Figure 3.3A). High resolution SDS-tricine gel data corresponding to a typical IC_{50} determination is shown for $Cy_5$2**P** (**1**) and $Cy_5$2A (**2**) (Figure 3.3B). Generally, the activity of conjugates with the form X-dC-puromycin falls over a fairly narrow range *in vitro*, with IC_{50} values ranging from ~4 to ~30 μM (Table 3.1). Also, control conjugates that lack the amino acid moiety, e.g., $Cy_5$2A (**2**) and BF2A (**9**), show little ability to inhibit protein synthesis even at high concentrations.

We next wished to confirm that our puromycin conjugates could become covalently attached to protein *in vitro*. To do this, we translated globin mRNA in the presence of increasing concentrations of FB2**P** (**3**), a conjugate containing fluorescein and biotin moieties (Figure 3.4A). Next, the concentration-dependent incorporation of FB2**P** was analyzed using neutravidin affinity chromatography of these same translation reactions (Figure 3.4B). These data indicate that puromycin conjugates are incorpo-

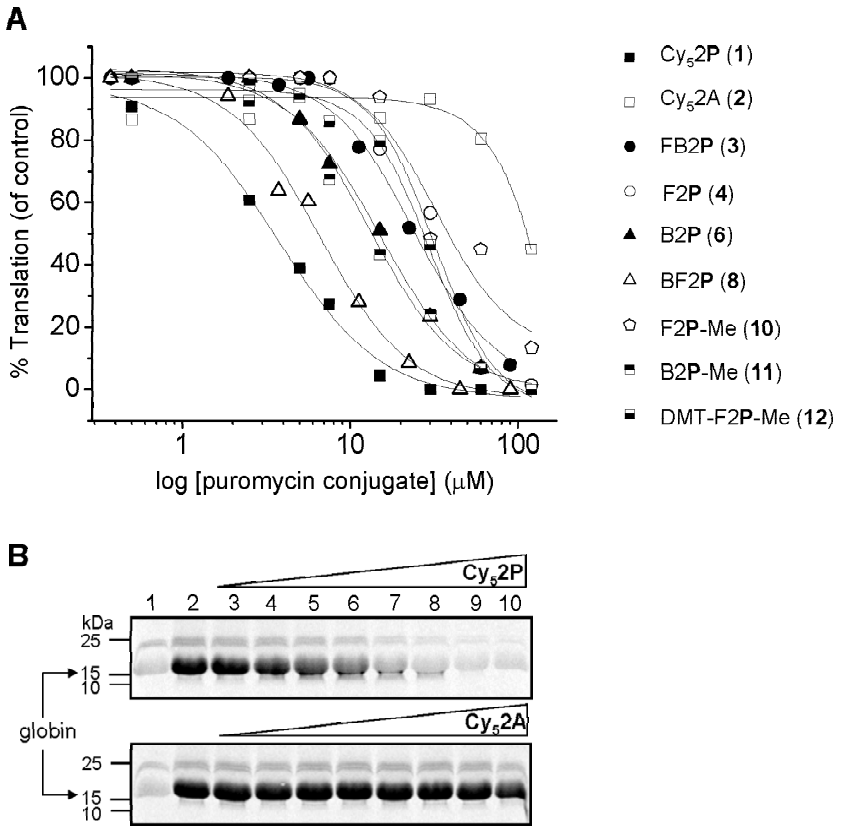

Figure 3.3: *In vitro* IC_{50} determination for puromycin conjugates. (A) Percent of globin translation relative to the no conjugate control for compounds **1**, **2**, **3**, **4**, **6**, **8**, **10**, **11**, **12**. (B) Tricine-SDS-PAGE analysis of globin translation reactions in the presence of $Cy_5$2**P** (**1**) (top) and $Cy_5$2A (**2**) (bottom): Lane 1, no template and no conjugate; lane 2, globin alone; lanes $3-10$, conjugate concentrations from 0.5 to 120 μM.

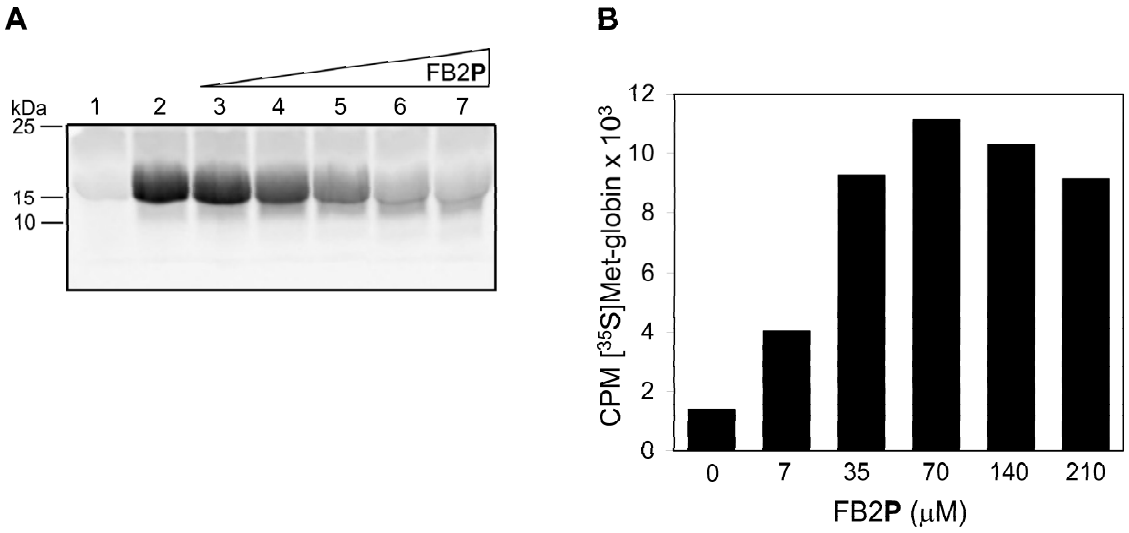

Figure 3.4: Protein labeling with the fluorescent puromycin conjugate FB2P (**3**). (A) Tricine-SDS-PAGE analysis of globin translation reactions incubated with increasing concentrations of **3**: Lane 1, no template, no conjugate; lane 2, globin alone; lane 3, 7 μM; lane 4, 35 μM; lane 5, 70 μM; lane 6, 140 μM; and lane 7, 210 μM. (B) Neutravidin-purified globin-FB2**P** complexes from translation reactions in (A).

Conjugate	IC_{50} (μM)
(**1**) $Cy_5$2**P**	3.8
(**2**) $Cy_5$2A	>100
(**3**) FB2**P**	24
(**4**) F2**P**	22
(**5**) F2**P**-Me	25
(**6**) DMT-F2**P**	29
(**7**) BF2**P**	5.8
(**8**) B2**P**	15
(**9**) B2**P**-Me	16

Table 3.1: The concentration of puromycin conjugate required for 50% inhibition of globin translation (IC_{50}). In replicate experiments, the standard error is <5%).

rated efficiently over a broad concentration range ranging from 2- to 3-fold below the IC_{50} to well above it. Thus labeling is possible even at concentrations where protein synthesis is not greatly inhibited.

These observations support the development of a broad range of puromycin-based reagents for two reasons. First, compounds of the form X-dC-puromycin appear tolerant to a wide variety of substitutions, including molecules containing more than one detection handle (e.g., BF2**P** and FB2**P**). Interestingly, even the methyl phosphonate versions (F2**P**-Me, **10**; B2**P**-Me, **11**; DMT-F2**P**-Me, **12**) showed good levels of *in vitro* activity. Second, the IC_{50} values indicate that even modest concentrations of each of these reagents in the low micromolar range will be sufficient to achieve good levels of protein labeling. This is because our data here (Table 3.1; Figures 3.3 and 3.4) as well as previous data (17, 18), demonstrate that protein labeling is achieved at or below the IC_{50} value. Thus, these *in vitro* translation and protein labeling assays provide a starting concentration range for analysis in live cells.

3.2.3 Analysis of Puromycin-conjugate Activity *In Vivo*

In order to analyze the activity of puromycin conjugates *in vivo*, we needed to choose both an appropriate cell line and an appropriate quantitation and detection scheme. While microscopy is a powerful means to analyze individual cells and small sections of tissue, we wished to perform experiments where thousands to millions of cells could be examined for protein labeling. We therefore chose flow cytometry as our primary means to analyze uptake and incorporation of our conjugates. In addition to providing a quantitative measure of fluorescence and cell size, flow cytometry methods enable live cells and dead cells to be readily distinguished (19). We chose the mammalian thymocyte D9 cell line (16610D9) (20) for our experiment for four reasons: 1) they have relatively uniform size and shape, 2) they do not aggregate, making single cell detection possible, 3) they are suspension cells, which allows for ready growth in culture with subsequent acquisition of a large number of single cell readings using flow cytometry and 4) they are amenable to routine infection techniques to introduce selectable markers and GFP-based tags.

We began by comparing the concentration and time dependence of labeling with F2**P** (**4**) and the negative control conjugate F2A (**5**) (Figure 3.5A,B). For F2**P**, progressively increased fluorescence is seen with increasing time (Figure 3.5A,B) and the greatest enhancement is seen after the 24 h incubation at both 5 μM and 25 μM of the conjugate. At both concentrations, a substantial population of live cells is detected and demonstrates up to 4-fold enhanced fluorescence relative to the F2A control molecule. Longer incubation (48 hours) in the presence of F2**P** eventually kills the majority of cells at both concentrations tested. In contrast, the background fluorescence from F2A reaches a maximum of $\sim 10^1$ units after a 7 h incubation for both 5 and 25 μM incubations (Figure 3.5A,B) and F2A has no apparent effect on cell viability. The fluorescence enhancement beyond 10^1 units for cells treated with F2**P** is consistent with C-terminal protein labeling by the fluorescein-puromycin conjugate. These experiments also suggest that there is an optimum concentration

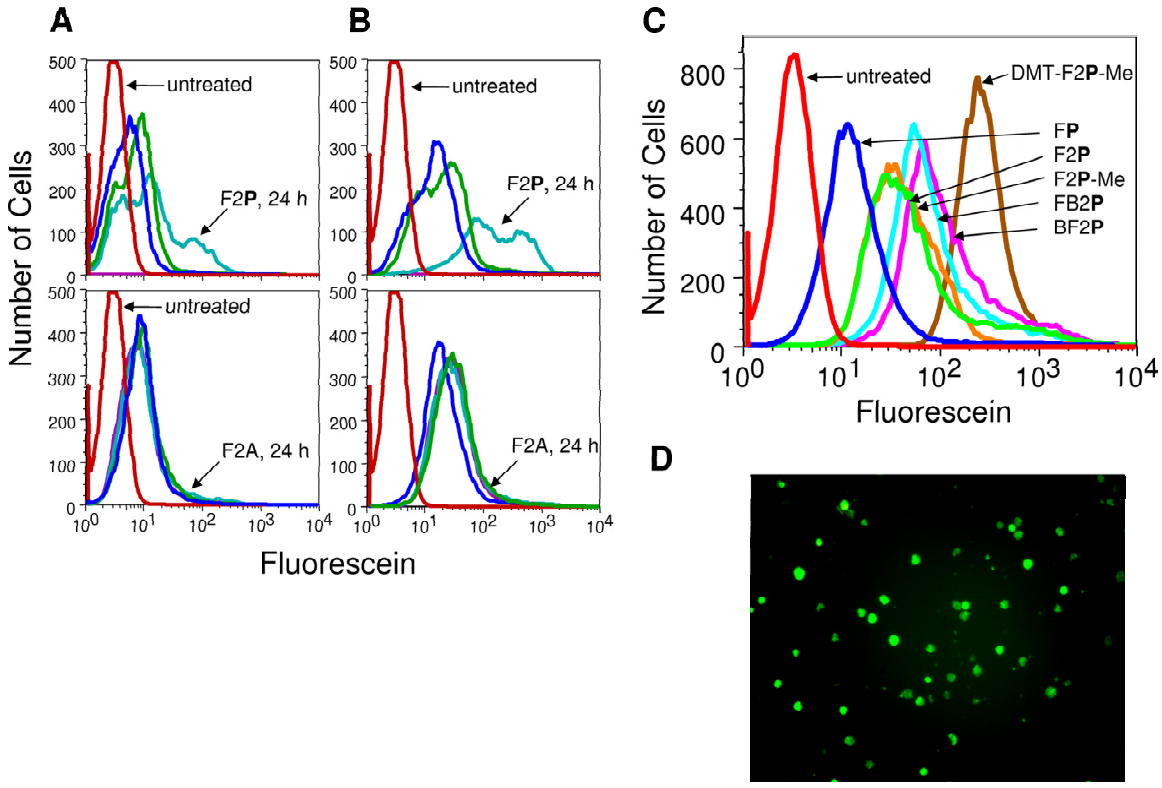

Figure 3.5: Analysis of puromycin conjugate activity in D9 thymocyte cells. Dose-response analysis of D9 thymocyte cells treated with F2**P** or F2Λ at (Λ) 5 μM and (B) 25 μM. Incubation times are 1 (■), 7 (■), 24 (■), and 48 h (■). Untreated cells incubated for 1h are indicated with (■). Cells were analyzed using a flow cytometer and gated on a live cell population according to forward and side scatter plots. (C) Flow cytometry analysis of untreated cells (■); Fluorescein-puromycin, F**P** (■); F2**P**, **4** (■); F2**P**-Me, **10** (■); FB2**P**, **3** (■); BF2**P**, **8** (■); DMT-F2**P**-Me, **12** (■). Cells were incubated for 24 h with puromycin conjugates at 50 μM. Analysis was performed using flow cytometry using a live cell gate as in Λ and B. (D) Epi-fluorescence microcopy of D9 cells treated with DMT-F2P-Me (25 μM) with 200 X magnification.

and incubation time for labeling expressed proteins without killing the cells.

We next wanted to examine the relative level of fluorescence enhancement for a series of conjugates. To do this, a uniform population of D9 cells was split into separate containers, each containing identical concentrations of a different puromycin conjugate, incubated for 24 hours, and analyzed by flow cytometry with a live-cell gate as before (Figure 3.5C). In this series, DMT-F2**P**-Me (**12**) gives the strongest enhancement and the rank order of compounds follows DMT-F2**P**-Me (**12**) > FB2**P** (**3**) ~ BF2**P** (**8**) > F2**P** (**4**) ~ F2**P**-Me (**10**) > F**P**. The IC_{50} values for all the compounds with the exception of F**P** (IC_{50} = 120 μM (17)) are relatively similar, while addition of the DMT group in compound (**12**) would be expected to confer increased hydrophobicity and membrane permeability. Compounds containing a phosphate (F2**P** (**4**)) or a methylphosphonate (F2**P**-Me (**10**)) bridging the puromycin and dC residue show little difference in IC_{50} (Figure 3.3 and Table 3.1) and *in vivo* labeling (Figure 3.5C), arguing that charge at this position does not play a key role in either the activity as a substrate or entry into the cell. The poor IC_{50} for F**P** *in vitro* (17) correlates with the small fluorescence enhancement seen for this compound *in vivo* (Figure 3.5C). Epi-fluorescence microscopy confirms that the conjugate DMT-F2**P**-Me (**12**) readily enters and labels D9 cells brightly (Figure 3.5D).

Following these experiments, we next wished to confirm that two of the best compounds, BF2**P** (**8**) and DMT-F2**P**-Me (**12**) also showed fluorescence enhancement *in vivo* relative to control molecules containing only a terminal adenosine. Indeed, comparison of cells treated with BF2**P** (**8**) versus BF2A (**9**) (Figure 3.6A) and DMT-F2**P**-Me (**12**) versus DMT-F2A-Me (**13**) (Figure 3.6B), indicates that compounds bearing the terminal puromycin moiety show a 3- to 4-fold fluorescence enhancement as compared with the control molecules.

This shift in fluorescence is consistent with labeling protein during rounds of translation. Overall, the combination of our *in vitro* and *in vivo* observations is consistent with the notion that the overall fluorescence enhancement reflects both

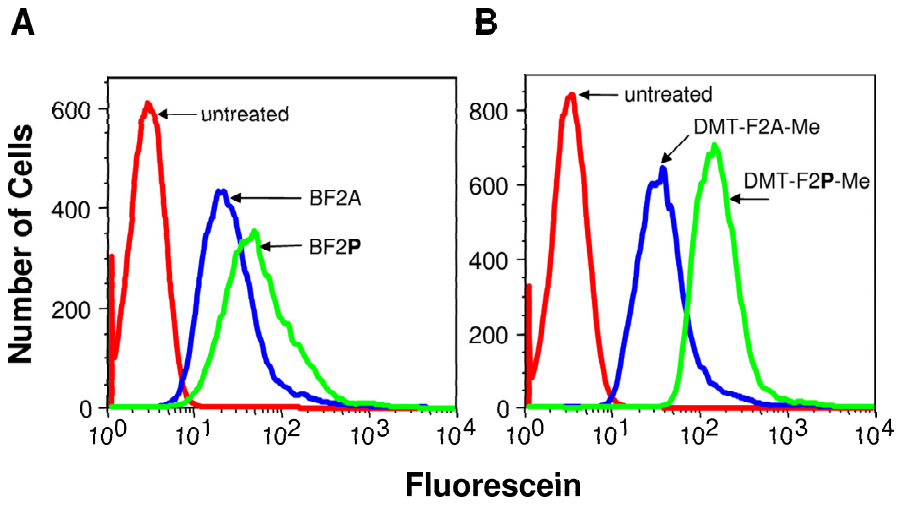

Figure 3.6: Fluorescence shift analysis for puromycin conjugates versus negative control molecules in D9 thymocyte cells. (A) Untreated cells (■); BF2A, **9** (■); BF2**P**, **8** (■). (B) Untreated cells (■); DMT-F2A-Me, **13** (■); DMT-F2**P**-Me, **12** (■). Analysis was performed using flow cytometry using a live cell gate as described for Figure 3.5.

the efficacy and the cellular permeability of the compounds.

3.2.4 Mechanism of Puromycin Conjugate Activity *In Vivo*

We next wished to demonstrate that the puromycin conjugates we had constructed were acting *in vivo* by the same mechanism as puromycin itself. Puromycin can be used as a selection agent in mammalian cell culture to kill cells that lack the resistance gene encoding puromycin *N*-acetyl-transferase (PAC) (21). This enzyme *N*-acetylates the reactive amine on puromycin and blocks its ability to participate in peptide bond formation (22, 23). In a mixed population of cells, those that lack a vector expressing PAC can be selectively killed by long incubations (>48 hours) with puromycin, leaving only vector-containing cells alive. Previously, we showed that chemical acylation inactivates puromycin-mediated translation inhibition *in vitro* (17). Thus, we wished to see if the D9 cells bearing PAC would be resistant to killing (and thus enriched in the mixed population) by long incubations with puromycin itself or our puromycin conjugates *in vivo*.

Foreign genes can be inserted into D9 cells by infection with a viral vector (see Experimental Procedures). Vectors that express GFP provide a straightforward means to measure the fraction of cells that become infected and a direct means to monitor any vector-mediated enrichment. We infected D9 cells with a viral vector driven by a mouse stem cell virus promoter (MSCV) containing an internal ribosome entry site (IRES) upstream from enhanced green fluorescent protein (EGFP) referred to as MIG (MIG = MSCV-IRES-GFP; Figure 3.7A) (24). MIG expresses GFP so that infection efficiency can be monitored by GFP fluorescence (Figure 3.7A). A second vector containing the PAC gene was also constructed (MIG_{PAC}; Figure 3.7B) and results in a bicistronic mRNA in which both PAC and GFP can be translated (Figure 3.7B).

Flow cytometry was used to examine both the infection efficiency and confirm the ability to perform puromycin-based enrichment. After infection with the MIG or MIG_{PAC} vectors, 5.0% and 4.3% of the D9 cells were infected and alive based

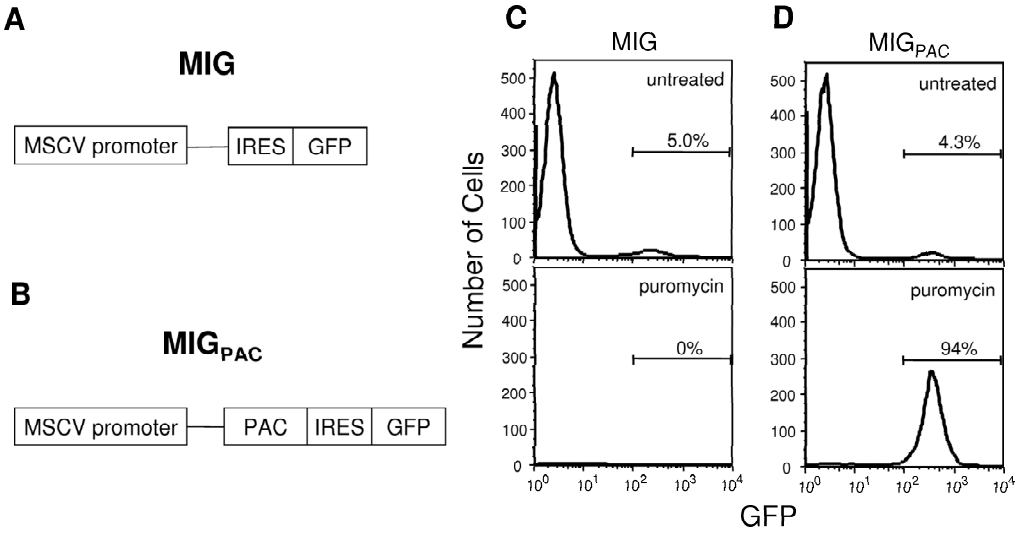

Figure 3.7: Mechanism of action of puromycin in D9 thymocyte cells infected with MIG (A) and MIG_{PAC} (B) constructs. Cells infected with MIG are sensitive (C) and MIG_{PAC} are resistant (D) to puromycin action.

on GFP expression, respectively (Figure 3.7C,D; upper panels). In both cases, the other 95% of the cells showed no GFP-based signal. Puromycin was then added to both MIG and MIG_{PAC} infected cells followed by incubation for 48 h at 37 °C. For MIG infected cells, puromycin results in almost complete killing of both GFP-positive and GFP-negative cells (Figure 3.7C; lower panel). For MIG_{PAC} infected cells, puromycin selectively kills only those cells lacking GFP, such that after 48 hours the population is completely dominated by GFP-positive cells (94%) (Figure 3.7D; lower panel). Enrichment of GFP-positive cells occurs because they express the PAC resistance protein that acylates puromycin, rendering it inactive. These experiments demonstrate that puromycin acylation is sufficient to rescue cells from puromycin toxicity and that *N*-blocked puromycin is non-toxic to D9 cells. The selective enrichment of PAC-expressing cells argues that puromycin exerts its effect on D9 cells by acting on the translation apparatus *in vivo*.

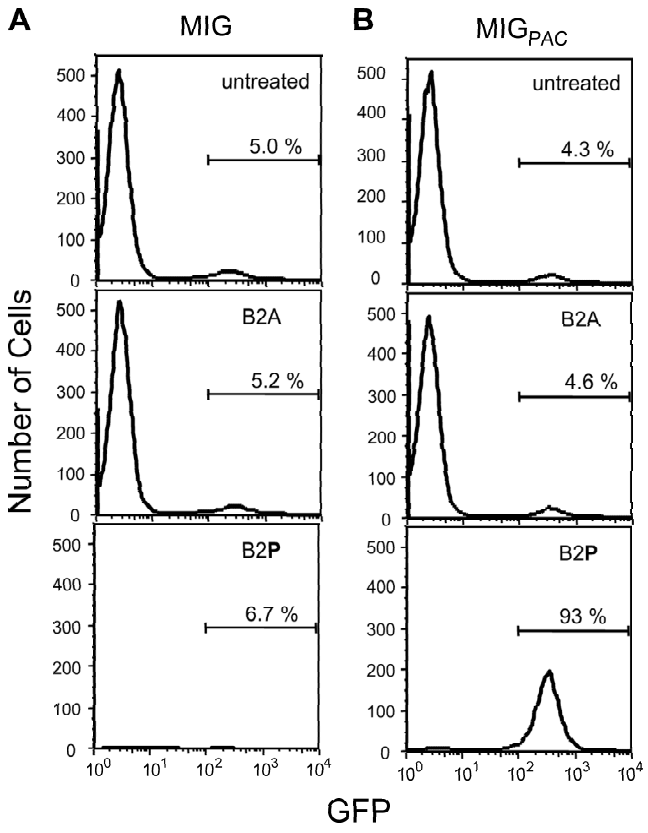

Figure 3.8: Mechanism of action of puromycin conjugates in D9 thymocyte cells. Cells infected with (A) MIG or (B) MIG_{PAC} were treated with biotinylated-puromycin conjugates B2A (**7**) and B2**P** (**6**), both at 25 μM.

We next wished to examine if B2**P** (**6**) could act in a biochemically similar fashion as puromycin itself. As with puromycin, flow cytometry indicated that long exposures of B2**P** (**6**) kills the vast majority of the cells infected with MIG (Figure 3.8A; bottom panel), while B2A (**7**), a control molecule lacking the amino acid, had no effect (Figure 3.8A; middle panel). Importantly, cells infected with MIG_{PAC} show selective enrichment when incubated with B2**P** (**6**) (Figure 3.8B; bottom panel), while B2A shows no change in GFP-positive and negative populations (Figure 3.8B; middle panel). These experiments are fully consistent with B2**P** (**6**) acting by the same mech-

anism as puromycin itself. Further, these data also provide the first demonstration that PAC can act on puromycin conjugates bearing 5'-extensions *in vivo*.

In line with this conclusion, two other puromycin conjugates show similar activity with B2**P**. We examined a Cy_5-bearing conjugate $Cy_5$2**P** (**1**) and compared its action with an analogous control molecule, $Cy_5$2A (2), using both MIG and MIG_{PAC} infected cells. Cy_5 provides a useful spectroscopic handle in this context because its red-shifted fluorescence allows the emission of the conjugate to be unambiguously separated from that of GFP. As with B2**P** versus B2A, MIG-infected cells were insensitive to $Cy_5$2A, while long exposure of $Cy_5$2**P** killed both GFP-positive and negative populations, since they lacked the PAC resistance determinant (data not shown). $Cy_5$2**P** also selectively enriched MIG_{PAC} infected cells from 4.3% to 90% (data not shown). Additionally, B2**P**-Me (**11**) also resulted in selective enrichment of MIGPAC-bearing cells and had similar potency with B2**P** (**6**) (data not shown). Taken together, these data support the idea that our various X-dC-puromycin conjugates act by the same mechanism as puromycin *in vivo* and that conjugates lacking the 3'-amino acid moiety have no effect.

3.2.5 Western Blot Analysis of Puromycin Conjugate Labeling in Live Cells

Action of puromycin and our conjugates should result in proteins bearing these compounds at their C-terminus *in vivo*. We chose to use Western blot analysis of cellular lysates to examine if incorporation occurred *in vivo* and compare the resulting signal with our control conjugates. Cells were incubated with either BF2**P** (**8**) or the control molecule BF2A (**9**), washed, and a whole-cell lysate was prepared for each sample (see Experimental Procedures). Proteins were run on a SDS-PAGE gel and transferred to nitrocellulose. Equal protein loading was confirmed in each lane using Ponceau S (data not shown). The Ponceau S stain was rinsed away and the blot was probed with an anti-fluorescein antibody to detect any fluorescein-conjugated protein containing

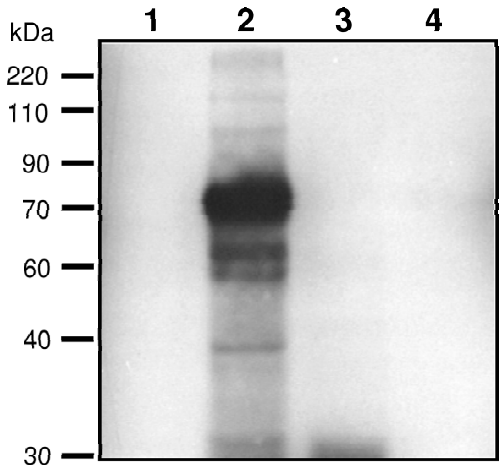

Figure 3.9: Western blot analysis of D9 thymocyte cells treated with a puromycin conjugate and analyzed using an α-fluorescein antibody: Lane 1, untreated cells; lane 2, BF2**P**, **8** (25 μM); lane 3, BF2A, **9** (25 μM); and anisomycin (250 ng/mL). Ponceau S stain was used to confirm equal protein loading. BF2**P**-conjugated protein is seen at many molecular weights indicating that the conjugate could target all translating ribosomes.

BF2**P** or BF2Λ. Cells treated with BF2**P** (Figure 3.9; lane 2) show good levels of incorporation in this assay, while lanes with cells alone (lane 1), cells treated with BF2Λ (lane 3), or anisomycin (lane 4) show essentially no signal (Figure 3.9). The Western-blot analysis of BF2**P** thus shows good correlation with flow cytometry data and is consistent with a model where puromycin conjugates are stably incorporated into proteins *in vivo* during protein synthesis.

3.2.6 Imaging of NIH 3T3 Cells Treated with Fluorescent Puromycin Conjugates

Adherent cells, such as NIH 3T3 cells, allow for spatial resolution of fluorescent molecule localization using fluorescent confocal microscopy. NIH 3T3 cells were treated with various fluorescent puromycin conjugates and imaged to ascertain the regions of conjugate localization (Figure 3.10). Cells were preincubated with anisomycin to inhibit translation and then incubated with either FB2**P** (**3**) or BF2**P** (**8**). Fluorescent confocal images clearly show that samples preincubated with anisomycin followed by incubation with either FB2**P** or BF2**P** (Figure 3.10Λ,C) have lower levels of fluorescence relative to samples not preincubated with anisomycin (Figure 3.10B,D). The images indicate that fluorescent puromycin conjugates localize in the cytoplasm, predominantly outside the nuclear membrane. NIH 3T3 cells were also treated with $Cy_3$2**P** (**1**) and imaged using fluorescent confocal microscopy (Figure 3.11). This shows the same pattern of conjugate localization as seen with FB2**P** and BF2**P** above. These results confirm that fluorescent puromycin conjugates enter cells and label protein during rounds of translation.

3.3 Discussion

In the present study, we developed a technique to detect protein synthesis in live cells that does not require gene transfection or radiolabeling. Our strategy thus provides

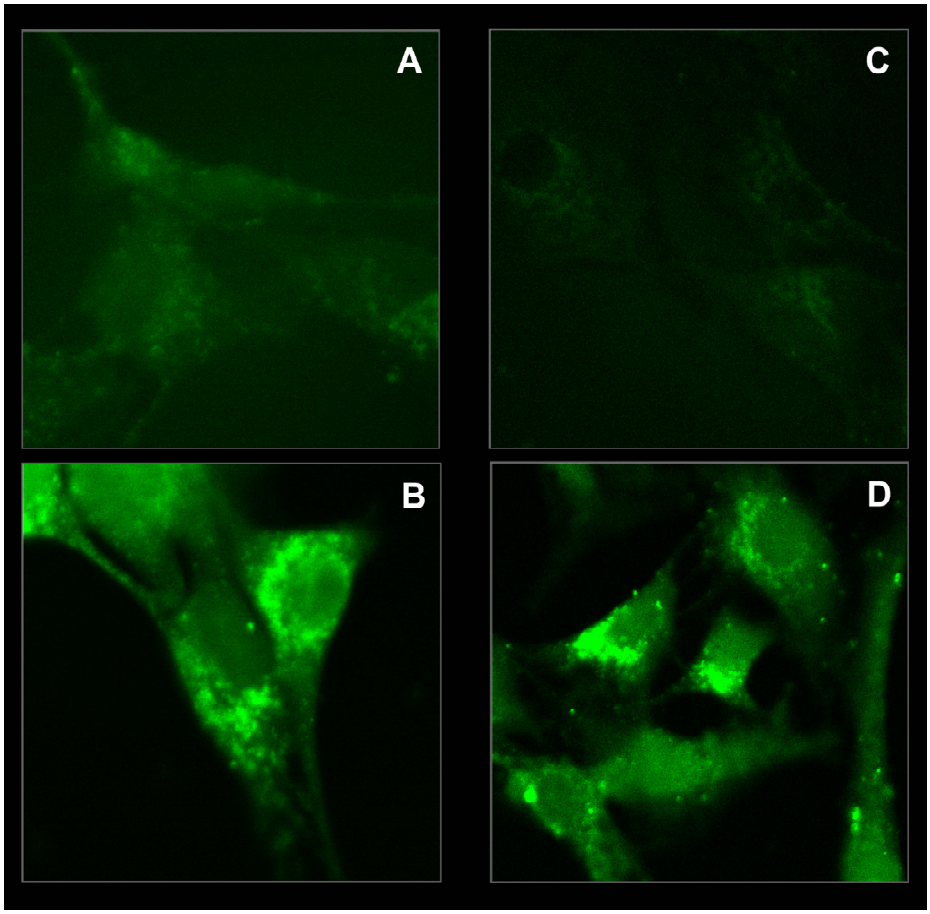

Figure 3.10: Fluorescent confocal microscopy of NIH 3T3 cells treated with 25 μM FB2**P** (**3**) and 25 μM BF2**P** (**8**)with (A and C) and without (B and D) anisomycin preincubated.

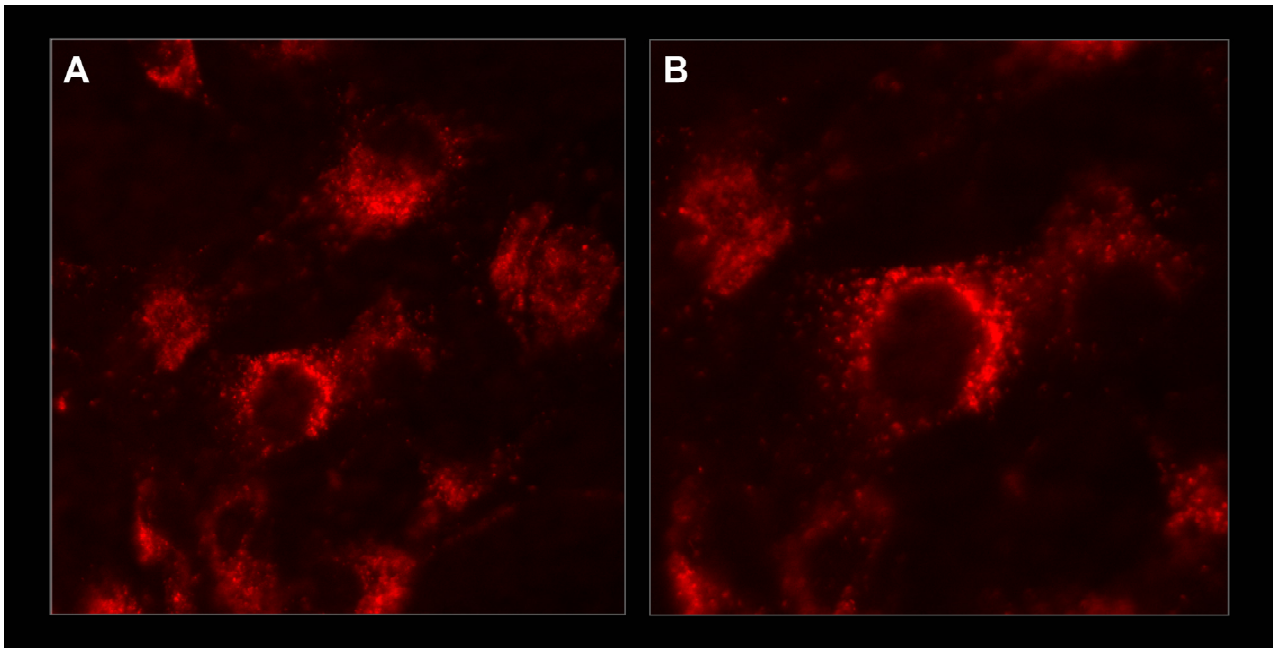

Figure 3.11: Fluorescent confocal microscopy of NIH 3T3 cells treated with $Cy_3$2**P** (**1** at 7.5 μM). Panel B is higher magnification of a cell in panel A.

an important potential alternative to these methods for studying protein expression *in vivo*. Generally, a great diversity of reagents of the class X-dC-puromycin, where X can be one or two fluorescent or affinity tags, can be constructed and show good activity in protein synthesis *in vitro* and *in vivo*. These reagents all appear to act by the same basic mechanism, entering the ribosomal peptidyl transferase site during translation, followed by covalent attachment to proteins being actively synthesized. Ribosome entry and attachment occurs predominantly at a few discrete sites in the open reading frame including the stop codon, rather than at every position in the chain (25). Previous work also demonstrates that over a 50-fold concentration range that brackets the IC_{50}, the length of truncated products is the same and that shorter products are favored as the conjugate concentration is increased substantially.

Despite the intermediate size of these molecules (1163 – 1730 Da), all the conjugates appear to be competent to enter the D9 suspension tissue culture cells used here and act at modest concentrations ($5 - 25\,\mu$M). Experiments with other mammalian and insect cell types support the idea that the ability of these compounds to cross membranes and act in protein synthesis is a general phenomenon (W. B. Smith, E. Schuman, B. Hay, unpublished observations). All of the conjugates we have examined show a significant and measurable shift in the fluorescence intensity of live cells as compared to the control conjugates. Western analysis and selective enrichment studies support the idea that this shift is due to the specific covalent attachment of the conjugates to nascent proteins during translation. Demonstration that affinity tags may be inserted into expressed proteins *in vivo* provides the future opportunity to examine protein expression in response to various cellular stimuli and subsequent identification of the individual polypeptides through a combination of affinity purification and mass spectrometry-based sequence analysis.

In the short term (~24 hours), these compounds are non-toxic based on the proportion of live cells seen in our flow cytometry experiments. The robust labeling and signal to noise we observe thus makes these compounds useful for a great diversity of

cell, tissue, and organism-level experiments. The long-term toxicity of the present set of compounds may provide some limitations for their use. In that context, non-toxic variants that can be photoactivated or presented as pro-drugs may provide useful paths for future conjugate development. The general class of compounds described here should therefore serve as useful cell biology tools to evaluate *in vivo* protein synthesis in areas such as nuclear protein synthesis (26, 27), neuron dentritic protein synthesis (10), dendritic cell aggresome-like induced structures (DALIS) (28), and other novel proteome functions.

3.4 Significance

Existing methods to study *in vivo* protein synthesis generally require choice of a candidate gene, radioactivity, or the destruction of cells. To overcome these limitations, we have developed a new class of reagents that enable detection of protein synthesis in live cells using fluorescent and biotinylated puromycin conjugates. These reagents, of the general form X-dC-puromycin, are active *in vitro* and *in vivo* and provide a non-toxic alternative for the study of protein synthesis in live cells. A wide variety of detection moieties appear to be accommodated at the X-position allowing for facile custom reagent design and development. Initial *in vitro* studies correlate the function of our compounds in peptide bond formation during protein synthesis. Subsequent *in vivo* experiments in a mouse thymocyte cell line demonstrate the usefulness of these molecules as indicators of protein synthesis in live cells. Selective enrichment studies with several conjugates as well as Western analysis demonstrate that these compounds all label protein in cells by the same general mechanism, attachment to nascent proteins during translation. The present results thus provide evidence that puromycin conjugates may serve as an alternative to existing tools to elucidate the proteome.

3.5 Experimental Procedures

3.5.1 Reagents and Materials

L-Puromycin hydrochloride, rabbit globin mRNA, and carboxypeptidase Y (CPY) were obtained from Sigma Chemical Co. (St. Louis, MO). Rabbit reticulocyte Red Nova lysate was purchased from Novagen (Madison, WI). L-[^{35}S]methionine ([^{35}S]Met) (1175 Ci/mmol) was obtained from NEN Life Science Products (Boston, MA). Immunopure immobilized Neutravidin-agarose was from Pierce (Rockford, IL). GF/A glass microfiber filters were from Whatman. The PAC gene was a kind gift from Joel Pomerantz and David Baltimore.

3.5.2 Puromycin Conjugates

Puromycin conjugates were synthesized using standard phosphoramidite chemistry at the California Institute of Technology oligonucleotide synthesis facility. Puromycin-CPG was obtained from Glen Research (Sterling, VA). Oligonucleotides were synthesized with the 5'-trityl intact, desalted via OPC cartridge chromatography (Glen Research) (DNA oligonucleotides only), cleaved, and evaporated to dryness. 5'-Biotin phosphoramidite, Biotin phosphoramidite, 5'-Fluorescein phosphoramidite, 6-Fluorescein phosphoramidite (Glen Research) were used to make the biotin- and dye-puromycin conjugates. Ac-dC-Me-phosphonamidite (Glen Research) was used to prepare the phosphonate puromycin conjugates. The dried samples were resuspended and desalted on Sephadex G-25 (Sigma). Puromycin, puromycin-conjugate, and control molecule concentrations were determined with the following extinction coefficients ($M^{-1}cm^{-1}$): puromycin (ϵ_{260} = 11,790; in H_2O); B2**P** and B2**P**-Me (ϵ_{260}= 19,100; in H_2O); F2**P**, F2**P**-Me, DMT-F2**P**-Me, FB2**P**, BF2**P**, F2A, and BF2A ($\epsilon_{471} = 66,000$; in 1X PBS); $Cy_3$2**P** $\epsilon_{650} = 150,000$; in 1X PBS), $Cy_5$2**P** and $Cy_5$2A ($\epsilon_{650} = 250,000$; in 1X PBS).

3.5.3 *In Vitro* Potency Determination for Puromycin Conjugates

Translation reactions containing [^{35}S]Met were mixed in batch on ice and added in aliquots to microcentrifuge tubes containing an appropriate amount of puromycin-conjugate (or control molecule) dried in vacuo. Typically, a 20 μl translation mixture consisted of 0.8 μL of 2.5 M KCl, 0.4 μL of 25 mM MgOAc, 1.6 μL of 12.5X translation mixture without methionine, (25 mM dithiothreitol (DTT), 250 mM HEPES (pH 7.6), 100 mM creatine phosphate, and 312.5 μM of 19 amino acids, except methionine), 3.6 μL of nuclease-free water, 0.6 μL (6.1 μCi) of [^{35}S]Met (1175 Ci/mmol), 8 μL of Red Nova nuclease-treated lysate, and 5 μL of 0.05 μg/μL globin mRNA. Inhibitor, lysate preparation (including all components except template), and globin mRNA were mixed simultaneously and incubated at 30 °C for 60 min. Each reaction (2 μL) was combined with 8 μL of tricine loading buffer (80 mM Tris-Cl (pH 6.8), 200 mM DTT, 24% (v/v) glycerol, 8% sodium dodecyl sulfate (SDS), and 0.02% (w/v) Coomassie blue G-250), heated to 90 °C for 5 min, and applied entirely to a 4% stacking portion of a 16% tricine-SDS-polyacrylamide gel containing 20% (v/v) glycerol (29)(30 mA for 1h, 30 min). Gels were fixed in 10% acetic acid (v/v) and 50% (v/v) methanol, dried, exposed overnight on a PhosphorImager screen, and analyzed using a Storm PhosphorImager (Molecular Dynamics).

3.5.4 Neutravidin Capture of *In Vitro* Translated Protein-puromycin-conjugate Products

Neutravidin-agarose [50% slurry (v/v)] was washed 3 times with 1X PBS + 0.1% Tween-20 and resuspended in 1 mL of 1X PBS + 0.1% Tween-20. To 200 μL of this suspension, 12 μL of the reaction lysate and 0.8 mL of 1X PBS + Tween-20 were added. The samples were rotated at 4 °C for 3 h and washed with 1X PBS + Tween-20 until the CPM of [^{35}S]Met were < 500 in the wash. The amount of immobilized

[^{35}S]Met-protein-puromycin conjugate was determined by scintillation counting of the Neutravidin-agarose beads.

3.5.5 Preparation of MIG_{PAC} Infected 16610D9 Cells

The PAC gene was cloned into MIG using BgII and EcoRI restriction sites to yield MIG_{PAC}. 293T-HEK fibroblasts (American Tissue Culture Collection) were co-transfected with pECL-Eco (30) and MIG or MIG_{PAC} by calcium phosphate precipitation. After 12 hours, the precipitate was removed, cells were washed once with PBS, and 4 mL of fresh complete Dulbecco's Modified Eagle Medium (DMEM) supplemented with 10% fetal calf serum (FCS). Viral supernatant was removed 24 hours later and used in infection of 16610D9 cells. One million D9 cells were spin-infected with 0.4 mL of viral supernatant suplemented with 5 μg/ml Polybrene (Sigma-Aldrich).

3.5.6 Enrichment of GFP(+) 16610D9 Cells using Puromycin and Puromycin Conjugates

16610D9 cells infected with either MIG of MIG_{PAC} were cultured in RPMI media with 10% FBS and grown at 37 °C in a humidified atmosphere with 5% CO_2. For each experiment, 16610D9 cells (0.25 x 10^6/well) were added to 24-well microtiter plates along with puromycin, puromycin-conjugate, and control molecules dissolved in the minimum amount of either media or PBS. After a 48 h incubation, the cells were washed twice in 2 mL PBS + 4% FCS and resuspended in PBS + 4% FCS supplemented with 2% formaldehyde along with incubation at 37 °C for 10 min. Flow cytometry was carried out on a Beckman FACScabilur Flow Cytometer.

3.5.7 Detection of Protein Synthesis Events *In vivo* using Flow Cytometry

16610D9 cells (0.5 million mL^{-1}) were combined with the various puromycin conjugates and control molecules resuspended in the minimum volume of PBS or media as described above. After a 24 h incubation, the cells were washed twice in 2 mL PBS + 4% FCS and resuspended in PBS + 4% FCS supplemented with 2% formaldehyde followed by incubation at 37 °C for 10 min or used directly after washing for immediate flow cytometry analysis.

3.5.8 Western Blot Analysis of 16610D9 Cells Treated with Puromycin Conjugates

Cells were prepared as described above except as indicated anisomycin was added to a final concentration of 250 μg mL^{-1} and washed twice in PBS. Live cell number was determined using trypan blue exclusion dye and each sample was adjusted to contain an equal number of live cells. Cell pellets were resuspended in 2X lysis buffer (100 mM $\beta-$glycerophosphate, 3 mM EGTA, 2 mM EDTA, 0.2 mM sodium-orthovanadate, 2 mM DTT, 20 μg/ml aprotinin, 20 μg/ml leupeptin, 50 μg/ml trypsin inhibitor, and 4 μg/ml pepstatin, and 1% Triton X-100) and incubated on ice for 30 min. Cell debris was removed by centrifugation at 20,000 x g for 30 min. Cell lysate was combined with SDS loading buffer (0.12 M Tris-Cl (pH 6.8), 20% glycerol, 4% (w/v) SDS, 2% (v/v) $\beta-$mercaptoethanol, and 0.001% bromophenol blue) and heated at 90 °C for 10 min. Samples were applied entirely to a 4% stacking portion of a 10% glycine-SDS-polyacrylamide gel (30 mA for 1h, 30 min). Protein was transferred using standard Western transfer transfer techniques and the blot was probed with an anti-fluorescein antibody followed by an anti-rabbit-horseradish peroxidase conjugate (Pierce chemicals). The chemiluminescence reaction was carried out using the ECL PLUS Western Blotting Detection System (Amersham Biosciences).

3.5.9 Confocal Microscopy of NIH 3T3 cells Treated with Fluorescent Puromycin Conjugates

NIH 3T3 cells were plated (50,000 cells/slide) on glass bottom cell culture imaging chambers. After 24 h, cells were preincubated with anisomycin in a total volume of 400 μL (50 μM) for 4 h. The cells were incubated with the fluorescent puromycin conjugates in a total volume of 400 μL (resuspended in media) for 7 h. After washing the cells 4 times with 1X PBS and adding a HEPES-buffered solution, images were collected on a Zeiss LSM 510-META confocal microscope using a 63X oil immersion lens.

Acknowledgements

We gratefully acknowledge the help and useful discussions from our collaborators Erin Schuman, W. Bryan Smith, and Bruce Hay who have examined puromycin-dye conjugates in various *in vivo* systems. This work was supported by NIH Grant R01 GM60416 to R.W.R. and by NIH training grant GM 07616 (S.R.S.).

References

[1] The International Human Genome Sequencing Consortium. Initial sequencing and analysis of the human genome. *Nature*, 409:860–921, 2001.

[2] J.C. Venter, M.D. Adams, E.W. Myers, P.W. Li, R.J. Mural, G.G. Sutton, H.O. Smith, M. Yandell, C.A. Evans, and R.A. et al. Holt. The sequence of the human genome. *Science*, 291:1304–1351, 2001.

[3] R.F. Duncan, H. Peterson, C.H. Hagedorn, and A. Sevanian. Oxidative stress increases eukaryotic initiation factor 4E phosphorylation in vascular cells. *Biochem. J.*, 369:213–225, 2003.

[4] J.H. Lipschutz, V.R. Lingappa, and K.E. Mostov. The exocyst affects protein synthesis by acting on the translocation machinery of the endoplasmic reticulum. *J. Biol. Chem.*, 278:20954–20960, 2003.

[5] C. Constantinou, M. Bushell, I.W. Jeffrey, V. Tilleray, M. West, V. Frost, J. Hensold, and M.J. Clemens. p53-induced inhibition of protein synthesis is independent of apoptosis. *Euro. J. Biochem.*, 270:3122–3132, 2003.

[6] D.L. Lockhart and E.A. Winzeler. Genomics, gene expression and DNA arrays. *Nature*, 405:827–836, 2000.

[7] P. van Roessel and A.H. Brand. Imaging into the future: Visualizing gene expression and protein interactions with fluorescent proteins. *Nat. Cell Biol.*, 4, 2003.

[8] A. Miyawaki, J. Llopis, R. Heim, J.M. McCaffery, J.A. Adams, M. Ikura, and R.Y. Tsien. Fluorescent indicators for Ca^{2+} based on green fluorescent proteins and calmodulin. *Nature,* 288:882–887, 1997.

[9] A.Y. Ting, K.H. Kain, R.L. Klemke, and R.Y. Tsien. Genetically encoded fluorescent reporters of protein tyrosine kinase acitivities in living cells. *Proc. Natl. Acad. Sci. U.S.A.*, 98:15003–15008, 2001.

[10] O. Steward and E.M. Schuman. Protein synthesis at synaptic sites on dendrites. *Annu. Rev. Neurosci.*, 24:299–325, 2001.

[11] G. Aakalu, W.B. Smith, N. Nguyen, C.G. Jiang, and E.M. Schuman. Dynamic visualization of local protein synthesis in hippocampal neurons. *Neuron*, 30:489–502, 2001.

[12] D. Nathans. Puromycin inhibition of protein synthesis: incorporation of puromycin into peptide chains. *Proc. Natl. Acad. Sci. U.S.A.*, 51:585–592, 1964.

[13] M.B. Yarmolinsky and G. de la Haba. Inhibition by puromycin of amino acid incorporation into protein. *Proc. Natl. Acad. Sci. U.S.A.*, 45:1721–1729, 1959.

[14] N. Doi, H. Takashima, M. Kinjo, K. Sakata, Y. Kawahashi, Y. Oishi, R. Oyama, E. Miyamoto-Sato, T. Sawasaki, Y. Endo, and H. Yanagawa. Novel fluorescence labeling and high-throughput assay technologies for *in vitro* analysis of protein interactions. *Genome Res.*, 12:487–492, 2002.

[15] Y. Kawahashi, N. Doi, H. Takashima, C. Tsuda, Y. Oishi, R. Oyama, M. Yonezawa, E. Miyamoto-Sato, and H. Yanagawa. *In vitro* protein microarrays for detecting protein-protein interactions: Application of a new method for fluorescence labeling of proteins. *Proteomics*, 3:1236–1243, 2003.

[16] N. Nemoto, E. Miyamoto-Sato, Y. Husimi, and H. Yanagawa. *In vitro* virus: Bonding of mRNA bearing puromycin at the 3'-terminal end to the C-terminal

end of its encoded protein on the ribosome *in vitro*. *FEBS Lett.*, 414:405–408, 1997.

[17] S.R. Starck and R.W. Roberts. Puromycin oligonucleotides reveal steric restrictions for ribosome entry and multiple modes of translation inhibition. *RNA*, 8:890–903, 2002.

[18] S.R. Starck, X. Qi, B.N. Olsen, and R.W. Roberts. The puromycin route to assess stereo- and regiochemical constraints on peptide bond formation in eukaryotic ribosomes. *J. Am. Chem. Soc.*, 125:8090–8091, 2003.

[19] *In Living Color: Protocols in Flow Cytometry and Cell Sorting*. Springer-Verlag: Berlin, 2000.

[20] L. Van Parijs, Y. Refaeli, J.D. Lord, B.H. Nelson, A.K. Abbas, and D. Baltimore. Uncoupling IL-2 signals that regulate T cell proliferation, survival, and Fas mediated activation-induced cell death. *Immunity*, 11:281–288, 1999.

[21] S. de la Luna and J. Ortin. Pac gene as efficient dominant marker and reporter gene in mammalian cells. *Methods Enzymol.*, 216:376–385, 1992.

[22] J.N. Porter, R.I. Hewitt, C.W. Hesseltine, G. Krupka, J.A. Lowery, W.S. Wallace, N. Bohonos, and J.H. Williams. Achromycin: A new antibiotic having trypanocidal properties. *Antibiotics and Chemo.*, 11:409–410, 1952.

[23] J.A. Pérez-González, J. Vara, and A. Jiménez. Acetylation of puromycin by *Streptomyces alboniger* the producing organism. *Biochem. Biophys. Res. Commun.*, 113:772–777, 1983.

[24] G. Bain, M.W. Quong, R.S. Soloff, S.M. Hedrick, and C. Murre. Thymocyte maturation is regulated by the activity of the helix-loop-helix protein. *J. Exp. Med.*, 190:1605–1616, 1999.

[25] S.L. Wolin and P. Walter. Ribosome pausing and stacking during translation of a eukaryotic mRNA. *EMBO*, 7:3559–3569, 1988.

[26] F.J. Iborra, D.A. Jackson, and P.R. Cook. Coupled transcription and translation within nuclei of mammalian cells. *Science*, 293:1139–1142, 2001.

[27] L. Nathanson, T. Xia, and M.P. Deutscher. Nuclear protein synthesis: a re-evaluation. *RNA*, 9:9–13, 2003.

[28] H. Lelouard, V. Ferrand, D. Marguet, J. Bania, V. Camosseto, A. David, E. Gatti, and P. Pierre. Dendritic cell-aggresome-like induced structures are dedicated areas for ubiquitination and storage of newly synthesized defective proteins. *Cell Biol.*, 164:667–675, 2004.

[29] H. Schagger and G.V. von Jagow. Tricine-sodium dodecyl sulfate-polyacrylamide gel electrophoresis for the separation of proteins in the range from 1 to 100 kDa. *Anal. Biochem.*, 166:368–379, 1987.

[30] R.K. Naviaux, E. Costanzi, M. Haas, and I.M. Verma. The pCL vector system: Rapid production of helper-free, high-titer, recombinant retroviruses. *J. Virology*, 70:5701–5705, 1996.

Chapter 4

The Puromycin Route to Assess Stereo- and Regiochemical Constraints on Peptide Bond Formation in Eukaryotic Ribosomes

This chapter has previously appeared as: S.R. Starck, X. Qi, B.N. Olsen, R.W. Roberts. The puromycin route to assess stereo- and regiochemical constraints on peptide bond formation in eukaryotic ribosomes. *J. Am. Chem. Soc.* 125:8090-8091, 2003.

4.1 Introduction

The protein synthesis machinery can be used to incorporate unnatural amino acids into peptides (1, 2, 3) proteins (4, 5), and molecular libraries (6, 7) (see references (8, 9, 10, 11, 12) for reviews). These studies indicate that the ribosome displays a broad ability to utilize residues beyond the 20 naturally occurring amino acids. Chemically misacylated-tRNA fragments and tRNAs have provided one route to probe the stereo- and regiospecificity of isolated ribosomes (13, 14, 15, 16) and intact translation systems (10, 17). This approach has expanded our understanding of the range of residues incorporated by the ribosome (18, 19, 20, 21). However, entry of both β-

and D-amino acids has proved challenging (2, 4, 13, 14, 15, 16). Analysis of these residues would deepen our understanding of the stereo- and regiochemical constraints of ribosome-mediated peptide bond formation. Here, we have used a series of synthetic puromycin analogs to measure the activity of both β- and D-amino acids in an intact eukaryotic translation system. Puromycin is a small-molecule mimic of aminoacyl-tRNA (aa-tRNA), and acts as a universal translation inhibitor by entering the ribosomal A site and participating in peptide bond formation with the nascent peptidyl chain (22). Puromycin and puromycin analogs have been very useful in exploring the activity of nucleophiles (-OH versus -NH_2 versus -SH) in peptide bond formation and the structural requirements for inhibition of translation (23, 24, 25, 26). Unlike aa-tRNA, puromycin is able to enter the ribosome independently, does not induce EF-Tu·GTPase activiy (27), and does not require soluble translation factors for function (28). Puromycin and related compounds therefore provide a direct means to address ribosome-mediated peptide bond formation in the context of a fully competent translation extract.

4.2 Results and Discussion

We synthesized a series of puromycin derivatives (Figure 4.1) that differ in the 1) amino acid moiety, 2) amino acid stereochemistry, and 3) number of carbon units in the amino acid backbone. We then measured the activity of each compound (Figure 4.2 and Table 4.1) in a high dynamic-range IC_{50} potency assay using the rabbit reticulocyte protein synthesis system (Figure 4.2A) (28). The naturally occurring compound, L-puromycin (**1a**), inhibits globin mRNA translation with an IC_{50} of 1.8 μM (Figure 4.2B). Surprisingly, D-puromycin (**1b**) also inhibited translation giving an IC_{50} of 280 μM (Figure 4.2B), a difference of 150-fold (Table 4.1). We reasoned that stereoselectivity should be a function of the sidechain size and geometry. To test this, we constructed compounds where the puromycin sidechain was altered to bear either

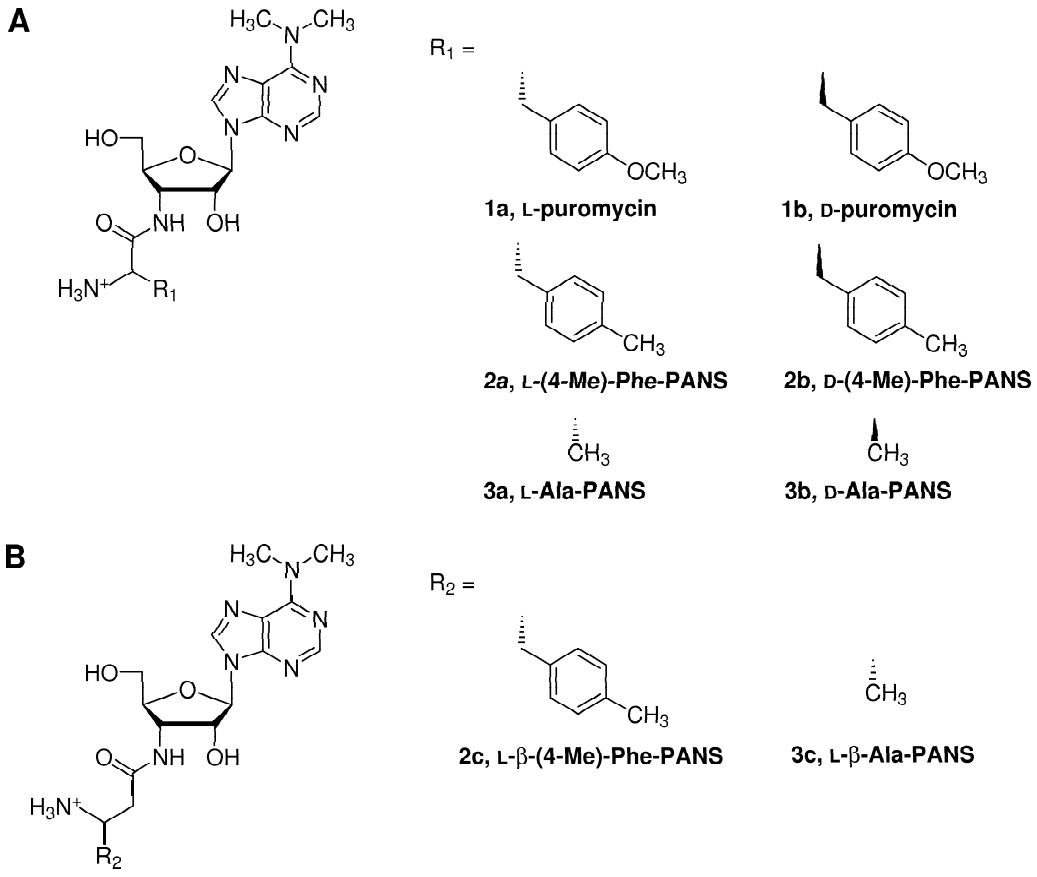

Figure 4.1: Puromycin analogs with (A) L- and D-α-amino acid sidechains and (B) L-β-amino acid sidechains.

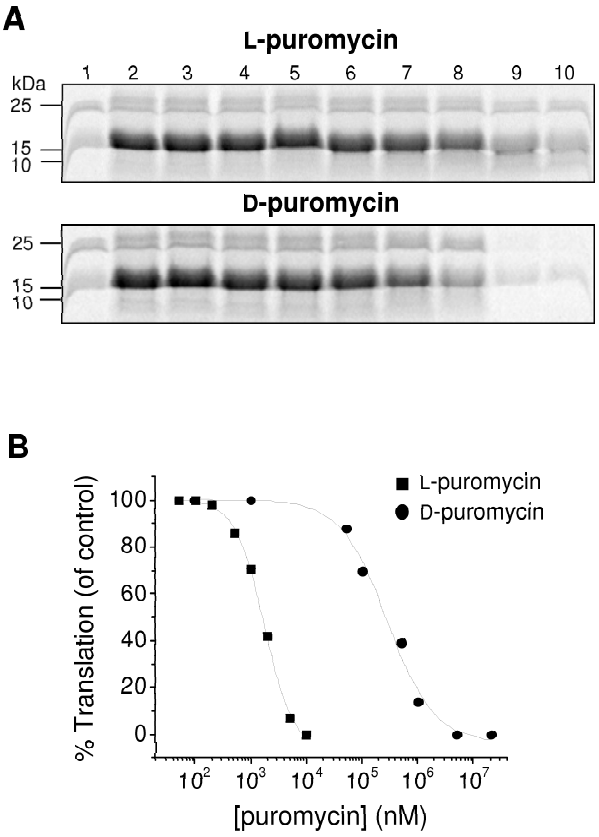

Figure 4.2: IC_{50} determination for L- and D-puromycin. (A) Tricine-SDS-PAGE analysis of [^{35}S]Met-globin translation reactions in the presence of L-puromycin (**1a**) and D-puromycin (**1b**): Lane 1, no template; lane 2, globin alone; lanes 3 – 10, concentrations from 50 nM to 10 mM for **1a** and from 100 nM to 20 mM for **1b**. (B) Percent globin translation relative to the globin only control for L-puromycin (**1a**) and D-puromycin (**1b**).

Puromycin analog	IC_{50} (μM)
1a, L-puromycin	1.8
1b, D-puromycin	280
2a, L-(4-Me)-Phe-PANS	1.0
2b, D-(4-Me)-Phe-PANS	2400
2c, D-β-(4-Me)-Phe-PANS	600
3a, L-Ala-PANS	730
3b, D-Ala-PANS	1900
3c, L-β-Ala-PANS	1700

Table 4.1: IC_{50} values for puromycin analogs.

a bulky (L- or D-4-methyl-phenylalanine; **2a** and **2b**) or a small substituent (L- or D-alanine; **3a** and **3b**). Compound **2a** inhibits translation better than puromycin itself (IC_{50} = 1.0 μM; Table 4.1) and is the most potent compound we constructed. The D-amino acid variant (**2b**) shows much lower activity (IC_{50} = 2400 μM), is ~9-fold lower than D-puromycin (**1b**), and is 2400-fold less potent than the L-isomer. The alanine analogs (R = CH_3) show only 3-fold selectivity for the L- versus D- isomers (**3a** versus **3b**; Table 4.1).

These observations argue that ribosomal stereoselectivity falls over a broad range and is primarily dictated by the size and geometry of the pendant sidechain. Within the L-amino acid series (**1a**, **2a**, and **3a**), marked variation is also seen based solely on sidechain identity. Larger, hydrophobic sidechains provide improved function, consistent with previous observations (14, 25). In the D-amino acid series, the 4-*O*-methyltyrosine derivative (**1b**) functions the best overall, and has ~3-fold better activity than the natural L-alanine variant (**3a**).

We next examined puromycin derivatives bearing β-amino acids. β-amino acids have been previously incorporated at low levels using nonsense suppression techniques (2, 4). In our experiments, both L-β-(4-Me)-Phe-PANS (**2c**) and L-β-Ala-PANS (**3c**)

were able to fully inhibit translation (IC_{50} = 600 and 1700 μM, respectively; Table 4.1).

Finally, we wished to confirm that our puromycin analogs participated in peptide bond formation within the ribosome. Incorporation of puromycin blocks the C-terminus, rendering the protein carboxypeptidase resistant (22). Previous work in our laboratory demonstrated that covalent puromycin incorporation is most efficient near the IC_{50} value (28). Consistent with this observation, protein synthesis performed in the presence of our puromycin derivatives near the IC_{50} resulted in a 12- to 16-fold increase in carboxypeptidase Y (CPY)-resistant protein compared with the no drug control (Figures 4.3A,B). All derivatives also produce truncated protein fragments, consistent with entry and attachment both internally and at the end of the template (Figure 4.4) (28).

The structural basis for stereoselectivity in rabbit ribosomes cannot be addressed presently, as there are no high-resolution structures available. However, modeling D-puromycin (**1b**) into the active site of the *Haloarcula marismortui* 50S subunit (29) is consistent with the idea that steric effects play a role in chiral discrimination. In the atomic resolution structure, U2620 (U2585 *E. coli*) is the closest nucleotide to the D-sidechain (Figure 4.5). Also, while many of the ribosome active site nucleotides are highly conserved, the fact that critical residues can be mutated (30), implies that construction of ribosomes with altered stereo- and regiospecificity may be possible.

4.3 Conclusions

Our data lead us to conclude that L-, D-, and β-amino acids can participate in ribosome-mediated peptide bond formation when constructed as analogs of puromycin. This route allows us to rank both natural and unnatural residues as substrates in a physiologically complete protein-synthesizing system. Analysis using intact systems is important as reconstituted or purified systems that are incapable of synthe-

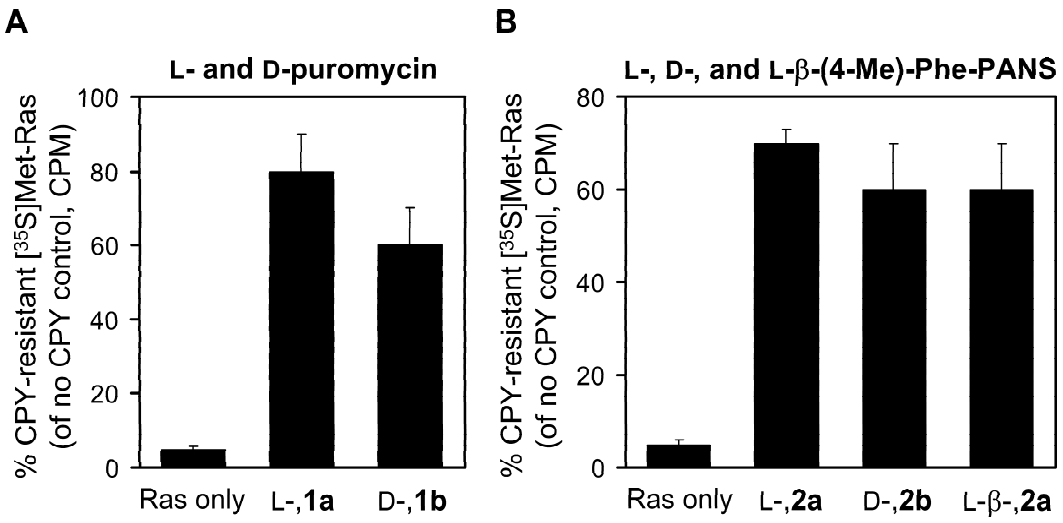

Figure 4.3: Carboxypeptidase Y (CPY) analysis of protein-puromycin products. TCA precipitation of [^{35}S]Met-protein (Ras) from translation reactions after CPY treatment containing (A) Ras only, L-puromycin (**1a**) at 2 μM and D-puromycin (**1b**) at 500 μM. (B) Ras only, L-(4-Me)-Phe-PANS (**2a**) at 1 μM, D-(4-Me)-Phe-PANS (**2b**) at 1500 μM, and L-β-(4-Me)-Phe-PANS (**2c**) at 1000 μM. Data represent the mean $\pm$ standard error for at least three independent experiments.

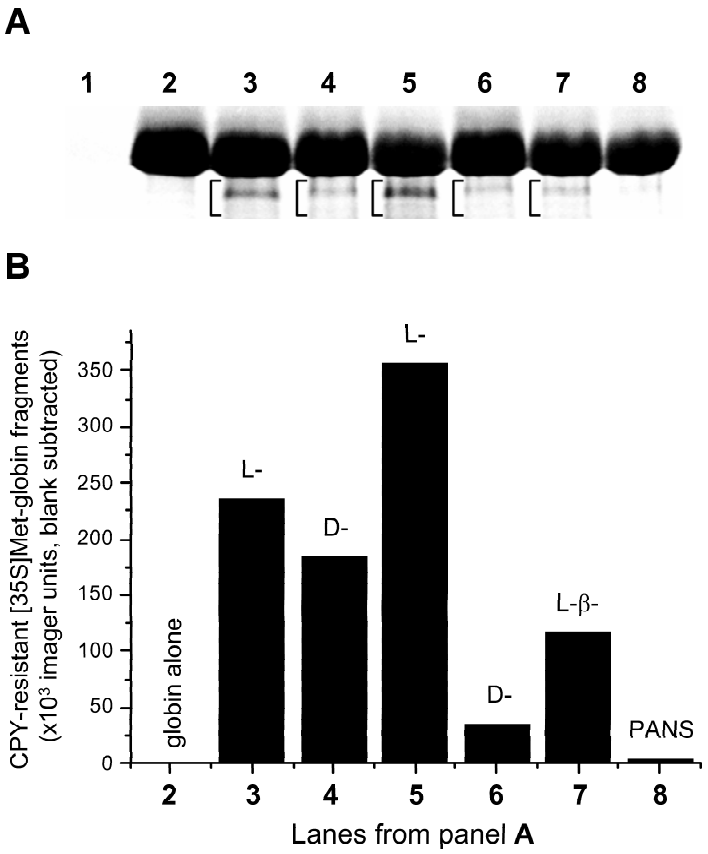

Figure 4.4: (A) Tricine-SDS-PAGE analysis of globin fragments resulting from puromycin and puromycin analog attachment to the C-terminus. Lane 1, no template, no puromycin (blank); lane 2, globin alone, no puromycin; lane 3, L-puromycin (2 μM); lane 4, D-puromycin (500 μM); lane 5, L-(4-Me)-Phe-PANS (2 μM); lane 6, D-(4-Me)-Phe-PANS (1500 μM); lane 7, L-β-(4-Me)-Phe-PANS (1200 μM); lane 8, puromycin aminonucleoside (PANS) (5 mM). PANS is a negative control molecule (no amino acid moiety) to evaluate the production of protein fragments in the presence of high exogenous molecule concentrations. The globin fragment-puromycin complexes are indicated by brackets. (B) Quantification of the globin fragment-puromycin complexes from A.

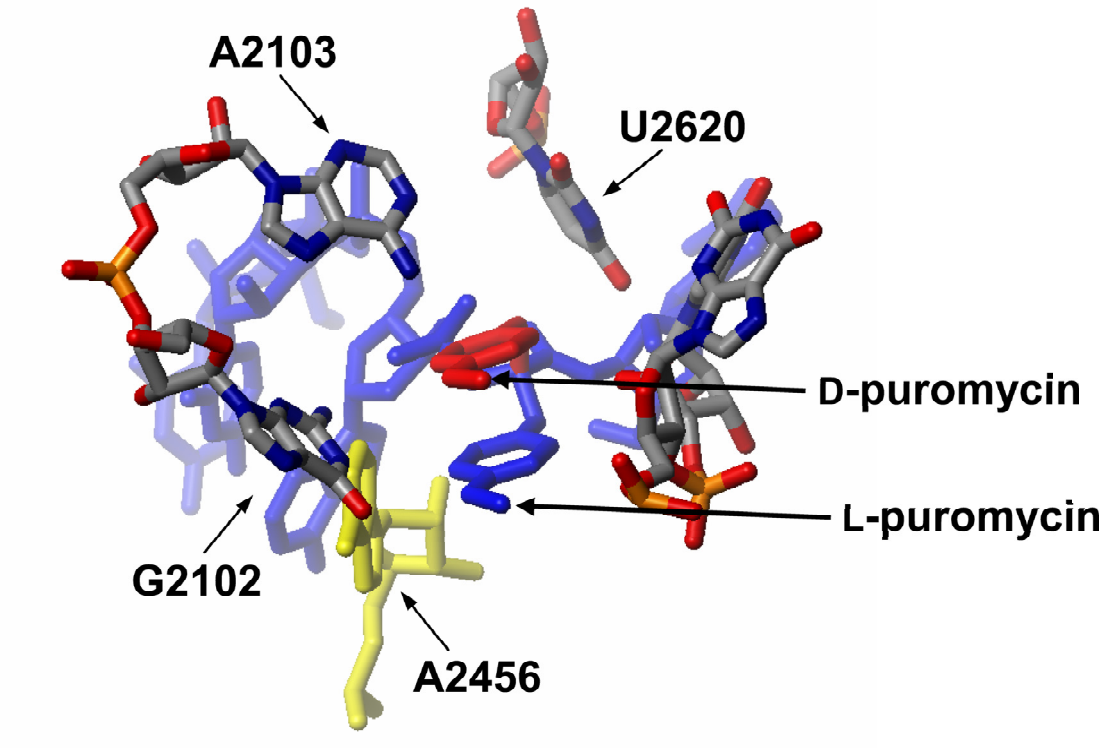

Figure 4.5: Model for D-puromycin (red) placement in the large 50S ribosome-CCdA-p-L-puromycin (blue) complex (29). U2620 is the closest nucleotide to the D-puromycin side chain which may cause steric clash. A2486 (yellow), the base originally identified as involved in peptidyl transferase catalysis, is also shown for reference.

sizing proteins can produce markedly different results (9, 28, 31, 32). The data here provide one metric of the chiral and regiospecificity of mammalian ribosomes. We are hopeful that this approach, along with other information such as the ability to optimize tRNA affinity for elongation factor Tu (EF-Tu) (33, 34) (EF1A in eukaryotes), will facilitate the incorporation of desirable but recalcitrant unnatural residues into peptides and proteins.

4.4 Experimental Procedures

4.4.1 General Information

^{1}H and ^{13}C NMR spectra were recorded on a Varian, Inc. UNITY INOVA instrument operating at 500 MHz using D_2O or DMSO-*d6* as the solvent. ^{1}H NMR data are reported as follows: s, singlet; d, doublet; t, triplet; q, quartet; m, multiplet; br s, broad singlet; dd, doublet of doublets. High-resolution mass spectra (FAB) were recorded on a JMS-600H double-focusing, high-resolution, magnetic sector mass spectrometer at the Mass Spectrometry Laboratory, Division of Chemistry and Chemical Engineering, California Institute of Technology. Column chromatography was carried out on silica gel ($40-63$ μm, EM Science). Analytical HPLC was performed using a Vydac C18 column (5 mm, 4.5 x 250 mm) with buffer A (5 mM NH_4OAc, pH 5.5 with 10% acetonitrile) and buffer B (5 mM NH4OAc, pH 5.5 with 90% acetonitrile); a linear gradient of 100% buffer B in 50 min was used with a flow rate of 1 mL/min. All reagents were of highest available commercial quality and were used without further purification. Puromycin aminonucleoside (3'-amino-3'-deoxy-*N*,*N*'-dimethyladenosine) (PANS) was purchased from Sigma Chemical Co. FMOC-(4-methoxy-D-phenylalanine) and FMOC-(D-alanine) were purchased from Bachem. FMOC-(4-methyl-L-phenylalanine), FMOC-(L-alanine), and FMOC-(L-β-homoalanine) were purchased from Fluka. FMOC-(4-methyl-D-phenylalanine) and FMOC-(4-methyl-L-β-phenylalanine) were from Peptech. Puromycin and puromycin analog concentra-

tions were determined with the following extinction coefficients ($M^{-1}cm^{-1}$) at 260 nm: L- and D-puromycin (**1a** and **1b**) [ϵ = 11,790] in H_2O; L-(4-Me)-Phe-PANS, D-(4-Me)-Phe-PANS, and L-β-(4-Me)-Phe-PANS (**2a** – **2c**) [ϵ = 10,500] in H_2O; and L-Ala-PANS, D-Ala-PANS, and L-β-Ala-PANS (**3a** – **3c**) [ϵ = 11,000] in phosphate buffered saline (pH 7.3). Rabbit reticulocyte lysate was purchased from Novagen. Rabbit globin mRNA was obtained from Life Technologies Gibco BRL. L-Puromycin (**1a**) was purchased from Sigma Chemical Co. Ras mRNA was prepared by using two DNA primers complementary to the 5'- and 3'-ends of the coding region for H-Ras (pProEX HTb vector, a kind gift from Dafna Bar-Sagi) (35) to amplify the gene using PCR. mRNA was produced by T7 runoff transcription (36) of the H-Ras DNA in the presence of RNAsecure (Ambion) followed by gel purification via denaturing urea-PAGE and 'crush and soak' RNA isolation. L-[^{35}S]methionine (1,175 Ci/mmol) was purchased from NEN Life Science Products. Carboxypeptidase Y was obtained from Pierce. GF/A glass microfiber filters were from Whatman. Scintillation counting was carried out using a Beckman LS-6500 liquid scintillation counter.

4.4.2 General Procedure for Preparation of Puromycin Analogs

N, *N*'-dicyclohexylcarbodiimide (DCC) (0.0539 mmol) was added to a cold (0 °C) solution of PANS (0.0520 mmol), FMOC-protected amino acid (0.0541 mmol), and *N*-hydroxysuccinimide (NHS) (0.0556 mmol) in dried *N*,*N*'-dimethylformamide (DMF) (0.900 mL). The solution was stirred for 30 min in an ice-water bath and then for 25 h at ambient temperature. *N*,*N*'-dicyclohexylurea was filtered and washed (EtOAc, 4 mL), and the filtrate was concentrated *in vacuo*. For **1b**, the residue was resuspended in EtOAc, sonicated, and the mixture was filtered and then dried. The material was purified by gradient flash chromatography using $CHCl_3$ → MeOH/$CHCl_3$ (4:96) for **1b** or MeOH/$CHCl_3$ (7:93) for **2a** – **2c** and **3a** – **3c**. Homogenous product fractions were dried *in vacuo* to yield the FMOC-protected product. FMOC-deprotection was

carried out in 20% (v/v) piperidine in DMF (5mL) with stirring for 30 min at ambient temperature. The solvent was removed *in vacuo* and the residue was subjected to gradient flash chromatography using $CHCl_3 \rightarrow MeOH/CHCl_3$ (8:92) for **1b**, **2a**, and **2b** and TEA/MeOH/$CHCl_3$ (2:10:88) for **2c** and **3a**−**3c** to afford the titled products. Confirmation of purity was assessed using analytical HPLC.

9-3'-Deoxy-3'-[(4-methoxy-D-phenylalanyl)amino]-β-D-ribofuranosyl-6-(*N*, *N*'-dimethylamino)purine (D-puromycin) (**1b**) (37) White solid (31.5 mg, 87.3%): ^{1}H (DMSO-*d6*) δ 1.85 (br s, 2H), 2.58-2.63 (m, 1H), 2.93 (dd, J = 4.5, 14 Hz, 1H), 3.42 (dd, J = 4.5, 8.5 Hz, 2H), 3.51-3.56 (m, 2H), 3.72 (s, 6H), 3.93-3.96 (m, 1H), 4.47-4.51 (m, 4H), 5.17 (t, J = 5.5 Hz, 1H), 5.97 (d, J = 2.0 Hz, 1H), 6.17 (d, J = 5.0, 1H), 6.85 (d, J = 9.0 Hz, 2H), 7.15 (d, J = 8.5 Hz, 2H), 8.08 (br s, 1H), 8.24 (s, 1H), 8.45 (s, 1H); ^{13}C (DMSO-*d6*) δ 25.4, 50.6, 56.0, 56.8, 61.7, 73.8, 84.4, 90.2, 114.3, 131.0, 138.7, 150.4, 152.6, 158.0, 175.5; HRMS (FAB), *m/z* calculated for $C_{22}H_{30}N_7O_5$ $(M+H)^+$ 472.2311, found 472.2307.

9-3'-Deoxy-3'-[(4-methyl-L-phenylalanyl)amino]-β-D-ribofuranosyl-6-(*N*, *N*'-dimethylamino)purine [L-(4-Me)-Phe-PANS] (**2a**) Pale white solid (18.8 mg, 80.8%): ^{1}H NMR (DMSO-*d6*) δ 1.84 (br s, 2H), 2.26 (s, 6H), 2.52-2.57 (m, 1H), 2.94 (dd, J = 4.5, 14 Hz, 1H), 3.44-3.52 (m, 2H), 3.67-3.70 (m, 2H), 3.92-3.95 (m, 1H), 4.44-4.50 (m, 4H), 5.14 (t, J = 5.5 Hz, 1H), 5.98 (d, J = 3.0 Hz, 1H), 6.14 (d, J = 4.0 Hz, 1H), 7.10 (dd, J = 8.0, 18 Hz, 4H), 8.07 (d, J = 5.5 Hz, 1H), 8.24 (s, 1H), 8.45 (s, 1H); ^{13}C (DMSO-*d6*) δ 21.3, 41.2, 50.7, 56.9, 61.7, 73.9, 84.3, 90.2, 120.3, 129.4, 129.8, 135.7, 136.3, 138.7, 150.4, 152.6, 155.0, 175.5; HRMS (FAB), *m/z* calculated for $C_{22}H_{30}N_7O_4$ $(M+H)^+$ 456.2362, found 456.2367.

9-3'-Deoxy-3'-[(4-methyl-D-phenylalanyl)amino]-β-D-ribofuranosyl-6-(*N*, *N*'-dimethylamino)purine [D-(4-Me)-Phe-PANS] (**2b**) Pale white solid (20.7 mg, 88.8%): ^{1}H NMR (DMSO-*d6*) δ 1.85 (br s, 2H), 2.26 (s, 6H), 2.61 (dd, J = 8.0, 13 Hz, 1H) 2.96 (dd, J = 4.5, 14 Hz, 1H), 3.42-3.45 (m, 1H), 3.51-3.56 (m, 1H), 3.71-3.73 (m, 2H), 3.94-3.96 (m, 1H), 4.40-4.49 (m, 4H), 4.48 (d, J = 12 Hz, 1H), 5.17 (t, J = 5.5

Hz, 1H), 5.97 (d, J = 2.5 Hz, 1H), 6.19 (br s, 1H), 7.11 (dd, J = 8.0, 16 Hz, 4H), 8.10 (br s, 1H), 8.23 (s, 1H), 8.45 (s, 1H); ^{13}C (DMSO-*d6*) δ 21.4, 41.0, 50.6, 56.8, 61.7, 73.8, 84.4, 90.2, 120.3, 129.4, 129.9, 135.8, 136.1, 138.7, 150.4, 152.6, 155.0, 175.5; HRMS (FAB), m/z calculated for $C_{22}H_{30}N_7O_4$ $(M+H)^+$ 456.2362, found 456.2360.

9-3'-Deoxy-3-[(4-methyl-L-β-phenylalanyl)amino]-β-D-ribofuranosyl-6-(*N*, *N*'-dimethylamino)purine [L-β-(4-Me)-Phe-PANS] (**2c**) Pale white solid (17.8 mg, 73.0%): ^{1}H NMR (D_20) δ 2.06 (s, 6H), 2.45-2.49 (m, 1H), 2.67 (d, J = 6.5 Hz, 1H), 3.18 (t, J = 6.0 Hz, 1H), 3.28 (br s, 3H), 3.37-3.39 (m, 1H), 3.49-3.50 (m, 1H), 3.59-3.62 (m, 1H), 3.80 (dd, J = 2.0, 13 Hz, 1H), 4.08-4.10 (m, 1H), 4.35 (dd, J = 6.0, 8.5 Hz, 1H), 4.46 (dd, J = 3.0, 5.5 Hz, 1H), 5.94 (d, J = 2.5 Hz, 1H), 7.03 (s, 4H), 8.03 (s, 1H), 8.15 (s, 1H); ^{13}C NMR (D_20) δ 19.1, 26.0, 40.5, 49.8, 50.5, 54.5, 60.8, 73.6, 82.7, 89.7, 111.0, 120.0, 129.4, 129.6, 134.0, 137.2, 138.0, 148.8, 152.3, 173.6; HRMS (FAB), m/z calculated for $C_{23}H_{32}N_7O_4$ $(M+H)^+$ 470.2519, found 470.2508.

9-3'-Deoxy-3'-[(L-alanine)amino]-β-D-ribofuranosyl-6-(*N*, *N*'-dimethylamino)purine (L-Ala-PANS) (**3a**) Pale yellow solid (5.7 mg, 30.2%): ^{1}H NMR (D_2O) δ 1.41 (d, J = 7.0 Hz, 3H), 3.28 (br s, 6H), 3.63 (dd, J = 3.5, 13 Hz, 1H), 3.82 (dd, J = 2.5, 13 Hz, 1H), 3.97 (q, J = 7.0 Hz, 1H), 4.17-4.18 (m, 1H), 4.55-4.58 (m, 2H), 4.62-4.64 (m, 1H), 5.98 (d, J = 3.0 Hz, 1H), 8.03 (s, 1H), 8.17 (s, 1H); ^{13}C NMR (D_2O) δ 17.3, 39.0, 49.4, 51.0, 60.7, 73.5, 82.7, 89.6, 119.5, 138.0, 148.8, 152.2, 154.6, 172.4; HRMS (FAB), m/z calculated for $C_{15}H_{24}N_7O_4$ $(M+H)^+$ 366.1892, found 366.1889.

9-3'-Deoxy-3'-[(D-alanine)amino]-β-D-ribofuranosyl-6-(*N*, *N*'-dimethylamino)purine (D-Ala-PANS) (**3b**) Pale yellow solid (8.6 mg, 45.4%): ^{1}H NMR (D_20) δ1.43 (d, J = 7.5 Hz, 3H), 3.28 (br s, 6H), 3.65 (dd, J = 4.0, 13 Hz, 1H), 3.83 (dd, J = 2.5, 13 Hz, 1H), 4.02 (q, J = 7.5 Hz, 1H), 4.14-4.17 (m, 1H), 4.55-4.58 (m, 2H), 4.64-4.66 (m, 1H), 5.98 (d, J = 3.0 Hz, 1H), 8.04 (s, 1H), 8.17 (s, 1H); ^{13}C NMR (D_20) δ 17.0, 39.0, 49.3, 50.9, 60.8, 73.3, 82.8, 89.6, 106.0, 119.6, 138.1, 152.3, 154.8, 172.0; HRMS (FAB), m/z calculated for $C_{15}H_{24}N_7O_4$ $(M+H)^+$

366.1892, found 366.1898.

9-3'-Deoxy-3'-[(L-β-homoalanine)amino]-β-D-ribofuranosyl-6-(*N*, *N*'-dimethylamino)purine (L-β-Ala-PANS) (**3c**) Pale yellow solid (4.6 mg, 25.6%): ^{1}H NMR (D_20) δ 1.16 (d, J = 6.5 Hz, 3H), 1.74 (s, 1H), 2.52 (d, J = 3.5 Hz, 2H), 3.24 (br s, 6H), 3.52-3.61 (m, 2H), 3.78 (d, J = 13 Hz, 1H), 4.11 (d, J = 5.5 Hz, 1H), 4.62-4.64 (m, 2H), 5.93 (s, 1H), 7.99 (s, 1H), 8.13 (s, 1H); ^{13}C NMR (D_20) δ 18.2, 39.0, 39.5, 45.0, 50.7, 60.7, 73.5, 82.7, 89.6, 119.5, 138.0, 148.8, 152.2, 172.7; HRMS (FAB), m/z calculated for $C_{16}H_{26}N_7O_4$ $(M+H)^+$ 380.2049, found 380.2054.

4.4.3 IC_{50} Determination

Translation reactions containing [^{35}S]Met were made up in batch on ice and added in aliquots to microcentrifuge tubes containing an appropriate amount puromycin or puromycin analog dried *in vacuo*. Typically, a 20 μl translation mixture consisted of 0.8 μL of 2.5 M KCl, 0.4 μL of 25 mM MgOAc, 1.6 μL of 12.5X Translation Mixture without methionine (25 mM dithiothreitol (DTT), 250 mM HEPES (pH 7.6), 100 mM creatine phosphate, and 312.5 μM of 19 amino acids, except methionine), 3.6 μL of nuclease-free water, 0.6 μL (6.1 μCi) of [^{35}S]Met (1175 Ci/mmol), 8 μL of Red Nova nuclease-treated lysate, and 5 μL of 0.05 μg/μL globin mRNA. Inhibitor, lysate preparation (include all components except template), and globin mRNA were mixed simultaneously and incubated at 30 °C for 60 min. Then 2 μL of each reaction was combined with 8 μL of tricine loading buffer (80 mM Tris-Cl (pH 6.8), 200 mM DTT, 24% (v/v) glycerol, 8% sodium dodecyl sulfate (SDS), and 0.02 % (w/v) Coomassie blue G-250), heated to 90 °C for 5 min, and applied entirely to a 4% stacking portion of a 16% tricine SDS-polyacrylamide gel containing 20% (v/v) glycerol (38) (30 mA for 1.5h). Gels were fixed in 10% acetic acid (v/v) and 50% (v/v) methanol, dried, exposed overnight on a PhosphorImager screen, and analyzed using a Storm PhosphorImager (Molecular Dynamics). Analysis in Figure 4 was carried out as described above except 6 μL of each reaction and 24 μL of tricine loading buffer were loaded

(1.5-fold increase in stacking and resolving portion of gel; 30mA for 7 h).

4.4.4 Carboxypeptidase Assay

Translation reactions were prepared as described for IC_{50} determination except reactions (50 μL) contained 2 μL of 2.5 M KOAc, 1 μL of 25 mM MgOAc, 4 μL of 12.5X Translation Mixture without methionine (25 mM dithiothreitol (DTT), 250 mM HEPES (pH 7.6), 100 mM creatine phosphate, and 312.5 μM of 19 amino acids, except methionine), 16 μL (163 μCi) of [^{35}S]Met (1175 Ci/mmol), 20 μL of Red Nova nuclease-treated lysate, and 6.96 μL of 230 μg/mL Ras mRNA (35). Inhibitor, lysate components, and Ras mRNA were mixed simultaneously and incubated at 30 °C for 60 min. Then 2 μL of reaction was combined with 150 μL of 0.1 M sodium acetate (pH 5.0) and 17 μL carboxypeptidase Y (CPY) (1 mg/mL in 0.05 M sodium citrate (pH 5.3) Pierce), and incubated at 37 °C for 18 h. After incubation, reactions were mixed with 100 μL of 1 N NaOH/2% H_2O_2 (hydrolyzes charged tRNAs and removes the red color that may quench scintillation counting) and incubated at 37 °C for 10 min to hydrolyze the charged tRNAs. Then 0.9 mL of 25% trichloroacetic acid (TCA)/2% casamino acids was added to the samples, vortexed, and put on ice for 10 min. The samples were filtered on GF/A filters (pre-soaked in 5% TCA), washed 3 times with 3-mL portions of cold 5% TCA, and scintillation counted to determine the amount of [^{35}S]Met-Ras. For the no CPY-treated samples, [^{35}S]Met-Ras (2 μL of reaction) was TCA precipitated without CPY treatment as described above.

Acknowledgement

This work was supported by NIH grant (R01 60416) to R.W.R. and by NIH training grant GM07616 (S.R.S.).

References

[1] T.G. Heckler, Y. Zama, T. Naka, and S.M. Hecht. Dipeptide formation with misacylated RNA^{Phe}s. *J. Biol.Chem.*, 258:4492–4495, 1983.

[2] J.D. Bain, C.G. Glabe, T.A. Dix, and A.R Chamberlin. Biosynthetic site-specific incorporation of a non-natural amino-acid into a polypeptide. *J. Am. Chem. Soc.*, 111:8013–8014, 1989.

[3] J.D. Bain, D.A. Wacker, E.E. Kuo, and A.R Chamberlin. Site-specific incorporation of nonnatural residues into peptides - Effect of residue structure on suppression and translation efficiencies. *Tetrahedron*, 47:2389–2400, 1991.

[4] C.J. Noren, S.J. Anthony-Cahill, M.C. Griffith, and P.G. Schultz. A general method for site-specific incorporation of unnatural amino-acids into proteins. *Science*, 244:182–188, 1989.

[5] M.W. Nowak, P.C. Kearney, J.R. Sampson, M.E. Saks, C.G. Labarca, S.K. Silverman, W. Zhong, J. Thorson, J.N. Abelson, N. Davidson, P.G. Schultz, D.A. Dougherty, and H.A Lester. Nicotinic receptor binding site probed with unnatural amino acid incorporation in intact cells. *Science*, 268:439–442, 1995.

[6] S. Li, S. Millward, and R.W. Roberts. *In vitro* selection of mRNA display libraries containing an unnatural amino acid. *J. Am. Chem. Soc.*, 124:9972–9973, 2002.

[7] T.T. Takahashi, R.J. Austin, and R.W. Roberts. mRNA display: ligand discovery, interaction analysis and beyond. *Trends Biochem. Sci.*, 28:159–165, 2003.

[8] J. Ellman, D. Mendel, S. Anthony-Cahill, C.J. Noren, and P.G. Schultz. Site-specific incorporation of novel backbone structures into proteins. *Science*, 202:301–336, 1992.

[9] S.M. Hecht. Probing the synthetic capabilities of a center of biochemical catalysis. *Acc. Chem. Res.*, 25:545–552, 1992.

[10] V.W. Cornish, D. Mendel, and P.G. Schultz. Probing protein structure and function with an expanded genetic code. *Angew. Chem. Int. Ed. Engl*, 34:621–633, 1995.

[11] Gilmore M.A., L.E. Steward, and A.R. Chamberlin. Incorporation of noncoded amino acids by *in vitro* protein biosynthesis. *Topics Curr. Chem.*, 202:77–99, 1999.

[12] J.C.M. van Hest and D.A. Tirrell. Protein-based materials, toward a new level of structural control. *Chem. Comm.*, 19:1897–1904, 2001.

[13] T. Yamane, D.L. Miller, and J.J. Hopfield. Discrimination between D-tyrosyl and L-tyrosyl transfer ribonucleic-acids in peptide-chain elongation. *Biochemistry*, 20:1897–1904, 1981.

[14] S. Chládek and M. Sprinzl. The 3'-end of transfer-RNA and its role in protein biosynthesis. *Angew. Chem. Int. Ed. Engl.*, 24:371–391, 1985.

[15] T.G. Heckler, J.R. Roesser, C. Xu, P.-I. Chang, and S.M. Hecht.

[16] J.R. Roesser, C. Xu, R.C. Payne, C.K. Surratt, and S.M. Hecht. Preparation of misacylated aminoacyl-transfer RNA^{PHE}s useful as probes of the ribosomal acceptor site. *Biochemistry*, 28:5185–5195, 1989.

[17] D. Mendel, J. Ellman, and P.G. Schultz. Protein biosynthesis with conformationally restricted amino acids. *J. Am. Chem. Soc.*, 115:4359–4360, 1993.

[18] J.A. Killian, M.D. Van Cleve, Y.F. Shayo, and S.M. Hecht. Ribosome-mediated incorporation of hydrazinophenylalanine into modified peptide and protein analogues. *J. Am. Chem. Soc.*, 120:3032–3042, 1998.

[19] J.T. Koh, V.W. Cornish, and P.G. Schultz. An experimental approach to evaluating the role of backbone interactions in proteins using unnatural amino acid mutagenesis. *Biochemistry*, 36:11314–11322, 1997.

[20] B.M. Eisenhauer and S.M. Hecht. Site-specific incorporation of (aminooxy)acetic acid into proteins. *Biochemistry*, 41:11472–11478, 2002.

[21] P.M. England, Y. Zhang, D.A. Dougherty, and H.A. Lester. Backbone mutations in transmembrane domains of a ligand-gated ion channel: Implications for the mechanism of gating. *Cell*, 96:89–98, 1999.

[22] D. Nathans. Puromycin inhibition of protein synthesis - Incorporation of puromycin into peptide chains. *Proc. Natl. Acad. Sci. U.S.A.*, 51:585–592, 1964.

[23] S. Fahnestock, H. Neumann, and A. Shashoua, V. Rich. Ribosome-catalyzed ester formation. *Biochemistry*, 9:2477–2483, 1970.

[24] J. Gooch and A.O. Hawtrey. Synthesis of thiol-containing analogues of puromycin and a study of their interaction with *N*-acetylphenylalanyl-transfer ribonucleic-acid on ribosomes to form thioesters. *Biochem. J.*, 149:209–220, 1975.

[25] D. Nathans and A. Neidle. Structural requirements for puromycin inhibition of protein synthesis. *Nature*, 197:1076–1077, 1963.

[26] R.J. Harris, J.E. Hanlon, and R.H. Symons. Peptide bond formation on the ribosome - Structural requirements for inhibition of protein synthesis and of release of peptides from peptidyl-transferRNA on bacterial and mammalian ribosomes by aminoacyl and nucleotidyl analogues of puromycin. *Biochim. Biophys. Acta*, 240:244–262, 1971.

[27] S. Campuzano and J. Modolell. Hydrolysis of GTP on elongation-factor TU. Ribosome complexes promoted by 2'(3')-*O*-L-phenylalanyladenosine. *Proc. Natl. Acad. Sci. U.S.A.*, 77:905–909, 1980.

[28] S.R. Starck and R.W. Roberts. Puromycin oligonucleotides reveal steric restrictions for ribosome entry and multiple modes of translation inhibition. *RNA*, 8:890–903, 2002.

[29] P. Nissen, J. Hansen, N. Ban, P.B. Moore, and T.A. Steitz. The structural basis of ribosome activity in peptide bond synthesis. *Science*, 289:920–930, 2000.

[30] N. Polacek, M. Gaynor, A. Yassin, and A.S. Mankin. Ribosomal peptidyl transferase can withstand mutations at the putative catalytic nucleotide. *Nature*, 411:498–501, 2001.

[31] A.A. Krayevsky and M.K. Kukhanova. The peptidyltransferase center of ribosomes. *Prog. in Nucleic Acids Res.*, 23:2–51, 1979.

[32] P. Bhuta, G. Kumar, and S. Chládek. The peptidyltransferase center of *Escherichia coli* ribosomes: binding sites for the cytidine 3'-phosphate residues of the aminoacyl-tRNA 3'- terminus and the interrelationships between the acceptor and donor sites. *Biochim. Biophys. Acta*, 696:208–211, 1982.

[33] F.J. LaRiviere, A.D. Wolfson, and O.C. Uhlenbeck. Uniform binding of aminoacyl-tRNAs to elongation factor Tu by thermodynamic compensation. *Science*, 294:165–168, 2001.

[34] O. C. Asahara, H.; Uhlenbeck. The tRNA specificity of *Thermus thermophilus* EF-Tu. *Proc. Natl. Acad. Sci. U.S.A.*, 99:3499–3504, 2002.

[35] P.A. Boriack-Sjodin, S.M. Margarit, D. Bar-Sagi, and J. Kuriyan. The structural basis of the activation of Ras by Sos. *Nature*, 395:337–343, 1998.

[36] J.F. Milligan and O.C. Uhlenbeck. Synthesis of small RNAs using T7 RNA-polymerase. *Methods Enzymol.*, 180:51–62, 1989.

[37] M.J. Robins, R.W. Miles, and M.C. Samano. Nucleic acid related compounds, part 115. Syntheses of puromycin from adenosine and 7-deazapuromycin from tubercidin, and biological comparisons of the 7-aza/deaza pair. *J. Org. Chem.*, 66:8204–8210, 2001.

[38] H. Schagger and G.V. von Jagow. Tricine-sodium dodecyl sulfate-polyacrylamide gel electrophoresis for the separation of proteins in the range from 1 to 100 kDa. *Anal. Biochem.*, 166:368–379, 1987.

Chapter 5

The Puromycin Route to Assess Amine Substitution Constraints on Peptide Bond Formation

Abstract

The use of puromycin analogs to probe the stereo- and regiospecificity of the ribosome shows that our protein synthesis machinery tolerates a wide range of unnatural residues (e.g., D-residues and β-amino acids). This approach offers a direct means to study the allowances of translation without the drawbacks of using chemically misacylated-tRNAs. Here, the limits of translation are studied with respect to substitution of the primary amine (e.g., secondary amine or N-methyl amine). Surprisingly, the amine is extremely sensitive to substitution since the activity of N-substituted analogs are dramatically lower than analogues with primary amines (7- to 500-fold loss in activity relative to the unsubstituted counterpart). The loss in activity upon primary amine substitution is thought to result in part from a change in the rate-determining step of peptide bond formation or from altered basicity of the substituted amine.

5.1 Background

N-substituted amino acids are a class of residues that show potential utility in the area of peptide- or protein-based therapeutics. Several properties render these unnatural amino acids useful for such therapies because they are 1) less polar than normal α-amino acids, which increases their bioavailability and 2) resistant to common human proteases. Nature appears to already utilize substituted amino acids such as proline and hydroxyproline in type I collagen to insure conformational rigidity in the collagen triple helix (1, 2). Further, substitution of an *N*-substituted amino acid (*N*-methyl-glycine) for proline in Src homology 3 (SH3) ligands maintains the high-specificity recognition and affinity for the SH3 scaffold (3). Recently, the utility of *N*-substituted amino acids in therapeutics led to the discovery that *N*-methyl-*N*-pyrimidin-2-yl glycine derivatives have antiphlogistic activity (4). In addition, *N*-substituted peptide antagonists of the Bradykinin receptor, a receptor directly involved with several inflammatory disease states, prove to be therapeutic leads (5). For these reasons, incorporation of *N*-substituted amino acids into peptides and proteins has been an area of intense research.

There are a diverse set of *N*-substituted amino acids that have been incorporated into peptides and proteins through aminoacyl-tRNA delivery (Figure 5.1). These experiments show that incorporation of the *N*-substituted residues is measurable, with a ~5 to ~70 suppression efficiency (Figure 5.1) (6, 7). This result is encouraging but is convoluted by the necessity for an elongation factor (EF-Tu in prokaryotes and EF1A in eukaryotes) to escort the *N*-substituted amino acid-tRNA (aa-tRNA) complex into the ribosome. Improper interactions between the aa-tRNA complex and elongation factor are expected to decrease the efficiency amino acid incorporation. Amino acids that bind to EF-Tu too tightly or too weakly may offset the optimum affinity balance (8, 9). Although, the optimal affinity may be generated by using a tRNA body that compensates for the amino acid affinity. This is a solution inferred from data showing that affinity for EF-Tu is a function of the amino acid identity

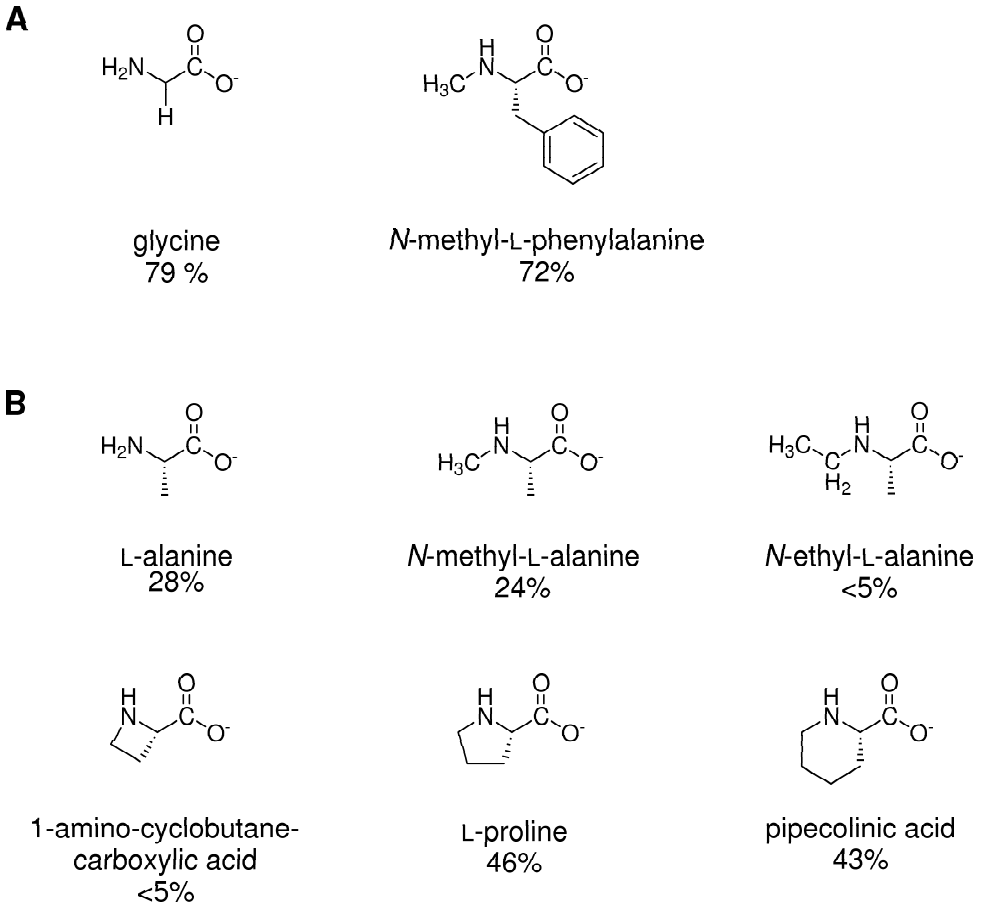

Figure 5.1: *N*-substituted amino acids inserted into (A) peptides (6) and (B) protein (7). Percent values indicate the extent of nonsense codon suppression using chemically misacylated-tRNAs

and the tRNA body sequence (8, 9).

Identification of *N*-substituted residues that are recognized by the ribosome and participate in peptidyl transferase is important for preparation of peptide-based libraries, such as those used in mRNA display (10, 11). Unnatural amino acid suppression techniques offer an excellent means to decipher those variants incorporated into protein. However, this strategy is labor intensive, burdened by low yields of unnatural aa-tRNA product, and costly. Further, extrapolation of ribosome toleration for *N*-substituted amino acids can not be directly assessed using this technique. In contrast, a direct means to examine the peptidyl transferase activity of *N*-substituted amino acids is to use puromycin analogs bearing *N*-methyl or other primary amine substitutions (12). Once the *N*-substituted amino acid is shown to participate in peptide-bond formation, use of an appropriate tRNA body to thermodynamically compensate for the unnatural amino acid, may yield an aa-tRNA complex readily recognized by EF-Tu or EF1A (8, 9). In this chapter, the peptidyl transferase activity of various *N*-substituted puromycin analogs is investigated.

5.2 Results and Discussion

Proline is the only naturally occurring substituted amino acid, bearing a secondary amine. Proline should be called an imino acid since the side chain is continuous within the backbone yielding a five-member ring. Proline is present 5.1% in proteins (13) and collagen is comprised from 25% of proline and hydroxyproline (14), its incorporation is thought to be readily accommodation by the ribosome. Therefore, it was of interest whether a puromycin analog of proline, called L-Pro-PANS (**1**) (Figure 5.2), would be recognized by the ribosome. The literature already had demonstrated that small, non-aromatic amino acids such as proline or alanine function poorly in translation (15). But this is thought to result from poor interactions within the A-site, which could be favorable between aromatic rings such as phenylalanine and tyrosine with the RNA

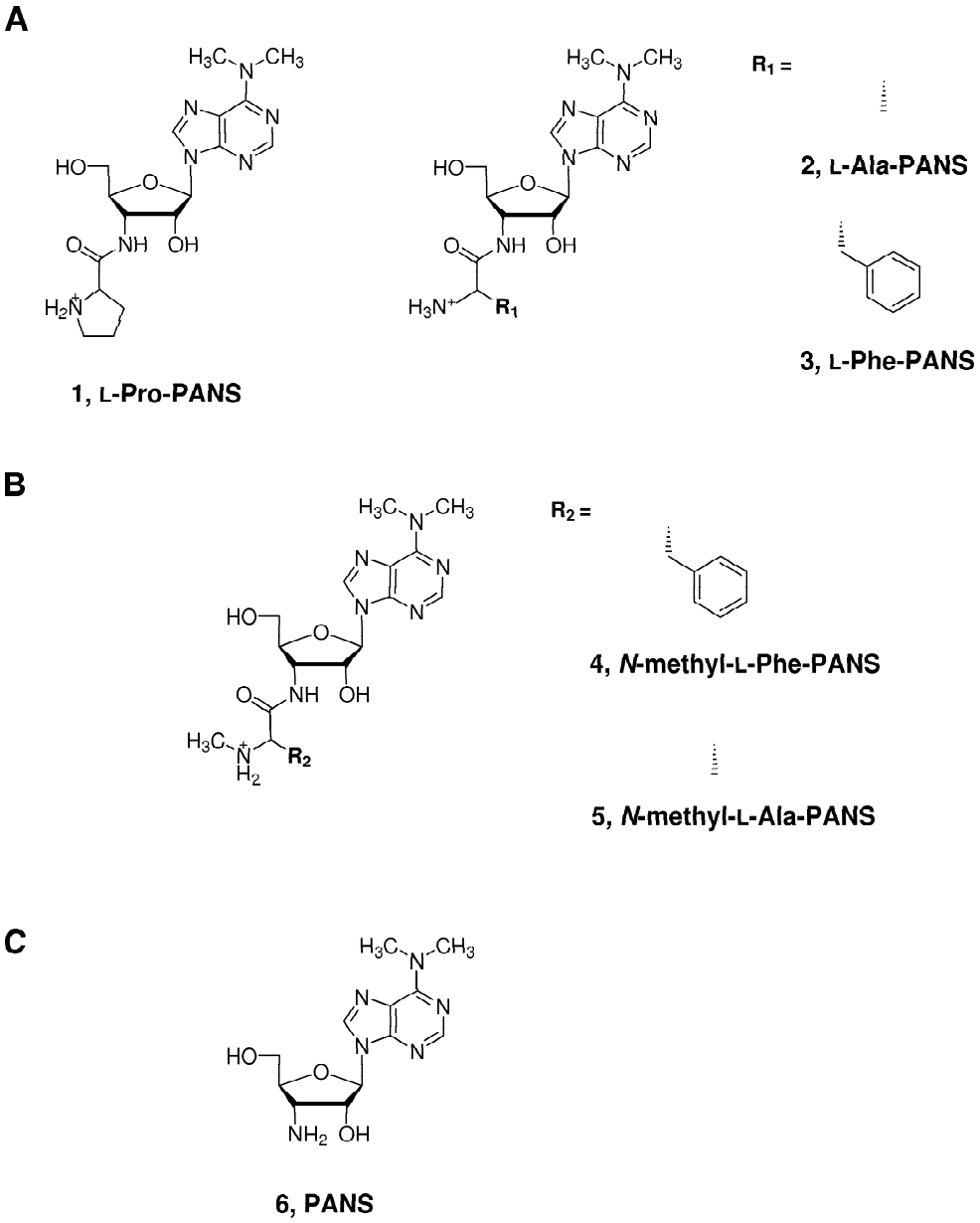

Figure 5.2: Puromycin analogs. (A) Analogs with naturally occurring amino acids, (B) *N*-methyl-substituted amino acid analogs, and (C) puromycin aminonucleoside (PANS)

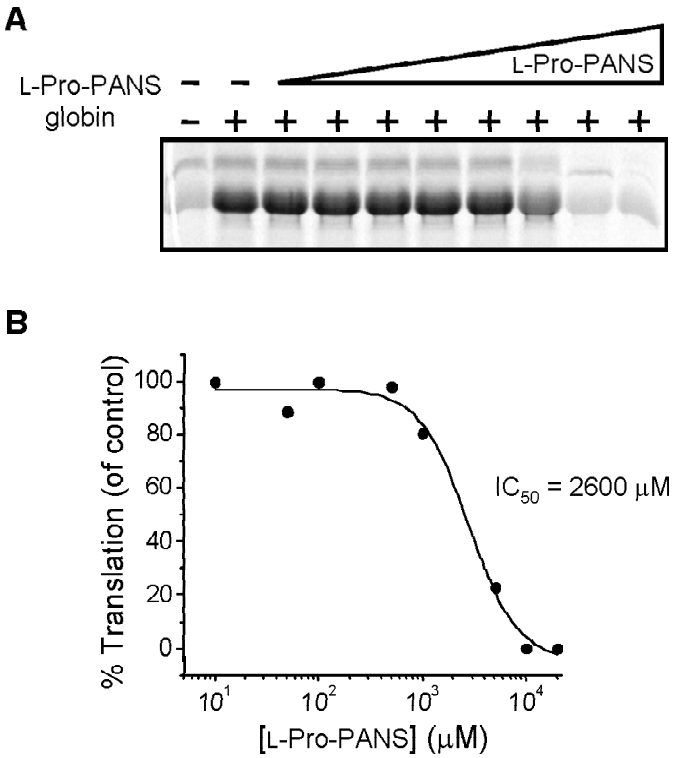

Figure 5.3: IC_{50} determination for L-Pro-PANS (**1**). Globin mRNA was translated with increasing amounts of **1**, resolved using tricine-SDS-PAGE, and quantitated by detection of [^{35}S]Met-globin. (A) Translation of globin with **1**: lane 1, no template; lane 2, globin alone; lanes 3 – 17, concentrations from 0.01 to 20 mM. (B) Percent of globin translation relative to a no-drug control.

bases. But how does L-Pro-PANS compare with previously tested small puromycin analogs (e.g., L-Ala-PANS and L-β-Ala-PANS)? Surprisingly, L-Pro-PANS inhibited translation of globin with an IC_{50} of 2.6 mM (Figure 5.3 and Table 5.1). This is nearly 4-fold less active than L-Ala-PANS (**2**) and 2-fold less potent than the unnatural amino acid analog L-β-Ala-PANS (IC_{50} = 0.73 and 1.7 mM, respectively) (Table 5.1 and reference (12)). This significant difference in activity between L-Pro-PANS (**1**) and L-Ala-PANS (**2**) is not expected to result from side chain size since L-Pro-PANS is actually larger than L-Ala-PANS (MW = 391 and 365 g/mol, respectively). Since

Puromycin analog	IC_{50} (μM)
1, L-Pro-PANS	2600
2, L-Phe-PANS	5.9
3, L-Ala-PANS	730*
4, *N*-methyl-L-Phe-PANS	2900
5, *N*-methyl-L-Ala-PANS	4800
6, PANS	3800

Table 5.1: IC_{50} values for *N*-substituted puromycin analogs (*Data from (12))

they are both non-polar, hydrophobic amino acid analogs, other conclusions based on hydrophobicity or charge-charge interactions do not apply. However, this dramatic lack of activity puts into question whether other *N*-substituted amino acid analogs would also show a significant loss in activity compared to the primary amino acid counterpart.

To address this question, a series of analogs with and without *N*-methylation were prepared and tested for inhibition of translation (Figure 5.2B). Once again, the presence of a *N*-methyl group appears to abolish the potency of the analog, even a highly active analog, such as L-phenylalanine-PANS (L-Phe-PANS, **3**). For example, L-Phe-PANS inhibits translation with an IC_{50} of 5.9 μM, while *N*-methyl-L-Phe-PANS (**4**) shows ~500-fold loss in activity (Table 5.1). This trend is seen further with *N*-methyl-L-Ala-PANS (**5**) which is ~7-fold less potent than L-Ala-PANS (**2**) (Table 5.1). The IC_{50} for puromycin aminonucleoside (PANS, **6**) (Figure 5.2C) was determined to be 3.8 mM (Table 5.1). Not only did addition of a methyl group on L-Ala-PANS diminish its potency, but to the extent that the analog was less active than PANS itself, which does not even bear a reactive amine. Although, it is unknown exactly why PANS inhibits translation, biochemical and structural data show that the equivalent base in aa-tRNA does make interactions with the ribosomal RNA within

the A-site (16, 17).

These results directly implicate the presence of a methyl group as responsible for activity loss. Apparently, substitution on the reactive nucleophile of puromycin analogs severely inhibits activity in the peptidyl transferase reaction. However, why does the addition of a methyl group or a natural amino acid analog such as L-Pro-PANS lack the expected level of potency?

Peptide bond formation is simply attack of an amine on an activated carbon through a tetrahedral intermediate (Figure 5.4). Depending on the natures of the ester and the amine, the breakdown of the intermediate or the attack of the amine on the carbonyl carbon of the ester can be the rate-limiting step in solution (19). Further insights may be inferred from experiments where the aminolysis of methyl formate is measured using various *N*-substituted amines (20). In this study, the rate of amine attack and the rate of the tetrahedral intermediate breakdown are determined using primary, secondary, and tertiary amines (20). The rate of amine attack (K_2) appeared to correlate positively with the basicity or pKa of the molecule (Figure 5.5A). More basic amines tended to attack methyl formate faster than less basic amines, which is expected. However, the rate of tetrahedral breakdown (K_4) showed that there is negative correlation between pKa and rate (Figure 5.5A). The increased basicity of the amine actually stabilizes the tetrahedral intermediate considerably.

The loss in activity with *N*-substitution, either with addition of a methyl group or with L-Pro-PANS, could reflect the stability of the tetrahedral intermediate with the P-site held aa-tRNA. While the IC_{50} determination assays are under multiple turnover conditions where the rate of the tetrahedral intermediate breakdown can not be derived, the effect of a more stable intermediate may decrease the inhibitory potential of the analog (Figure 5.5B). The stability of the intermediate may allow incoming aa-tRNAs to compete more effectively and exclude the *N*-substituted analog from the peptidyl transferase reaction.

Ab initio calculations of amino acids with and without *N*-substitution reveal that

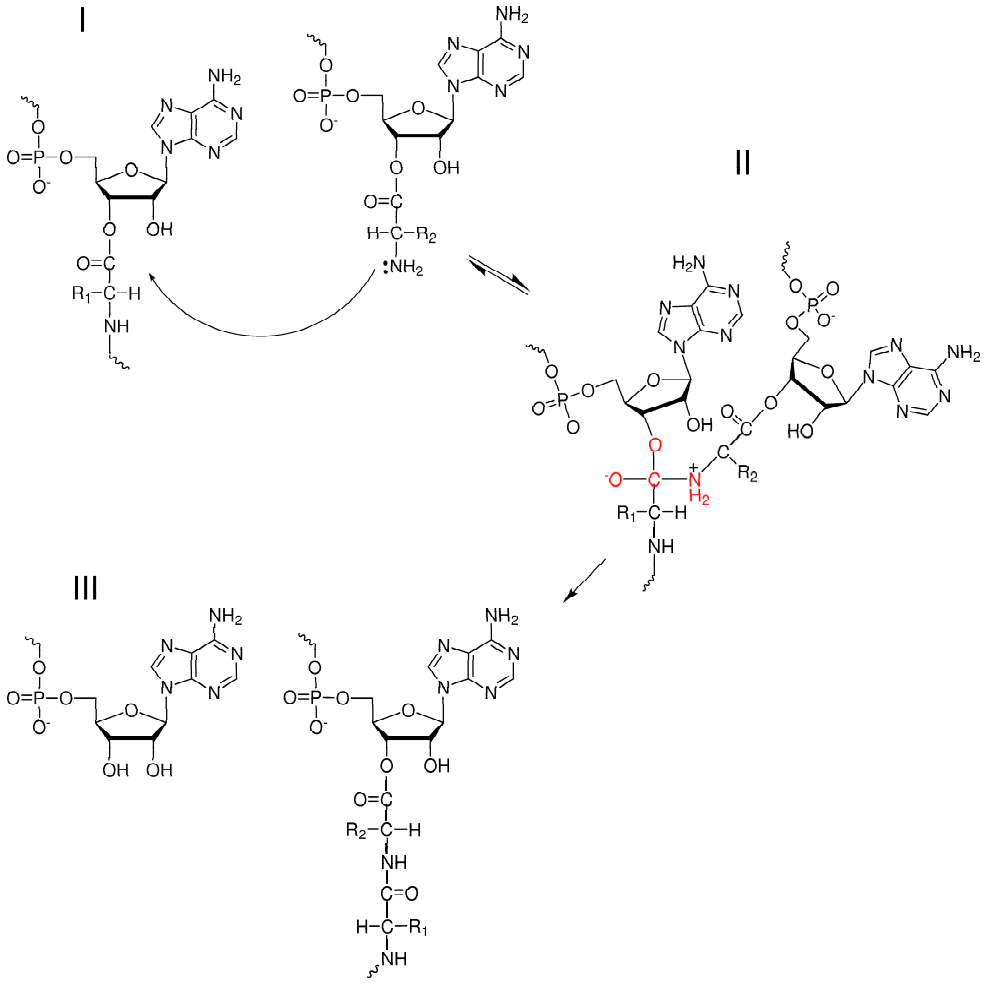

Figure 5.4: Mechanism of peptide bond formation in the ribosome. I, a free amine nucleophilically attacks an activated carbonyl carbon of a P-site held aa-tRNA; II, a zwitterionic tetrahedral intermediate (atoms in red) is formed; and III, the intermediate loses a proton to yield a new peptide bond and an empty P-site tRNA. Figure adapted from (18).

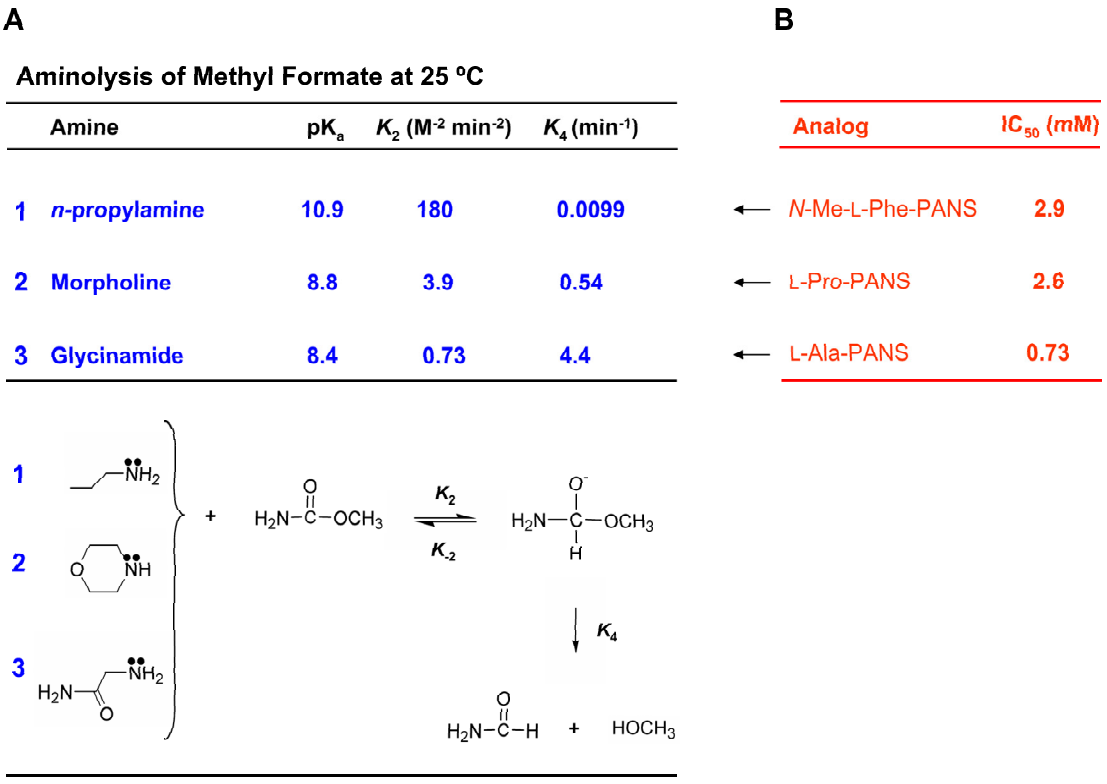

Figure 5.5: Comparison of amine attack rate on methyl formate [data from 19] to IC_{50} values for the *N*-substituted amino acid analogs *N*-Me-L-Phe-PANS (**4**), L-proline-PANS (**1**), and L-Ala-PANS (**2**) (Figure 5.2).

Amino acid	δ_N
L-Phe	-1.023
N-methyl-L-Phe	-0.761
N-ethyl-L-Phe	-0.941
N-isopropyl-L-Phe	-0.950
N-phenyl-L-Phe	-0.819

Table 5.2: Partial negative charge of *N*-substituted phenylalanine amino acids (calculations made using SPARTAN ESSENTIAL Copyright 1991-2001 by Wavefunction Inc. Hartree-Frock minimizations with a 6-31G* basis minimization set employed.)

the partial negative charge of the amine decreases with increased substitution (Table 5.2). This is a counterintuitive result based on the gas-phase basicity of amines where $NH_3 < CH_3CH_2NH_2 < (CH_3CH_2)_2NH < (CH_3CH_2)_3N$. However, the basicity of amines in solution follows a different pattern where $NH_3 < RNH_2 \sim R_3N < R_2NH$. This discontinuity results from the balance between electron release from alkyl groups (and dispersion of positive charge) and solvation effects from hydrogen bonding (Figure 5.6).

The SPARTAN calculation identifies the partial coulombic charge on the nitrogen. This calculation takes into account the electronic environment surrounding the nitrogen atom and depicts the change in bond polarity with different *N*-substituents. The decreased activity of *N*-substituted analogs may indicate that the optimum balance between positive charge dispersion and solvation through hydrogen bonding is seen with L-Phe-PANS (similar to A in Figure 5.6) instead of *N*-methyl-L-Phe-PANS (similar to B in Figure 5.6). While this calculation was carried out only with the amino acid group, not the entire amino acid-PANS derivative, there may be some validity with this analysis. As such, the presence of a larger *N*-substituent such as an ethyl or isopropyl group may preserve the nucleophilicity of the amine (greater

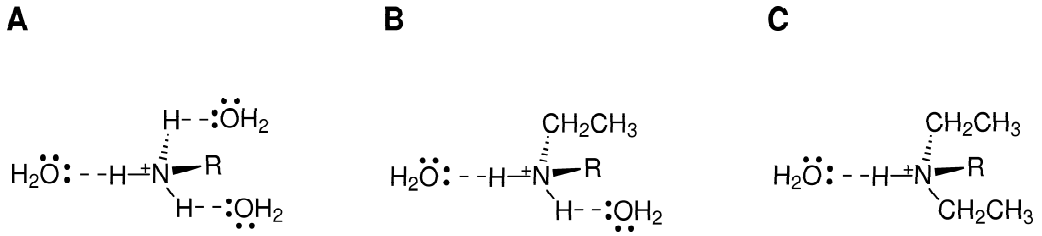

Figure 5.6: Schematic of hydrogen bonding potential for a A) primary amine with three protons on nitrogen available for H-bonding, B) secondary amine with two protons on nitrogen available for H-bonding, and C) tertiary amine with one proton on nitrogen available for H-bonding.

positive charge dispersion than by a methyl group) as evidenced by the higher δ_N values (Table 5.2). More *N*-substituted puromycin derivatives will need to prepared and tested for activity to assess the validity of these theories.

5.3 Conclusions

The peptidyl transferase reaction appears to be sensitive to substitution on the reactive amine in puromycin analogs. Even small substituents, such as a methyl group, diminish the potency of the amino acid analog. This is supported by data using puromycin analogs with *N*-substitution which shows that even a naturally occurring amino acid such as proline becomes a poor substrate when presented to the ribosome in the context of L-Pro-PANS (**1**), which is an effect that may also be seen with L-proline-tRNA at proline codons. Perhaps the kinetics of peptide bond formation vary with different amino acids even in tRNA-mediated peptidyl transferase. These studies may allow the unnatural amino acid incorporation data to be evaluated further since an amino acid bearing a substitution may still be active in peptide bond formation if the substituent does not increase the basicity (and the stability of the tetrahedral intermediate) of the amine dramatically. For example, a -CF_3 group on the α-nitrogen

would still inhibit protease activity, but not enhance the stability of the tetrahedral intermediate. However, the electronegativity of fluorine may reduce the reactivity of nitrogen or compete with nitrogen as a peptide bond acceptor. Nevertheless, these data provide a framework for the design of an *N*-substituted-unnatural amino acid that maintains high therapeutic value as well as reactivity in the peptidyl transferase reaction.

5.4 Experimental Procedures

5.4.1 General Information

Low-resolution mass spectra were recorded on a PE SCIEX API 365 triple quadruple electrospray mass spectrometer at the Beckman Institute Mass Spectrometry Laboratory, California Institute of Technology. High-resolution mass spectra (FAB) were recorded on a JMS-600H double-focusing, high-resolution, magnetic sector mass spectrometer at the Mass Spectrometry Laboratory, Division of Chemistry and Chemical Engineering, California Institute of Technology. Column chromatography was carried out on silica gel (40 – 63 μm, EM Science). Analytical HPLC was performed using a Vydac C18 column (5 mm, 4.5 x 250 mm) with buffer A (5 mM NH_4OAc, pH 5.5 with 10% acetonitrile) and buffer B (5 mM NH_4OAc, pH 5.5 with 90% acetonitrile); a linear gradient of 100% buffer B in 50 min was used with a flow rate of 1 mL/min. All reagents were of highest available commercial quality and were used without further purification. Puromycin aminonucleoside (3'-amino-3'-deoxy-*N*,*N*'-dimethyl-adenosine) (PANS) was purchased from Sigma Chemical Co. FMOC-(L-phenylalanine) and FMOC-(L-alanine) were obtained from Novabiochem and Fluka, respectively. FMOC-(L-proline), FMOC-*N*-methyl-L-(phenylalanine), FMOC-*N*-methyl-L-(alanine) were purchased from Novabiochem. Puromycin analog concentrations were determined with the following extinction coefficients ($M^{-1}cm^{-1}$) at 260 nm: Non-aromatic puromycin analogs such as L-Pro-PANS (**1**), L-Ala-PANS (**2**), *N*-methyl-

L-Ala-PANS (**5**) and PANS (**6**) [$\epsilon = 11,000$] in phosphate buffered saline (pH 7.3); aromatic puromycin analogs such as L-Phe-PANS (**3**) and *N*-methyl-L-Phe-PANS (**4**) [$\epsilon = 10,500$] in H_2O. Rabbit reticulocyte lysate was purchased from Novagen. Rabbit globin mRNA was obtained from Life Technologies Gibco BRL.

5.4.2 General Procedure for Preparation of Puromycin Analogs

N,N'-dicyclohexylcarbodiimide (DCC) (0.0539 mmol) was added to a cold (0 °C) solution of PANS (0.0520 mmol), FMOC-protected amino acid (0.0541 mmol), and *N*-hydroxysuccinimide (NHS) (0.0556 mmol) in dried *N,N*'-dimethylformamide (DMF) (0.900 mL). The solution was stirred for 30 min in an ice-water bath and then for 25 h at ambient temperature. *N,N*'-dicyclohexylurea was filtered and washed (EtOAc, 4 mL), and the filtrate was concentrated *in vacuo*. The material was purified by gradient flash chromatography using MeOH/$CHCl_3$ (7:93). Homogenous product fractions were dried *in vacuo* to yield the FMOC-protected product. FMOC-deprotection was carried out in 20% (v/v) piperidine in DMF (5mL) with stirring for 30 min at ambient temperature. The solvent was removed *in vacuo* and the residue was subjected to gradient flash chromatography using $CHCl_3 \rightarrow$ TEA/MeOH/$CHCl_3$ (7:10:83) for **1**; $CHCl_3 \rightarrow$ TEA/MeOH/$CHCl_3$ (2:10:88) for **2**

5.4.3 IC_{50} Determination

Translation reactions containing [^{35}S]Met were made up in batch on ice and added in aliquots to microcentrifuge tubes containing an appropriate amount puromycin or puromycin analog dried *in vacuo*. Typically, a 20μl translation mixture consisted of 0.8 μL of 2.5 M KCl, 0.4 μL of 25 mM MgOAc, 1.6 μL of 12.5X Translation Mixture without methionine (25 mM dithiothreitol (DTT), 250 mM HEPES (pH 7.6), 100 mM creatine phosphate, and 312.5 μM of 19 amino acids, pexcept methionine),

3.6 μL of nuclease-free water, 0.6 μL (6.1 μCi) of [^{35}S]Met (1175 Ci/mmol), 8 μL of Red Nova nuclease-treated lysate, and 5 μL of 0.05 μg/μL globin mRNA. Inhibitor, lysate preparation (all components except template), and globin mRNA were mixed simultaneously and incubated at 30 °C for 60 min. Then 2 μL of each reaction was combined with 8 μL of tricine loading buffer (80 mM Tris-Cl (pH 6.8), 200 mM DTT, 24% (v/v) glycerol, 8% sodium dodecyl sulfate (SDS), and 0.02 % (w/v) Coomassie blue G-250), heated to 90 °C for 5 min, and applied entirely to a 4% stacking portion of a 16% tricine SDS-polyacrylamide gel containing 20% (v/v) glycerol (21)(30 mA for 1.5h). Gels were fixed in 10% acetic acid (v/v) and 50% (v/v) methanol, dried, exposed overnight on a PhosphorImager screen, and analyzed using a Storm PhosphorImager (Molecular Dynamics).

Acknowledgements

I gratefully acknowledge Jennifer Treweek and Binghai Ling, SURF students during Summer 2003 at the California Institute of Technology, for their contributions to this chapter, including the synthesis and characterization of several puromycin analogs.

References

[1] J. Josse and W.F. Harrington. Role of pyrrolidine residues in structure + stabilization of collagen. *J. Mol. Biol.*, 9:269–287, 1964.

[2] N.K. Shah, J.A.M. Ramshaw, A. Kirkpatrick, C. Shah, and B. Brodsky. A host-guest set of triple-helical peptides: Stability of Gly-X-Y triplets containing common nonpolar residues. *Biochemistry*, 35:10262–10268, 1996.

[3] J.T. Nguyen, C.W. Turck, F.E. Cohen, R.N. Zuckermann, and W.A. Lim. Exploiting the basis of proline recognition by SH3 and WW domains; design of *N*-substituted inhibitors. *Science*, 282:2088–2092, 1998.

[4] O. Bruno, S. Schenone, A. Ranise, F. Bondavalli, W. Filippelli, G. Falcone, G. Motola, and F. Mazzeo. Antiinflammatory agents: new series of N-substituted amino acids with complex pyrimidine structures endowed with antiphlogistic activity. *Farmaco*, 54:95–100, 1999.

[5] V.S. Goodfellow, M.V. Marathe, K.G. Kuhlman, T.D. Fitzpatrick, D. Cuadrado, W. Hanson, J.S. Zuzack, S.E. Ross, M. Wieczorek, M. Burkard, and E.T. Whalley. Receptor antagonists containing *N*-substituted amino acids: *In vitro* and *in vivo* B-2 and B-1 receptor antagonist activity. *J. Med. Chem.*, 39:1472–1484, 1996.

[6] J.D. Bain, D.A. Wacker, E.E. Kuo, and A.R Chamberlin. Site-specific incor-

poration of nonnatural residues into peptides - Effect of residue structure on suppression and translation efficiencies. *Tetrahedron*, 47:2389–2400, 1991.

[7] J. Ellman, D. Mendel, S. Anthony-Cahill, C.J. Noren, and P.G. Schultz. Site-specific incorporation of novel backbone structures into proteins. *Science*, 202:301–336, 1992.

[8] F.J. LaRiviere, A.D. Wolfson, and O.C. Uhlenbeck. Uniform binding of aminoacyl-tRNAs to elongation factor Tu by thermodynamic compensation. *Science*, 294:165–168, 2001.

[9] O. C. Asahara, H.; Uhlenbeck. The tRNA specificity of *Thermus thermophilus* EF-Tu. *Proc. Natl. Acad. Sci. U.S.A.*, 99:3499–3504, 2002.

[10] T.T. Takahashi, R.J. Austin, and R.W. Roberts. mRNA display: ligand discovery, interaction analysis and beyond. *Trends Biochem. Sci.*, 28:159–165, 2003.

[11] A. Frankel, S.W. Millward, and R.W. Roberts. Encodamers: Unnatural peptide oligomers encoded in RNA. *Chem. Biol.*, 10:1043–1050, 2003.

[12] S.R. Starck, X. Qi, B.N. Olsen, and R.W. Roberts. The puromycin route to assess stereo- and regiochemical constraints on peptide bond formation in eukaryotic ribosomes. *J. Am. Chem. Soc.*, 125:8090–8091, 2003.

[13] P. McCaldon and P. Argos. Oligopeptide biases in protein sequences and their use in predicting protein coding regions in nucleotide-sequences. *Proteins-Struct. Func. Genet.*, 4:99–122, 1988.

[14] P.P. Fietzek and K. Kuhn. Information contained in amino-acid sequence of alpha1(I)-chain of collagen and its consequences upon formation of triple helix, of fibrils and crosslinks. *Mol. Cell Biochem.*, 8:141–157, 1975.

[15] D. Nathans and A. Neidle. Structural requirements for puromycin inhibition of protein synthesis. *Nature*, 197:1076–1077, 1963.

[16] R. Green, C. Switzer, and HF. Noller. Ribosome-catalyzed peptide-bond formation with an A-site substrate covalently linked to the 23S ribosomal RNA. *Science*, 280:286–289, 1998.

[17] P. Nissen, J. Hansen, N. Ban, PB. Moore, and Steitz TA. The structural basis of ribosome activity in peptide bond synthesis. *Science*, 289:920–930, 2000.

[18] R. Green and J.R. Lorsch. The path to perdition is paved with protons. *Cell*, 110:665–668, 2002.

[19] G.M. Blackburn and W.P. Jencks. The mechanism of the aminolysis of methyl formate. *J. Am. Chem. Soc.*, 90:2638–2645, 1968.

[20] A.C. Satterthwait and W.P. Jencks. The mechanism of the aminolysis of acetate esters. *J. Am. Chem. Soc.*, 96:7018–7031, 1974.

[21] H. Schagger and G.V. von Jagow. Tricine-sodium dodecyl sulfate-polyacrylamide gel electrophoresis for the separation of proteins in the range from 1 to 100 kDa. *Anal. Biochem.*, 166:368–379, 1987.

Chapter 6

Stereoselectivity of Translation in Live Cells

Abstract

Translation fidelity in living cells is attained through several steps during protein synthesis. For example, the elongation factor 1A (EF1A) preferentially delivers L-amino acids versus D-amino acids (via aminoacyl-tRNA) to the ribosome. However, D-residues can be introduced into protein by puromycin analogs since they act in an elongation-factor independent mode. Here, various puromycin analogs with L- and D- stereochemistry are used to test the effect on cell viability. D-amino acid analogs are toxic to cells but it appears that ribosomal stereospecificity is variable and a function of amino acid side chain identity. For a flexible side chain (biocytin), there appears to be negligible selectivity for the L- versus D-analog. These data have broad implications for the *in vivo* synthesis of peptides or proteins bearing stereochemically altered residues.

6.1 Background

Proteins synthesized on the ribosome are comprised entirely of L-amino acids. Several proofreading steps ensure that only L-amino acids are incorporated into protein. For example, EF-Tu which escorts aminoacyl-tRNA (aa-tRNA) into the ribosome, preferentially binds L-aa-tRNA over D-aa-tRNA (1). In addition, the peptidyl transferase reaction was not previously recognized to accommodate D-residues since a puromycin analog with a D-configuration (D-phenylalanine-PANS) did not inhibit translation in an *E. coli* extract and in rabbit reticulocyte lysate (2). In addition, incorporation of D-residues was unsuccessful using the chemically misacylated-tRNA strategy with D-residues (3, 4). Based on these data, the toxicity of D-amino acids in live cells is expected to be insignificant. However, *in vitro* analysis of L- and D-puromycin analogs (**1** and **2**, respectively; Figure 6.1) suggested that D-residues are active in translation (5). But whether D-puromycin would also function in live cells remained unexamined.

There is utility in determining whether D-residues are incorporated into protein in live cells and what influences there potency. D-residues are fundamental residues in many cyclic peptides, some of which are antibiotics such as gramicidin A or bacitracin. However, these peptides are synthesized by nonribosomal peptide synthetases (NRPS), which can utilize both L- and D-amino acids (6). These enormous protein complexes are highly specialized for the sequence to be synthesized, yet require large individual protein complexes for each amino acid to be coupled. Therefore, reconstitution of biosynthetic pathways (7) for novel peptides or peptide libraries remains a challenge. However, the discovery that ribosomes do utilize D-residues *in vitro* may allow peptide libraries (8, 9) to be screened for novel antibiotics, immunosuppressants, or even D-peptide-based drugs that are amenable to oral administration.

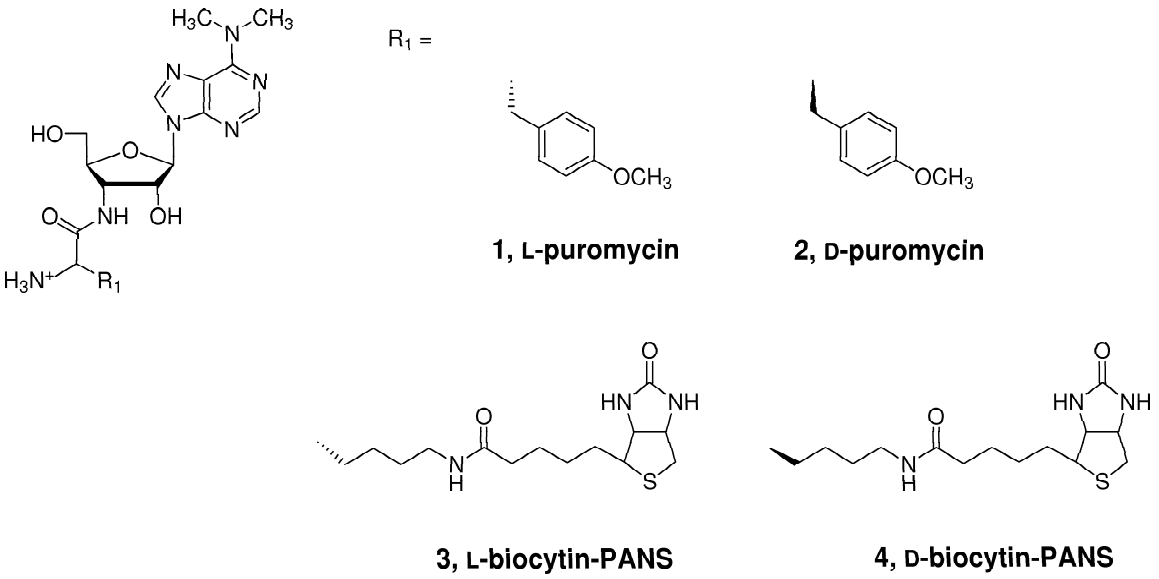

Figure 6.1: L- and D-amino acid analogs used in live cell assays.

6.2 Results and Discussion

The first experiment was to determine the cell sensitivity to to L- (**1**) and D-puromycin (**2**) (Figure 6.1). L-puromycin is known to be toxic to cells, but the concentration varies according to the cell line. The cell line used for these studies was a stable mammalian thymocyte 16610D9 cell line (D9) (10) which was used previously to test the labeling of protein by fluorescent puromycin conjugates (11). D9 cells were incubated with an L-puromycin concentration (10 μM) shown to be highly toxic to mammalian cells (optimal working concentration for L-puromycin varies from $2-20$ μM for mammalian cell lines). A D-puromycin concentration 100-fold greater (1000 μM) was used since *in vitro* analysis showed D-puromycin to have $\sim$150-fold reduced potency for inhibition of translation (5). Indeed, D-puromycin was also toxic to cells (24 h) and at a concentration that was only 100-fold greater than L-puromycin (Figure 6.2A). After a 48 h incubation with increasing amounts of D-puromycin, the concentration that killed 50% of the cells (EC_{50}) was 580 μM (Figure 6.2B).

These data establish for the first time that a D-amino acid analog is toxic to

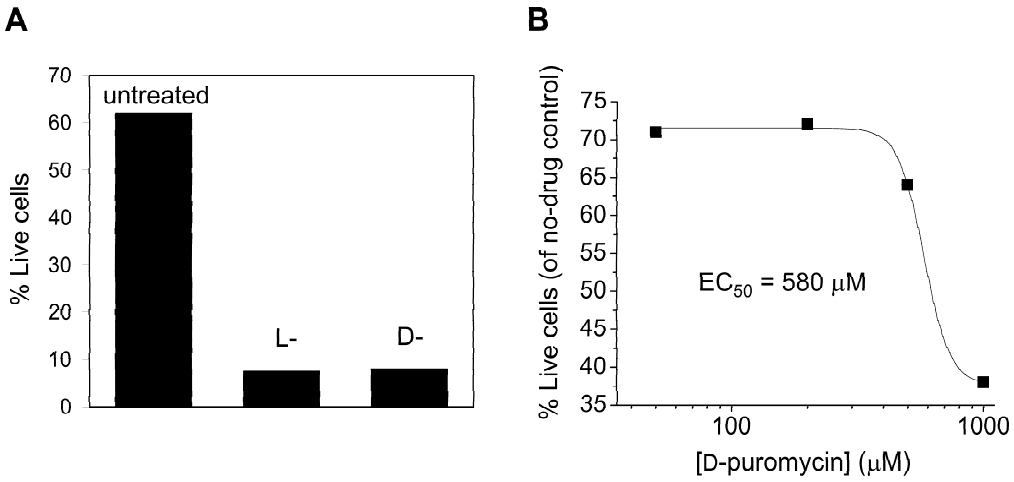

Figure 6.2: (A) Toxicity of L- (10μM) and D-puromycin (1000 μM) to live cells during a 24 h incubation. (B) D-puromycin concentration required to kill 50 percent of cells (EC_{50}) relative to an untreated control after a 48 h incubation.

mammalian cells. The concentration required for killing is rather high but reflects the fold discrimination (L- versus D-) obtained from *in vitro* translation experiments (5). L-puromycin toxicity is thought to result from participation in peptidyl transferase. This suggests that D-puromycin toxicity is also related to inhibition of translation through a similar mechanism.

The purity of the D-puromycin preparation is important in these experiments since any contaminating L-puromycin would cause the cells to die. Therefore, purity of the D-puromycin synthesis was assessed using HPLC chromatography. Isolated L- and D-amino acids are enantiomers and are expected to have identical chromatography profiles. But L- and D-puromycin derivatives are diastereomers and have unique physical properties which should be detectable from HPLC. Indeed, HPLC analysis of L- and D-puromycin shows that the D-puromycin sample is highly pure (Figure 6.3). This suggests that the effect observed results from D-puromycin toxicity, not from L-analog contamination.

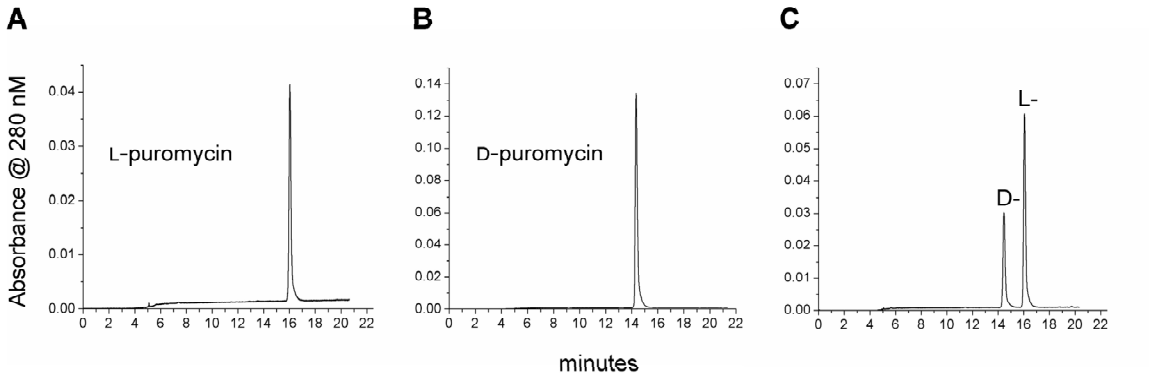

Figure 6.3: HPLC analysis of (A) L- and (B) D-puromycin and (C) L- and D-puromycin co-injection.

Another strategy to ensure the purity of the D-analog sample is to carry out selective enrichment experiments of cells containing puromycin *N*-acetyl-transferase (PAC) (12). This enzyme *N*-acetylates the reactive amine on L-puromycin and blocks its ability to participate in peptide bond formation (13, 14). In a mixed population of cells, those that lack a vector expressing PAC can be selectively killed by long incubations ($\geq$48 hours) with puromycin, leaving only vector-containing cells alive. The marker for PAC activity in these experiments was GFP from the construct (MIG_{PAC}) used previously to confirm the chemical activity of puromycin-dye conjugates *in vivo* (Figure 6.4) (11). Cells infected with MIG_{PAC} should be enriched by only L-puromycin since PAC is a typical, highly stereospecific enzyme. If the D-puromycin synthesis contains any contaminating L-puromycin, then selective enrichment of GFP(+) cells should also be detected. Incubation of D9 cells infected with MIG_{PAC} with either L- or D-puromycin showed that L-puromycin (5 μM) enriched for 98% of MIG_{PAC} cells (Figure 6.5A). However, D-puromycin did not yield MIG_{PAC} cell enrichment, even up to a 1 mM D-puromycin concentration (Figure 6.5B).

A 0.05% L-puromycin contamination in the D-sample is equivalent to 0.5 μM of the

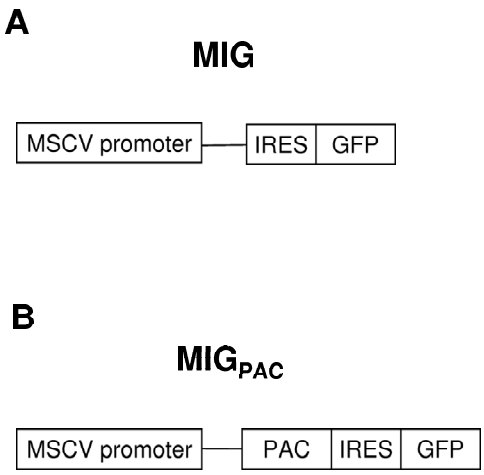

Figure 6.4: Constructs used to infect 16610D9 thymocyte cells. (A) MIG contains GFP and (B)MIG$_{\mathrm{PAC}}$ contains GFP and PAC rendering cells insensitive to puromycin action.

the L-species. Even this low level of L- contamination would yield detectable GFP(+) population enrichment, which is observed in the L-puromycin enrichment experiment (Figure 6.5A). This is strong evidence to support a highly pure D-puromycin preparation (<0.05%). Therefore, the toxic effect observed in the presence of D-puromycin results solely from the activity of the D-analog.

The stereoselectivity of ribosomes in mammalian cells (inferred from the toxicity of the analogs) showed ~100-fold discrimination between L- and D-puromycin (Figure 6.2). Previously, it was shown that *in vitro* ribosomal stereoselectivity falls over a broad range and is dictated by the size and geometry of the pendant side chain (5). Therefore, it was of interest to test the level of discrimination of other L- and D-amino acid analog pairs. The next pair tested was L-biocytin-PANS (**3**) and D-biocytin-PANS (**4**) (Figure 6.1).

The viability of D9 cells was determined after incubation with both L- and D-analogs. The % live cells in the presence of L- and D-puromycin at identical con-

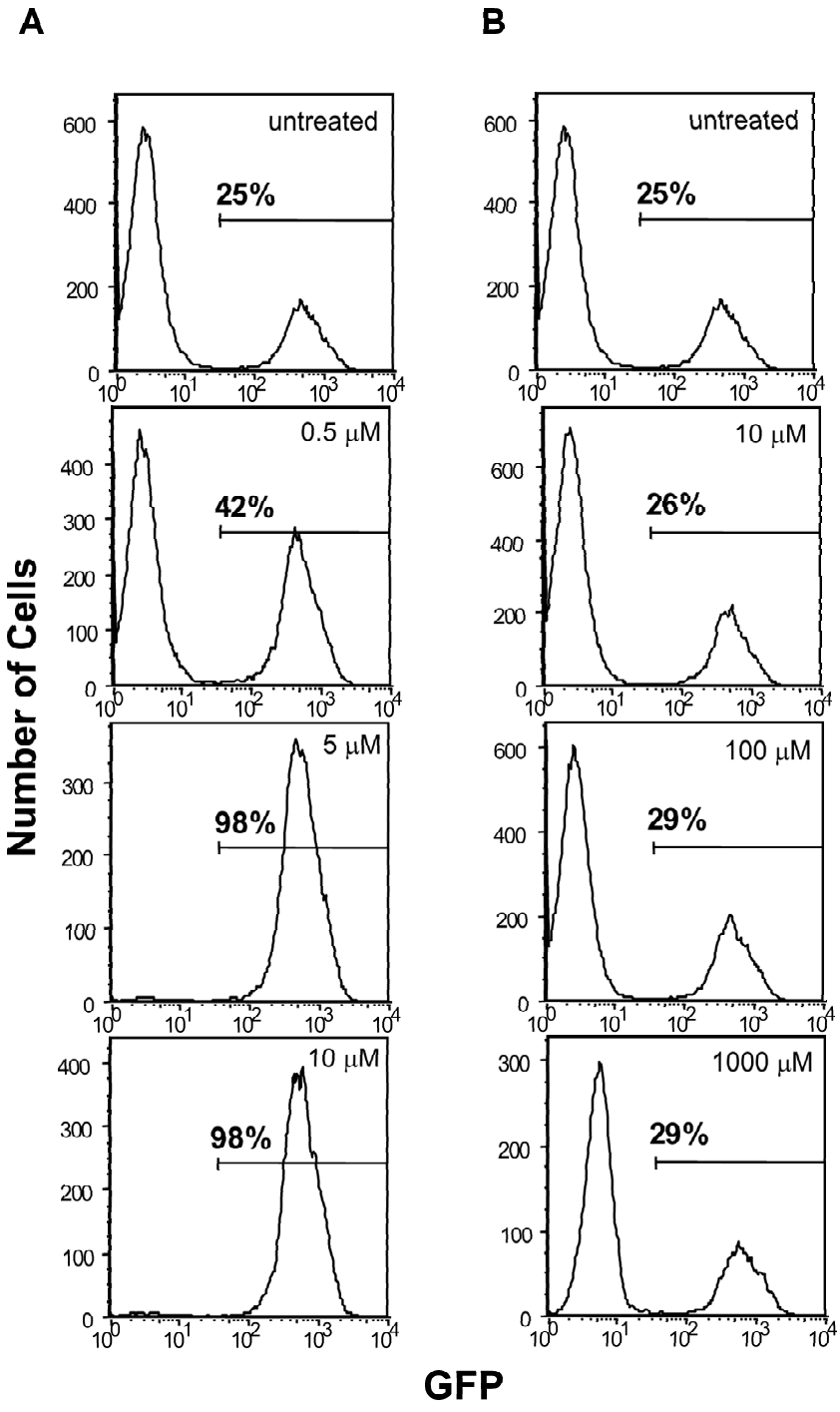

Figure 6.5: GFP(+) cell enrichment achieved with (A) L-puromycin but not with (B) D-puromycin.

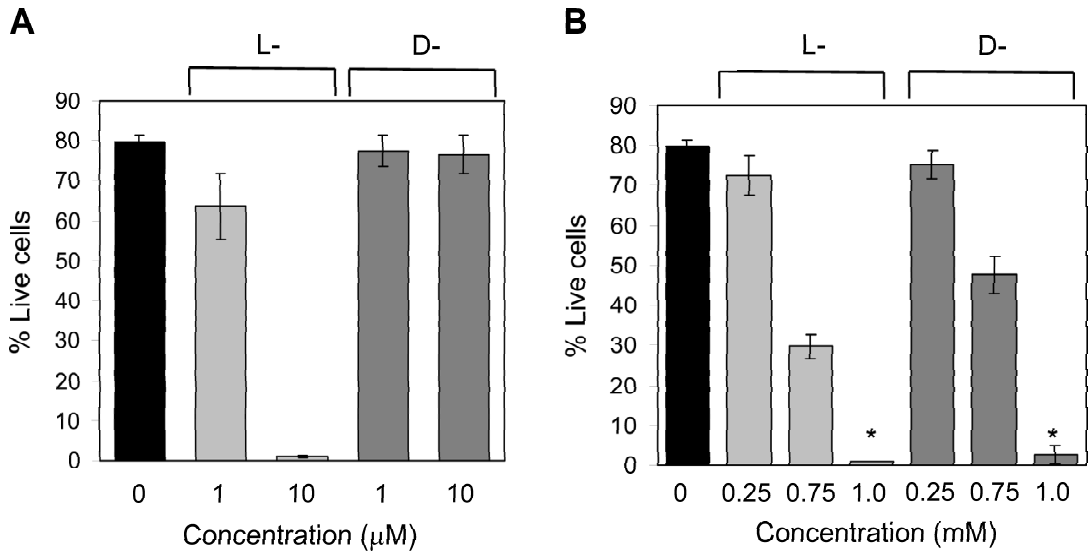

Figure 6.6: Viability of D9 thymocyte cells in the presence of L- and D-amino acid analogs. Cells are sensitive to the stereochemistry of (A) L- and D-puromycin but not (B) L- and D-biocytin-PANS. The mean ± standard error is calculated from three independent experiments except for *samples which were obtained from two independent experiments with minor changes (See Experimental Procedures).

centrations varies considerably (Figure 6.6A). However, for L- and D-biocytin-PANS at the same concentrations the % live cells is not dissimilar at each concentration tested (Figure 6.6B). In fact, the *in vitro* IC_{50} values for L- and D-biocytin-PANS are identical (Figure 6.7).

These data suggest that the side chain affects the level of discrimination the ribosome can make for the L-amino acid analog versus the D-analog (Figure 6.6). Assuming the loss in cell viability results from inhibition of translation, ribosomes in live cells also show a range of stereoselectivity. This reduced selectivity suggests that incorporation of D-residues may be possible with certain amino acids, given the ribosome shows little or no preference for the L- versus the D-variant.

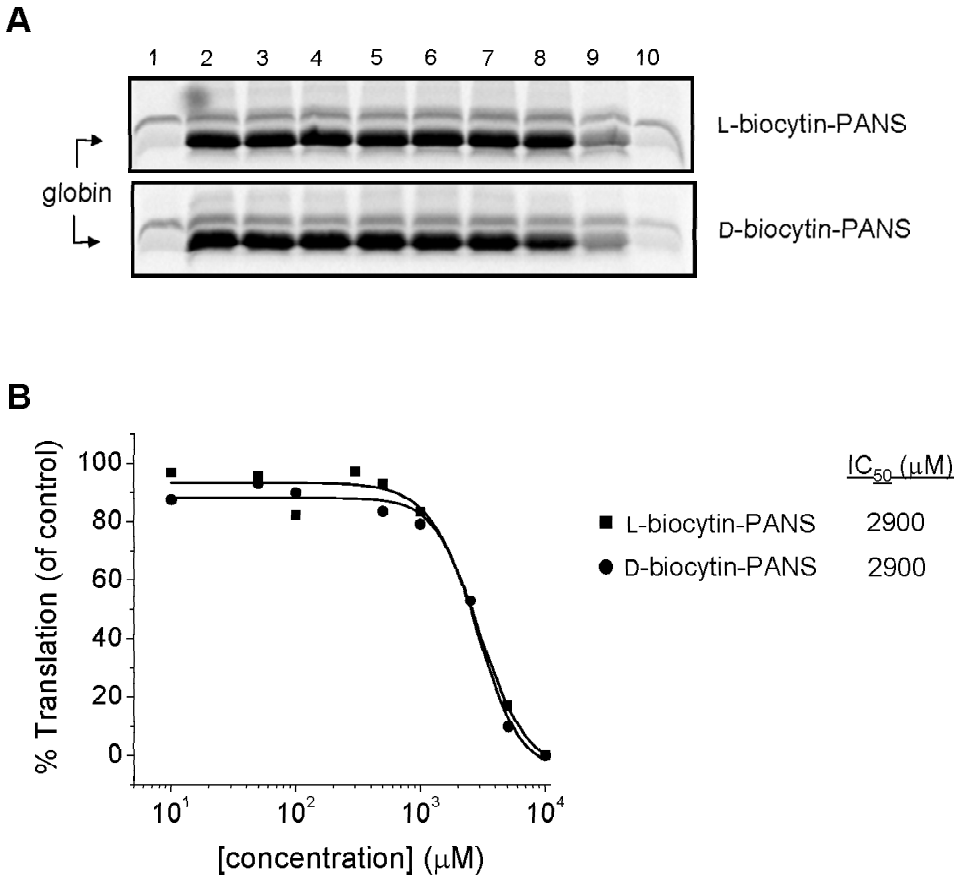

Figure 6.7: *In vitro* activity analysis (IC_{50}) for L- and D-biocytin-PANS. Globin mRNA was translated with increasing amounts of analog, resolved using tricine-SDS-PAGE, and quantitated by detection of [^{35}S]Met-globin as described (see Experimental Procedures). (A) Translation of globin with L-biocytin-PANS and D-biocytin-PANS: lane 1, no template; lane 2, globin alone; lanes $3-17$, concentrations from 0.01 to 10 mM. (B) % Translation of globin mRNA (of untreated control).

L- and D-alanine are also expected to be discriminated poorly by the ribosome in eukaryotic cells (yet this has yet to be tested) since there is a ~3-fold discrimination of L- and D-Ala-PANS by ribosomes *in vitro* (5). This low level of peptidyl transferase selectivity may allow D-alanine to be readily incorporated into protein. The following analysis demonstrates how measures can be taken to increase the recognition of D-amino acids via aa-tRNA-mediated protein synthesis.

Based on an analysis by Hopfield and co-workers partial selectivity at each stage of protein synthesis should exclude D-tyrosine from being incorporated into protein (1). For example, the EF-Tu-aa-tRNA complex of L-tyrosine-tRNA^{Tyr} is bound ~20 times more tightly than D-tyrosine-tRNA^{Tyr} (1). In addition, binding to ribosomes and subsequent peptide bond formation are favored for L-tyrosine-tRNA^{Tyr} by 3- and ~30-fold, respectively (1). Taken together the selectivity for L-tyrosine-tRNA^{Tyr} versus D-tyrosine-tRNA^{Tyr} is 10^4 (Figure 6.8; column I).

However, aminoacylation by a cognate synthetase is not required since a D-aa-tRNA could be prepared using the chemical misacylation strategy (15, 16). This decreases the discrimination of a D-aa-tRNA to 10^3-fold (Figure 6.8; column II). Further, the identification of an optimal tRNA body to use with D-amino acids to provide favorable thermodynamic compensation for EF-Tu or EF1A affinity would allow the tertiary complex to effectively compete with other naturally occurring aa-tRNA-EF-Tu complexes (17, 18). This improvement should further decrease the discrimination to $<10^2$-fold (Figure 6.8; column III).

Peptidyl transferase discrimination for an aminoacylated-tRNA with 4-*O*-methyl-tyrosine is expected to be 5-fold (1). This assumes that the discrimination between L- and D-tyrosine-tRNA and L- and D-4-*O*-methyl-tyrosine-tRNA in peptidyl transferase is equivalent, at 5-fold (1). Next, the stereoselectivity of peptidyl transferase between L- and D-alanine-tRNA can be calculated. The ~ 150-fold peptidyl transferase selectivity for L- and D-puromycin and the ~3-fold selectivity for L- and D-alanine-PANS (5) can be used to calculate the fold selectivity for peptidyl transferase

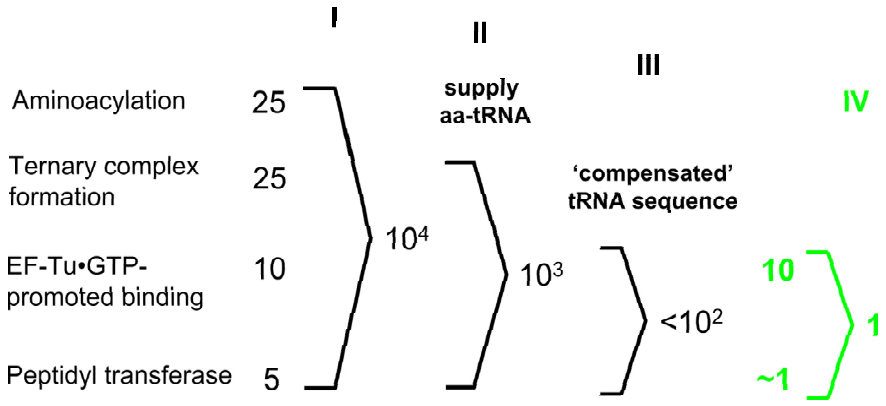

Figure 6.8: Analysis of ribosomal selectivity for D-alanine using an optimized tRNA body starting with the (I) maximal selectivity of L- versus D-tyrosine from (1).

activity in the ribosome for L- versus D-alanine-tRNA^{Ala} using the following equation:

$$\frac{[4\text{-}O\text{-methyl-tyrosine-tRNA-fold selectivity (1)}]}{[\text{puromycin-fold selectivity (5)}]} \times \frac{1}{[\text{alanine-PANS-fold selectivity (5)}]}$$

$$\frac{5}{150} \times \frac{1}{3} = 1$$

Replacing the 5-fold discrimination for peptidyl transferase between L- and D-tyrosine-tRNA (1) with that for L- and D-alanine-tRNA from this calculation changes the overall discrimination of D-residues from protein synthesis to ~1 (Figure 6.8; column IV). This calculation virtually eliminates the stereoselectivity of translation for incorporation of D-alanine-tRNA. This argument predicts that steps can be taken to reduce the stereoselectivity of protein synthesis at several levels: 1) supply excess of chemically misacylated-tRNA, 2) use a tRNA body that optimizes association with the elongation factor (EF-Tu or EF1A), and 3) use a D-residue that shows little peptidyl transferase selectivity, such as D-biocytin or D-alanine.

6.3 Conclusions

Until recently, D-amino acids were not considered to be important in the biology of higher organisms. The discovery that small peptides with D-amino acids are involved in development, hormone synthesis, and neurotransmission, as well as in age-related conditions such as Alzheimer's has challenged theories about the utility of D-amino acids. (reviewed in (19)). The data presented here highlight the possibility that D-amino acids do have biological relevance in live cells. This examination should facilitate the conception and design of experiments to elucidate the role that D-amino acids play both in normal and disease states *in vivo* as well as aid in construction of D-based peptide libraries for mRNA display selections (8).

6.4 Experimental Procedures

6.4.1 General information

Low-resolution mass spectra were recorded on a PE SCIEX API 365 triple quadruple electrospray mass spectrometer at the Beckman Institute Mass Spectrometry Laboratory, California Institute of Technology. Column chromatography was carried out on silica gel (40 – 63 μm, EM Science). Analytical HPLC was performed using a Vydac C18 column (5 mm, 4.5 x 250 mm) with buffer A (5 mM NH_4OAc, pH 5.5 with 10% acetonitrile) and buffer B (5 mM NH_4OAc, pH 5.5 with 90% acetonitrile); a linear gradient of 100% buffer B in 50 min was used with a flow rate of 1 mL/min. All reagents were of highest available commercial quality and were used without further purification. L-puromycin and puromycin aminonucleoside (3'-amino-3'-deoxy-*N*,*N*'-dimethyl-adenosine) (PANS) were purchased from Sigma Chemical Co. D-puromycin was prepared as described in (5). FMOC-L-biocytin was obtained from Novabiochem. FMOC-D-biocytin was prepared from coupling FMOC-D-lysine (Bachem) and D-biotin (>99.9%; Sigma Chemical Co.) as described below. Immobilized piperidine

beads (3-4 mmol/g) were purchased from Aldrich. Puromycin analog concentrations were determined with the following extinction coefficients ($M^{-1}cm^{-1}$) at 260 nm: Aromatic puromycin analogs such as L- and D-puromycin (**1** and **2**, respectively) [$\epsilon = 10,500$] in water; non-aromatic puromycin analogs such as L- and D-biocytin (**3** and **4**, respectively) [$\epsilon = 11,000$] in phosphate buffered saline (pH 7.3). Rabbit reticulocyte lysate was purchased from Novagen. Rabbit globin mRNA was obtained from Life Technologies Gibco BRL.

6.4.2 Procedure for Preparation of FMOC-D-biocytin

FMOC-D-lysine (0.204 mmol) was dissolved in dried *N*,*N*-α-dimethylformamide (DMF) (0.700 mL) at room temperature. To this solution was added 1-H-benzotriazolium (HBTU) (0.204 mmol) and 6-chloro-1-hydroxy-1H-benzotriazole (HOBT) (0.204 mmol) and stirred for 10 min. FMOC-D-lysine (0.204 mmol) dissolved in diisopropylethylamine (DIEA) (2.55 mL) was added slowly with stirring. The solution was stirred at ambient temperature overnight and then dried *in vacuo*. The product was resuspended in MeOH/CH_3COOH/$CHCl_3$ (7:13:80) and purified by flash chromatography using MeOH/CH_3COOH/$CHCl_3$ (7:10:83). Homogenous product fractions were dried *in vacuo* to yield FMOC-D-biocytin as a yellow-brown oil (120 mg, 99.0%). LRMS, *m/z* $(M+H)^+ = 595.2$.

6.4.3 General Procedure for Preparation of Puromycin Analogs

N,*N*'-dicyclohexylcarbodiimide (DCC) (0.0539 mmol) was added to a cold (0 °C) solution of PANS (0.0520 mmol), FMOC-protected amino acid (0.0541 mmol), and *N*-hydroxysuccinimide (NHS) (0.0556 mmol) in dried *N*,*N*-α-dimethylformamide (DMF) (0.900 mL). The solution was stirred for 30 min in an ice-water bath and then for 42 h at ambient temperature. *N*,*N*'-dicyclohexylurea was filtered and washed (EtOAc,

4 mL), and the filtrate was concentrated *in vacuo*. The material was resuspended in triethylamine/MeOH/$CHCl_3$ (2:8:90) and purified by flash chromatography using triethylamine/MeOH/$CHCl_3$ (2:8:90). Homogenous product fractions were dried *in vacuo* to yield the FMOC-protected products. FMOC-deprotection was carried out using immobilized piperidine in DMF (5mL) with stirring overnight at ambient temperature for L- and D-biocytin-PANS (**3** and **4**, respectively). The beads were filtered and the solvent was removed *in vacuo*. The residue was purified using HPLC to afford the products L- and D-biocytin-PANS. LRMS, m/z $(M+H)^+ = 649.4$. L- and D-puromycin (**1** and **2**, respectively) were prepared as described previously (5).

6.4.4 *In vivo* Analysis of Puromycin Analogs

16610D9 thymocyte cells (D9 cells; 25,000 cells) were combined with puromycin analogs (dried initially and dissolved in RPMI media with 10% FBS) in total volume of 100 μL in 48-well microtiter plates. After incubation at 37°C in a humidified atmosphere with 5% CO2 for 24 h, cells were analyzed directly using a Beckman FACScabilur flow cytometer to collect forward and side scatter measurements, which shows a characteristic plot for viable cells. A slight modification of the procedure as indicated in Figure 6.6 was using a total volume of 300 μM in 24-well microtiter plates in a separate experiment.

6.4.5 Preparation of MIG_{PAC} Infected 16610D9 Cells

The PAC gene was cloned into MIG using BgII and EcoRI restriction sites to yield MIG_{PAC}. 293T-HEK fibroblasts (American Tissue Culture Collection) were cotransfected with pECL-Eco and MIG or MIG_{PAC} by calcium phosphate precipitation [see reference (11)]. After 12 hours, the precipitate was removed, cells were washed once with PBS, and 4 mL of fresh complete Dulbecco's Modified Eagle Medium (DMEM) supplemented with 10% fetal calf serum (FCS) was added. Viral supernatant was

removed 24 hours later and used for infection of D9 cells. One million D9 cells were spin-infected with 0.4 mL of viral supernatant suplemented with 5 μg/ml Polybrene (Sigma-Aldrich).

6.4.6 Enrichment of GFP(+) 16610D9 Cells using Puromycin and Puromycin Conjugates

D9 cells infected with either MIG of MIG_{PAC} were cultured in RPMI media with 10% FBS and grown at 37 °C in a humidified atmosphere with 5% CO_2. For each experiment, D9 cells (0.25 x 10^6/well) were added to 24-well microtiter plates along with puromycin and puromycin analog dissolved in the minimum amount of media. After a 48 h incubation, the cells were washed twice in 2 mL PBS + 4% FCS and resuspended in PBS + 4% FCS supplemented with 2% formaldehyde along with incubation at 37 °C for 10 min and analyzed using flow cytometery.

6.4.7 IC_{50} Determination

Translation reactions containing [^{35}S]Met were mixed in batch on ice and added in aliquots to microcentrifuge tubes containing an appropriate amount of puromycin, puromycin-conjugate, or oligonucleotide dried in vacuo. Typically, a 20 μl translation mixture consisted of 0.8 μL of 2.5 M KCl, 0.4 μL of 25 mM MgOAc, 1.6 μL of 12.5X translation mixture without methionine, (25 mM dithiothreitol (DTT), 250 mM HEPES (pH 7.6), 100 mM creatine phosphate, and 312.5 μM of 19 amino acids, except methionine) (Novagen), 3.6 μL of nuclease-free water, 0.6 μL (6.1 μCi) of [^{35}S]Met (1175 Ci/mmol), 8 μL of Red Nova nuclease-treated lysate (Novagen), and 5 μL of 0.05 μg/μL globin mRNA (Gibco). Inhibitor, lysate preparation (all components except template), and globin mRNA were mixed simultaneously and incubated at 30 °C for 60 min. Then 2 μL of each reaction was combined with 8 μL of tricine loading buffer (80 mM Tris-Cl (pH 6.8), 200 mM DTT, 24% (v/v) glycerol, 8% sodium dodecyl

sulfate (SDS), and 0.02 % (w/v) Coomassie blue G-250), heated to 90 °C for 5 min, and applied entirely to a 4% stacking portion of a 16% tricine-SDS-polyacrylamide gel containing 20% (v/v) (20) (30 mA for 1h, 30 min). Gels were fixed in 10% acetic acid (v/v) and 50% (v/v) methanol, dried, exposed overnight on a PhosphorImager screen, and analyzed using a Storm PhosphorImager (Molecular Dynamics).

References

[1] T. Yamane, D.L. Miller, and J.J. Hopfield. Discrimination between D-tyrosyl and L-tyrosyl transfer ribonucleic-acids in peptide-chain elongation. *Biochemistry*, 20:1897–1904, 1981.

[2] D. Nathans and A. Neidle. Structural requirements for puromycin inhibition of protein synthesis. *Nature*, 197:1076–1077, 1963.

[3] J.D. Bain, D.A. Wacker, E.E. Kuo, and A.R Chamberlin. Site-specific incorporation of nonnatural residues into peptides - Effect of residue structure on suppression and translation efficiencies. *Tetrahedron*, 47:2389–2400, 1991.

[4] J. Ellman, D. Mendel, S. Anthony-Cahill, C.J. Noren, and P.G. Schultz. Site-specific incorporation of novel backbone structures into proteins. *Science*, 202:301–336, 1992.

[5] S.R. Starck, X. Qi, B.N. Olsen, and R.W. Roberts. The puromycin route to assess stereo- and regiochemical constraints on peptide bond formation in eukaryotic ribosomes. *J. Am. Chem. Soc.*, 125:8090–8091, 2003.

[6] J.W. Trauger, R.M. Kohli, H.D. Mootz, M.A. Marahiel, and C.T Walsh. Peptide cyclization catalysed by the thioesterase domain of tyrocidine synthetase. *Naure*, 407:215–218, 2000.

[7] T.A. Keating, C.G. Marshall, and C.T. Walsh. Reconstitution and characteriza-

tion of the Vibrio cholerae vibriobactin synthetase from VibB, VibE, VibF, and VibH. *Biochemistry*, 39:15522–15530, 2000.

[8] T.T. Takahashi, R.J. Austin, and R.W. Roberts. mRNA display: ligand discovery, interaction analysis and beyond. *Trends Biochem. Sci.*, 28:159–165, 2003.

[9] A. Frankel, S.W. Millward, and R.W. Roberts. Encodamers: Unnatural peptide oligomers encoded in RNA. *Chem. Biol.*, 10:1043–1050, 2003.

[10] L. Van Parijs, Y. Refaeli, J.D. Lord, B.H. Nelson, A.K. Abbas, and D. Baltimore. Uncoupling IL-2 signals that regulate T cell proliferation, survival, and Fas mediated activation-induced cell death. *Immunity*, 11:281–288, 1999.

[11] S.R. Starck, H.M. Green, J. Alberola-Ila, and R.W. Roberts. A general approach to detect protein expression *In Vivo* using fluorescent puromycin conjugates. *Chem. Biol.*, page In press, 2004.

[12] S. de la Luna and J. Ortin. Pac gene as efficient dominant marker and reporter gene in mammalian cells. *Methods Enzymol.*, 216:376–385, 1992.

[13] J.N. Porter, R.I. Hewitt, C.W. Hesseltine, G. Krupka, J.A. Lowery, W.S. Wallace, N. Bohonos, and J.H. Williams. Achromycin: A new antibiotic having trypanocidal properties. *Antibiotics and Chemo.*, 11:409–410, 1952.

[14] J.A. Pérez-González, J. Vara, and A. Jiménez. Acetylation of puromycin by *Streptomyces alboniger* the producing organism. *Biochem. Biophys. Res. Commun.*, 113:772–777, 1983.

[15] S.M. Hecht. Probing the synthetic capabilities of a center of biochemical catalysis. *Acc. Chem. Res.*, 25:545–552, 1992.

[16] C.J. Noren, S.J. Anthony-Cahill, M.C. Griffith, and P.G. Schultz. A general method for site-specific incorporation of unnatural amino-acids into proteins. *Science*, 244:182–188, 1989.

[17] F.J. LaRiviere, A.D. Wolfson, and O.C. Uhlenbeck. Uniform binding of aminoacyl-tRNAs to elongation factor Tu by thermodynamic compensation. *Science*, 294:165–168, 2001.

[18] O. C. Asahara, H.; Uhlenbeck. The tRNA specificity of *Thermus thermophilus* EF-Tu. *Proc. Natl. Acad. Sci. U.S.A.*, 99:3499–3504, 2002.

[19] H. Yang, G. Zheng, X. Peng, B. Qiang, and J. Yuan. D-Amino acids and D-Tyr-tRNA^{Tyr} deacylase: Stereospecificity of the translation machine revisited. *FEBS*, 552:95–98, 2003.

[20] H. Schagger and G.V. von Jagow. Tricine-sodium dodecyl sulfate-polyacrylamide gel electrophoresis for the separation of proteins in the range from 1 to 100 kDa. *Anal. Biochem.*, 166:368–379, 1987.

Chapter 7

Puromycin Analogs and the Homochirality of Life

Abstract

How nature evolved to use L-amino acids instead of the D-enantiomers to synthesize proteins remains an unanswered question. The physical basis for evolution of amino acid homochirality is proposed based on the physical properties of puromycin analogs bearing L- and D-amino acid residues. While L- and D-amino acids are enantiomers with similar physical properties, L- and D-puromycin analogs are diastereomers with unique physical properties as assessed by liquid chromatography and solubility determination. These data indicate that selection of L-amino acids could be made based on the different physical properties of aminoacyl-adenosine derivatives.

7.1 Introduction

The origin for homochirality of life continues to be a source of intense debate. Since Louis Pasteur first discovered the chirality of molecules in the 19^{th} century, scientists are divided on where and how enantiomer excess first originated. Enantiomer selection evolving on earth is supported by data that shows the surface of calcite crystals, a

widely present molecule on early earth, separate L- and D-amino acids on different faces of the crystal (1). Others speculate that sunlight, which shows a predominant direction of circular polarized light at dusk, directed enantiomer selection through light-induced reactions on early earth. Other data support models where molecular handedness was directed from events in space. One theory is that Earth formed from accretion of primordial dust containing an excess of left-handed amino acids (2). Further, enantiomer excess is thought to have originated from meteorites, which now have been shown to have L-enantiomeric excesses (3). A significant drawback for this theory is that L-enantiomer excesses were not found to exceed 3% for naturally occuring amino acids (4).

Biochemical experiments have also been carried out showing that while aminoacylation of RNA by amino acids is not stereoselective, RNA that is surface-bound (thought to mimic prebiotic surface monolayers) is aminoacylated specifically with L-residues (5). Another terrestrial process thought to play a role in homochirality is the observation that L- and D-enantiomers do not have exactly the same energy (6). However, this energy difference equates to an enantiomer excess of merely $10^{-13} - 10^{-16}\%$ (7).

How amino acid enantiomer excess evolved remains one of many 'origin of life' questions. Data collection can be gained not only from astrochemisty laboratories but also from chemistry and biochemistry experiments. Evaluating and understanding biological systems, such as ribosome-mediated protein synthesis (eukaryotes) or nonribosomal peptide synthesis (prokaryotes), could provide evidence for why handedness is a fundamental law of biology. Pushing the limits of such systems could yield results that support or refute existing models for enantiomeric selection. Development of reagents and assays to thoroughly elucidate the mechanism of protein synthesis, for example, is the starting point for drawing conclusions about how and why biological systems are stereospecific.

7.2 Results and Discussion

L- and D-amino acid pairs are enantiomers and have similar physical properties. This physical similarity puts into question how the L-enantiomer was selected to be used instead of the D-enantiomer. Current theories about enantiomer selection argue that this event occurred prior to the evolution of biological systems. However, the following data argue that selection of L-amino acids may have been possible based on the distinct physical properties of aminoacyl-nucleotides, such as puromycin. The theory presented assumes that the evolution of homochirality occurred at stages, i.e., D-sugars and then L-amino acids. Several pieces of data should be reviewed first in order to provide a framework for this argument.

A seminal discovery in 1967 showed that peptidyl transferase was carried out on isolated ribosomes in a reaction called the 'fragment reaction' where a peptide bond can be formed on isolated large 50S ribosomal subunits between a P-site held terminal hexanucleotide with a 3'-formylmethionine (CAACCA-Met-f) and puromycin (Figure 7.1) (8). Soon thereafter, peptidyl transferase activity under fragment assay conditions persisted despite the removal of most ribosomal protein (9).

This discovery led Francis Crick and Leslie Orgel to argue that the primitive ribosome may have consisted entirely of RNA (11). In their discussion, Crick and Orgel suggested that while the primordial ribosome may have been entirely RNA, present day ribosomes evolved to contain protein to 'do the job with greater precision' (12). Then tandem discoveries of catalytic RNA in 1980 (13) and experiments showing that stripping protein from 23S rRNA in 50S ribosomal subunits showed continued peptidyl transferase activity (14) further bolstered the theory of a primitive RNA only ribosome. Finally, in August 2000 Tom Steitz and co-workers published an atomic resolution crystal structure of the large ribosomal subunit with a transition state analog (10). This work unambiguously assigned the peptidyl transferase center (PTC) to be completely within a region of RNA (Figure 7.1). In fact, the closest amino acid side chain is more than 18 $\AA$ removed from the PTC (10). This confirmed the

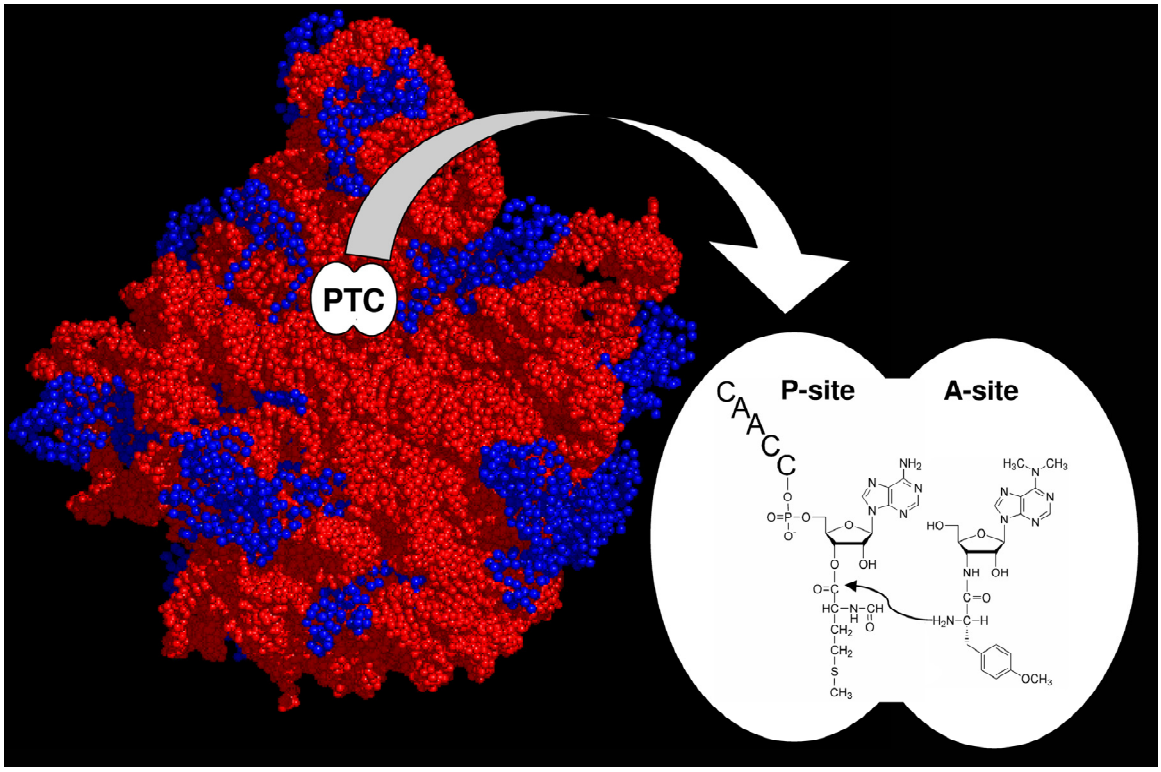

Figure 7.1: The fragment reaction between a P-site held CAACCA-Met-f and puromycin (RNA = red and protein = blue). Cystral structure of the 50S subunit from *H. marismortui* adapted from (10).

theory that the ribosome is a ribozyme (10). Taken together, these data are evidence that a primordial system for protein synthesis may have evolved from an RNA world where an RNA-only ribosome performed dipeptide bond formation between aa-tRNA fragments (15, 16).

At one point in evolution, prebiotic life had selected D-sugars, mastered RNA polymer synthesis, and the identification of the optimal RNA sequence and structure for basic ligation and cleavage reactions. However, the presence of amino acids in the prebiotic environment and pressure to search for alternative polymers prompted RNA to react with amino acids. In a scenario where the 'fragment reaction' was the progenitor of current day protein synthesis, the presence of puromycin-like molecules (e.g., 3'-*N*- and *O*-aminoacyl adenosine derivatives) would be expected. In fact, RNA catalysts have been selected that perform aminoacyl group transfer (17, 18). Therefore, primitive aminoacylation reactions may have yielded a variety of amino acid-nucleoside molecules. The current existence of puromycin, modified nucleosides, and co-factors such as S-adenosyl methionine (Figure 7.2) may be primordial remnants of the first amino acid-ribonucleoside compounds (19, 20, 21).

A primordial peptidyl transferase system may not have been stereospecific admist a racemic mixture of L- and D-amino acids. This phenomena is still apparent in current day aminoacylation reactions (for review see (22)). In this theory, both L- and D-amino acids became covalently linked to 2'-*N*- and 2'(3')-*O*-adenosine ribonucleosides by an RNA-based system yielding a series of 3'-*N*- and 2'(3')-*O*-L- and D-aminoacylnucleosides. These compounds recapitulate the 3'-end of every aa-tRNA molecule where the terminal nucleoside is an adenosine. Now, a series of dipeptides may have been coupled by the peptidyl transferase reaction of a primordial RNA-only ribosomal subunit. Since aminoacylation is not stereochemically controlled in this theory, the primitive ribosome would equally incorporate 3'-*N*- and -*O*-L- and D-aminoacylnucleosides (Figure 7.3).

As such, the homochirality of proteins may have resulted from a primordial RNA-

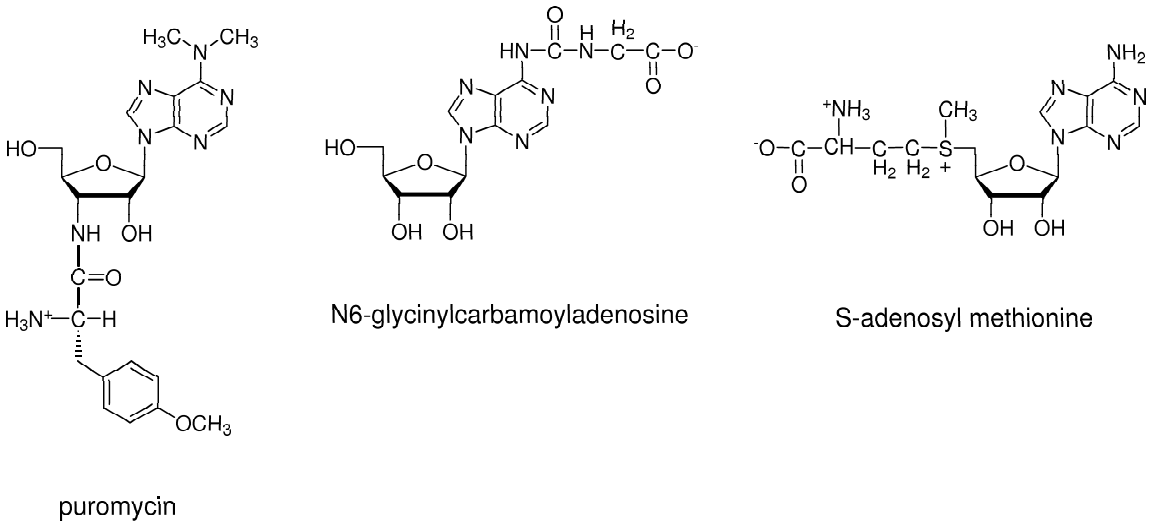

Figure 7.2: Current day ribonucleoside adenosine compounds with amino acid moieties.

only ribosome evolving to preferentially select L-amino acids. The data presented herein suggest that based on chemical differences between 3'-*N*- and L- and D-aminoacylnucleosides the ribosome was able to differentiate the L-isomer from the D-isomer. Two pieces of data are presented: 1) HPLC analysis of L- and D-puromycin analogs and 2) Solubility data for L- and D-analogs.

HPLC analysis shows the retention times for L- and D-puromycin analogs are different for each diastereomer (Figure 7.4A). This pattern is also observed for L- and D-Phe-PANS, *N*-methyl-L- and D-Phe-PANS, and L- and D-biocytin-PANS (Figure 7.4B-D). One interesting result is that D-analogs consistently elute before their L-counterparts (Figure 7.4). L- and D-amino acid pairs are expected to have identical chromatographic behavior, but when linked to puromycin aminonucleoside (PANS) the molecules are diastereomers with different physical properties. Overall, the presence of a D-side chain changes the solubility of the molecule, independent of the side chain identity (e.g., 4-*O*-methyl-tyrosine or biocytin side chains) or amine substitution (e.g., *N*-methyl-Phe-PANS) (Figure 7.4). The solubility of several L- and

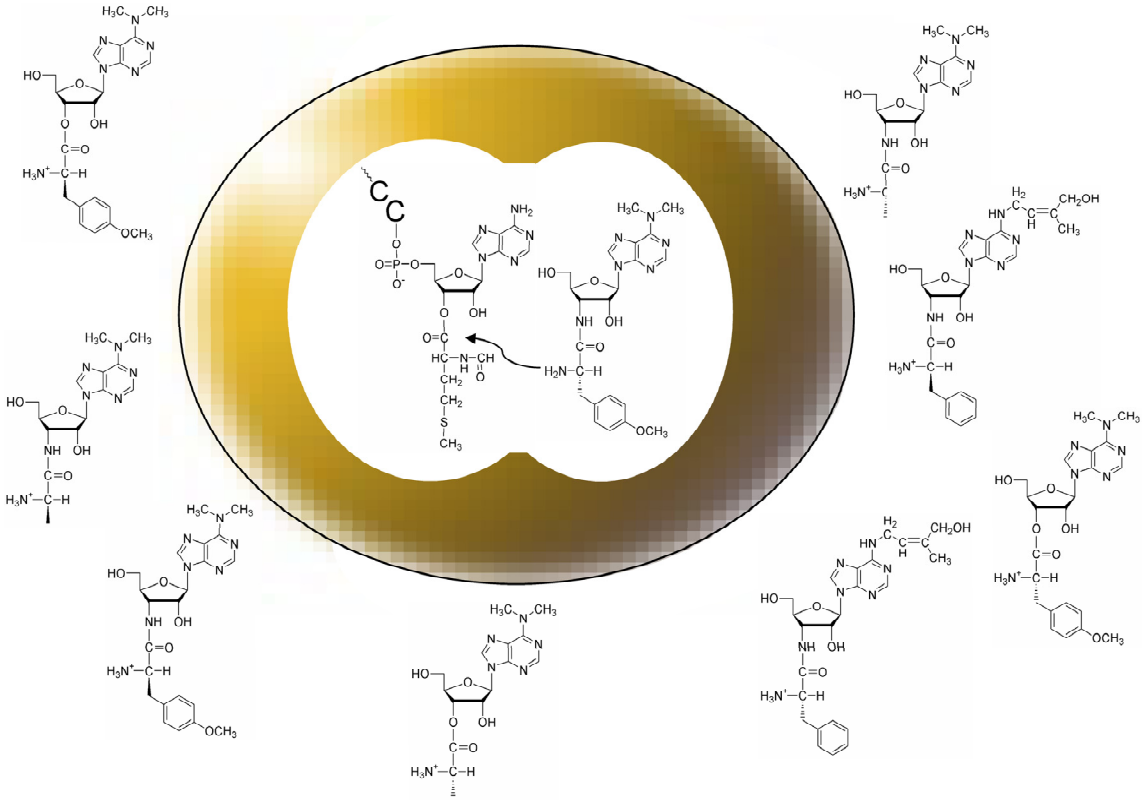

Figure 7.3: A primordial RNA-only ribosome may have generated dipeptides by coupling CAACCA-Met-f and 3'-*N*- and 2'-(3')-*O*-L- and D-aminoacylnucleosides.

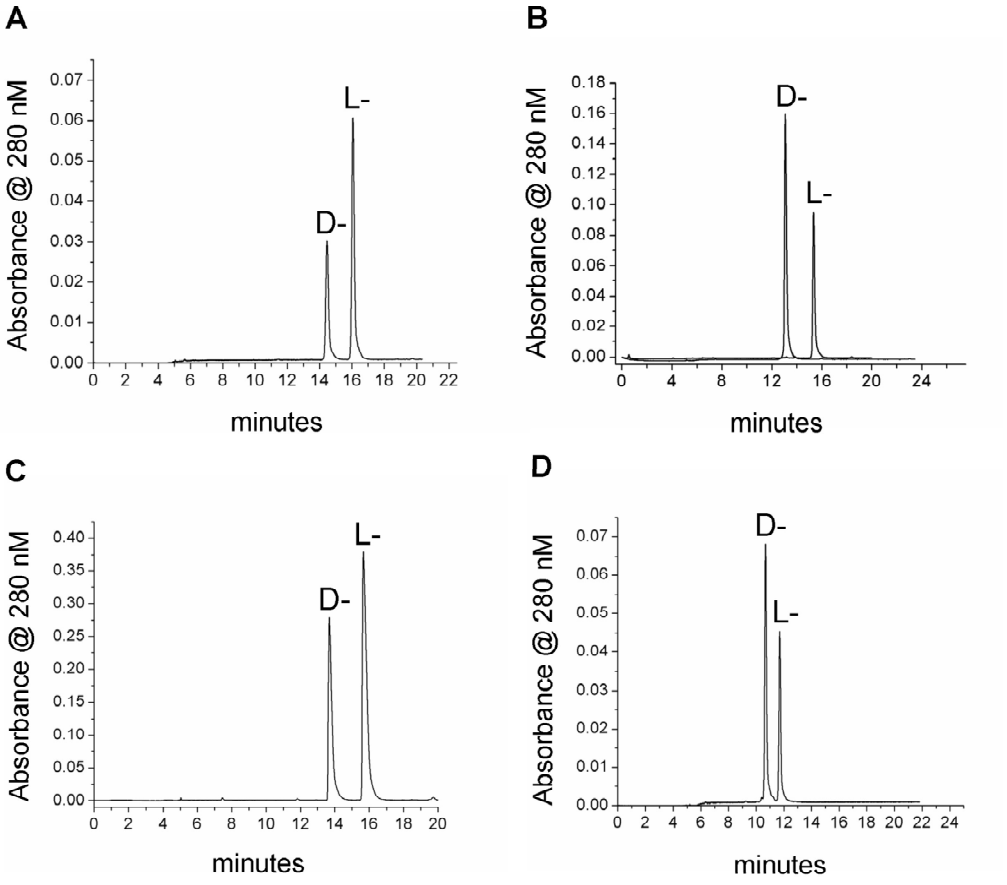

Figure 7.4: HPLC analysis of L- and D-amino acid analogs: (A) L- and D-puromycin; (B) L- and D-Phe-PANS; (C) *N*-methyl-L- and D-Phe-PANS; and (D) L- and D-biocytin-PANS.

Analog	Solubility (K_{sp}, μM)	ΔK_{sp}
L-puromycin	48.0	
D-puromycin	0.45	~100-fold
L-Phe-PANS	23.2	
D-Phe-PANS	4.44	~5-fold
L-Ala-PANS	1120	
D-Ala-PANS	10.4	~100-fold
PANS	147	

Table 7.1: Solubility determination for puromycin analogs.

D-puromycin analog pairs was also determined (Table 7.1).

The solubility of the L-analogs is consistently greater than their D-counterparts. In fact, the D-variants were all less soluble than any one L-variant (Table 7.1). Once the amino acid is coupled to PANS (K_{sp} = 147 mM) the analog solubility decreases for each molecule except L-Ala-PANS which becomes more soluble (Table 7.1). This observation may be related to the high solubility (g/100g, 25 °C) of free alanine which is 16.65 (6th most soluble amino acid) while free phenylalanine is 2.965 (23, 24). Perhaps, the presence of an L-alanine moiety increased the solubility of the L-Ala-PANS derivative relative to PANS alone (Table 7.1). The solubility data shows a consistent pattern for the D-analogs tested since they were all were less soluble than their L-counterparts. This pattern is comparable to that seen from the HPLC data where D-analogs consistently eluted before their L-counterparts (Figure 7.4). However, there does not appear to be a direct relationship between the potency of the analogs and their solubility. A problem with attempting to make this correlation stems from the effect of the amino acid side chain for affinity within the A-site of the ribosome. This variation was first noted by Nathans and Neidle which showed that hydrophobic, aromatic side chains produce the most potent puromycin derivatives

while smaller side chains lead to a less active analog (25).

The HPLC and water solubility data identify physical differences between L- and D-puromycin analogs. While this property can not be reconciled with the absolute potency of the analogs, the consistently low solubility of the D-variants is a property that primitive ribosomes may have been able to discern. Previous observations that D-puromycin analogs are incorporated into protein (26) may represent a residual activity that has not yet been lost through evolution. It should be noted that the significant physical difference between L- and D-analogs may not have required such an evolutionarly mature selective step, such as peptidyl transferase. Simply, the solubilty differences between 3'-*N*- and 2'(3')*O*-L- and D-aminoacylnucleosides dictated the concentrations available for subsequent reactions.

7.3 Conclusions

The RNA world hypothesis argues that an RNA-only ribosome (the progenitor of the current day large 50S or 60S subunits) may have carried out reactions analogous to the 'fragment reaction' to yield dipeptides. Assuming that 3'-*N*- and 2'(3')*O*-L- and D-aminoacylnucleosides were present in this primordial reaction, the primitive ribosome would be poised to discriminate between L- and D-molecules based on their distinct physical differences. The solubility data presented here reflect the unique properties of L- and D-puromycin analogs. The primordial ribosome may have initially been able to accommodate L- and D-variants equally and evolved to use only L-variants. This theory is specifically supported by the identification of mutations in RNA of the peptidyl transferase center of *E. coli.* 23S RNA that allow for enhanced incorporation of D-amino acids into protein (27). The confirmation that a primitive ribosome evolved to preferentially select L-residues instead of D-residues would stand as the first terrestrial process known to break the parity of racemic mixtures.

7.4 Experimental Procedures

7.4.1 General Information

Low-resolution mass spectra were recorded on a PE SCIEX API 365 triple quadruple electrospray mass spectrometer at the Beckman Institute Mass Spectrometry Laboratory, California Institute of Technology. High-resolution mass spectra (FAB) were recorded on a JMS-600H double-focusing, high-resolution, magnetic sector mass spectrometer at the Mass Spectrometry Laboratory, Division of Chemistry and Chemical Engineering, California Institute of Technology. All reagents were of highest available commercial quality and were used without further purification. L-puromycin and puromycin aminonucleoside (3′—amino-3′—deoxy-*N*,*N*'-dimethyl-adenosine) (PANS) were purchased from Sigma Chemical Co. D-puromycin and L- and D-alanine-PANS were prepared as described in (26). L- and D-phenylalanine-PANS and *N*-methyl-L- and D-phenylalanine-PANS were prepared as described in Chapter 5. L- and D-biocytin-PANS were prepared as described in Chapter 6. Puromycin analog concentrations were determined with the following extinction coefficients ($M^{-1}cm^{-1}$) at 260 nm: Aromatic puromycin analogs such as L- and D-puromycin, L- and D-phenylalanine, and *N*-methyl-L- and D-phenylalanine-PANS [$\epsilon = 10,500$] in H_2O. Non-aromatic puromycin analogs, such as L-and D-biocytin-PANS and L- and D-Ala-PANS [$\epsilon = 11,000$] in phosphate buffered saline (pH 7.3). Rabbit reticulocyte lysate was purchased from Novagen. Rabbit globin mRNA was obtained from Life Technologies Gibco BRL.

7.4.2 HPLC Analysis

Column chromatography was carried out on silica gel (40 – 63 μm, EM Science). Analytical HPLC was performed using a Vydac C18 column (5 mm, 4.5 x 250 mm) with buffer A (5 mM NH4OAc, pH 5.5 with 10% acetonitrile) and buffer B (5 mM NH4OAc, pH 5.5 with 90% acetonitrile); a linear gradient of 100% buffer B in 50 min

was used with a flow rate of 1 mL/min.

7.4.3 Solubility (K_{sp}) Determination

Saturated solutions were prepared by dissolving the analytes in 0.75 mL of water in 1.5-mL eppendorf tubes. The samples were shaken for 3 days at 25 °C and then filtered. The resulting saturated solution was quantified as described in General Information and K_{sp} = [analyte].

References

[1] R.M. Hazen, T.R. Filley, and G.A. Goodfriend. Selective adsorption of L- and D-amino acids on calcite: Implications for biochemical homochirality. *Proc. Natl. Acad. Sci. U.S.A.*, 98:5487–5490, 2001.

[2] T. Henning and F. Salama. Carbon-carbon in the universe. *Science*, 282:2204–2210, 1998.

[3] J.R. Cronin and S. Pizzarello. Enantiomeric excesses in meteoritic amino acids. *Science*, 275:951–955, 1997.

[4] S. Pizzarello and J.R. Cronin. Non-racemic amino acids in the Murray and Murchison meterorites. *Geochim. Cosmo. Acta*, 64:329–338, 2000.

[5] J.M. Bailey. Rna-directed amino acid homochirality. *FASEB J.*, 12:503–507, 1998.

[6] S.L. Barron. *Molecular Light Scattering and Optical Activity.* Cambridge University Press, Cambridge, 1982.

[7] K. Plankensteiner, A. Righi, B.M. Rode, R. Gargallo, J. Jaumot, and R. Tauler. Indications towards a stereoselectivity of the salt-induced peptide formation reaction. *Inorgan. Chim. Acta*, 357:649–656, 2004.

[8] RE. Monro and KA. Marcker. Ribosome-catalysed reaction of puromycin with a formylmethionine-containing oligonucleotide. *J. Mol. Biol.*, 25:347–350, 1967.

[9] T. Stachelı, D. Maglot, and R.E. Monro. On the catalytic center of peptidyl transfer: apart of the 50-S ribosome structure. In *Cold Spring Harb. Symp. Quant. Biol. XXXIV*, pages 39–48, 1969.

[10] P. Nissen, J. Hansen, N. Ban, P.B. Moore, and T.A. Steitz. The structural basis of ribosome activity in peptide bond synthesis. *Science*, 289:920–930, 2000.

[11] L.E. Orgel. Evolution of the genetic apparatus. *J. Mol. Biol.*, 38:381–393, 1968.

[12] F.H.C. Crick. The origin of the genetic code. *J. Mol. Biol.*, 38:367–379, 1968.

[13] A.J. Zaug and T.R. Cech. *In vitro* splicing of the ribosomal RNA precursor in nuclei of *Tetrahymena*. *Cell*, 2:331–338, 1980.

[14] HF. Noller, V. Hoffarth, and Zimniak L. Unusual resistance of peptidyl transferase to protein extraction procedures. *Science*, 256:1416–1419, 1992.

[15] *The RNA World*, chapter On the origin of the ribosome: coevolution of subdomains of tRNA and rRNA, pages 197–209. Cold Spring Harbor Press, New York, 1999.

[16] M. Yarus. On translation by RNAs alone. In *Cold Spring Harb. Symp Quant Biol 66*, pages 207–215, 2001.

[17] J.A. Piccirilli, T.S. McConnell, A.J. Zaug, H.F. Noller, and T.R. Cech. Aminoacyl esterase-activity of the *Tetrahymena* ribozyme. *Science*, 256:1420–1424, 1992.

[18] M. Illangasekare, G. Sanchez, T. Nickels, and M. Yarus. Aminoacyl-RNA synthesis catalyzed by an RNA. *Science*, 267:643–647, 1995.

[19] *In The Pyridine Nucleotide Coenzymes*, pages 1–17. Academic Press, New York, 1982.

[20] W. Gilbert. Origin of life - the RNA world. *Nature*, 319:618–618, 1986.

[21] H.B. White. Coenzymes as fossils of an earlier metabolic state. *J. Mol. Biol.*, 7:101–104, 1986.

[22] H. Yang, G. Zheng, X. Peng, B. Qiang, and J. Yuan. D-Amino acids and D-Tyr-tRNA^{Tyr} deacylase: Stereospecificity of the translation machine revisited. *FEBS*, 552:95–98, 2003.

[23] *The Merck Index.* Number ISBN 911910-28-X. Merck and Co., Inc., Nahway, N.J., 1989.

[24] *CRC Handbook of Chemistry and Physics.* Number ISBN 0-8493-0458-X. CRC Press, Inc., Cleveland, Ohio, 1977.

[25] D. Nathans and A. Neidle. Structural requirements for puromycin inhibition of protein synthesis. *Nature*, 197:1076–1077, 1963.

[26] S.R. Starck, X. Qi, B.N. Olsen, and R.W. Roberts. The puromycin route to assess stereo- and regiochemical constraints on peptide bond formation in eukaryotic ribosomes. *J. Am. Chem. Soc.*, 125:8090–8091, 2003.

[27] L.M. Dedkova, N.E. Fahmi, S.Y. Golovine, and S.M. Hecht. Enhanced D-amino acid incorporation into protein by modified ribosomes. *J. Am. Chem. Soc.*, 125:6612–6617, 2003.